**Author(s):** Rostami, Hossein; Valio, Johanna; Suominen, Pekka; Tynjälä, Pekka; Lassi, Ulla

**Title:** Advancements in cathode technology, recycling strategies, and market dynamics : A comprehensive review of sodium ion batteries

**Year:** 2024

**Version:** Published version



Rostami, H., Valio, J., Suominen, P., Tynjälä, P., & Lassi, U. (2024). Advancements in cathode technology, recycling strategies, and market dynamics : A comprehensive review of sodium ion batteries. Chemical Engineering Journal, 495, Article 153471. https://doi.org/10.1016/j.cej.2024.153471

Chemical Engineering Journal 495 (2024) 153471

Contents lists available at ScienceDirect

Chemical Engineering Journal

journal homepage: www.elsevier.com/locate/cej

Review

# Advancements in cathode technology, recycling strategies, and market dynamics: A comprehensive review of sodium ion batteries

Hossein Rostami [a,b,*], Johanna Valio [b], Pekka Suominen [b], Pekka Tynjälä [a,c], Ulla Lassi [a,c]

[a] University of Oulu, Research Unit of Sustainable Chemistry, P.O.Box 3000, FI-90014, Finland
[b] Satakunta University of Applied Sciences (SAMK), Satakunnankatu 23, FI-28130 Pori, Finland
[c] University of Jyvaskyla, Kokkola University Consortium Chydenius, Talonpojankatu 2B, FI-67100 Kokkola, Finland

ARTICLE INFO

*Keywords:*
Sodium-ion battery
Cathode materials
Recycling
Material recovery
Sustainability

ABSTRACT

The rising demand for sodium-ion batteries (SIBs) in commercial applications emphasizes the importance of meeting commercial criteria. Despite their potential, SIBs encounter challenges related to specific energy, cycling life, and specific power due to the unique characteristics of sodium ions. Design strategies, surface engineering, and structural modifications for cathode materials have been devised to improve the electrochemical performance of SIBs. In SIBs, the energy density primarily depends on the choice of cathode materials. Common cathode materials nowadays include transition metal oxides, polyanionic compounds, and Prussian blue analogs (PBAs). Enhancing these materials through targeted modifications to overcome their limitations is crucial for transitioning them from lab-scale to practical use. However, there are still some challenges to address before cathode materials can be effectively utilized for large-scale energy storage in SIBs.

Recycling spent SIBs poses significant economic and environmental challenges, particularly compared to lithium-ion batteries (LIBs). Despite progress in cathode materials, thorough environmental assessments and detailed inventory data are lacking for SIBs. The early stage of their development restricts metal recycling in SIBs, underscoring the significance of end-of-life treatment. Pyrometallurgy and hydrometallurgy are commonly employed for metal recovery, with pyrometallurgy favored for SIBs due to reduced sodium evaporation risks.

The marketing and commercialization trends in SIBs reflect the growing demand for renewable energy solutions. SIBs, with their potential for grid-scale energy storage, are expected to support the expansion of renewable energy infrastructure. However, overcoming technological challenges and reducing costs are key to SIB commercialization. In this regard, startups are playing a significant role in advancing SIB technologies for large-scale energy storage applications. The collaboration between companies and advancements in manufacturing facilities are driving SIB production, marking substantial progress towards commercialization. This paper aims to provide a comprehensive review of the current research and advancements in SIB technology.

## 1. Introduction

Globally, there is substantial dependence on non-renewable fossil fuels, which results in considerable environmental degradation. Addressing this urgent global energy challenge necessitates a transformative strategy. However, renewable energy sources encounter limitations imposed by natural constraints. Hence, there is a critical need for an energy storage solution characterized by simplicity, efficiency, resource abundance, and environmental friendliness. Encouragingly, emerging electrochemical energy storage technology exhibits promising adaptability advantages, attracting significant attention in academic circles [1].

Lithium-ion batteries (LIBs) are of significant interest in advanced energy storage systems due to their high energy density, long cycle lifespan, and environmentally benign attributes. However, the availability of lithium in the Earth's crust is limited. As a result, the price of lithium has increased due to the growing demand for LIBs in electronic devices and electric vehicles (EVs). In response to this challenge, scientists are exploring sodium-ion batteries (SIBs) as a potential alternative because sodium is more abundant and widely distributed. However, SIBs face challenges in achieving optimal performance and stability of sodium host materials, mainly because sodium ions are larger and

* Corresponding author at: University of Oulu, Research Unit of Sustainable Chemistry, P.O.Box 3000, FI-90014, Finland.
*E-mail addresses:* h.rostami64@gmail.com, hossein.rostamimalkhalifeh@oulu.fi (H. Rostami).

https://doi.org/10.1016/j.cej.2024.153471
Received 11 April 2024; Received in revised form 6 June 2024; Accepted 24 June 2024
Available online 24 June 2024

heavier than lithium ions. Therefore, a comprehensive understanding of the reaction mechanisms is essential for developing reliable and durable electrodes for high-performance SIBs [2–4].

The emergence of modern Na-ion batteries can be traced back to initial studies demonstrating successful alkali-ion intercalation in solid materials. Notably, the first papers on Na-ion and Li-ion intercalation were published in successive months in 1976 [5]. These studies showed effective $Na^+$ intercalation into $TiS_2$ using a Na–Hg amalgam counter electrode and $Li^+$ intercalation in $TiS_2$ using a Li metal counter electrode. This research prompted further exploration into intercalation-based active materials for both Li-ion and Na-ion batteries. Subsequent developments included successfully demonstrating a Na metal anode in a $TiS_2$ half-cell in 1980, although cycling stability was limited [6]. The same year, Professor Goodenough's group discovered high-voltage oxide-based cathodes that could intercalate $Li^+$ reversibly [7]. This discovery paved the way for the development of the first high-voltage oxide-based Na-ion cathodes by Delmas et al. in 1981 [8]. They studied layered oxides' structural classification and properties with the formula $Na_xMO_2$. They categorized these compositions into $O_3$, $P_2$, and $P_3$ types based on the crystallographic site of Na and the stacking sequence of $MO_2$ slabs, a classification still commonly used today. The focus on Li-ion battery research overshadowed Na-ion battery development, leading to the breakthrough of lithiated graphite anodes in 1982 [9]. However, it took almost eight years for Sony to reveal this seminal demonstration in 1990 [10]. In 1987, Shacklette et al. demonstrated a rocking-chair type Na-ion battery featuring specific cathode, electrolyte, and anode components [9]. Following this, Shishikura et al. filed a patent for an alternative battery design, highlighting remarkable cycling stability in their system [11]. Between 1990 and 2000, sodium-ion battery research declined as lithium-ion batteries soared in market dominance after Sony's commercialization. Rising cobalt prices spurred the search for cheaper alternatives like spinel $LiMn_2O_4$ (LMO) and olivine $LiFePO_4$ (LFP) [12,13]. Despite the decline in sodium-ion battery research, considerable progress has been made in high-temperature sodium batteries, such as sodium-sulfur and sodium-nickel chloride systems, demonstrating their feasibility for large-scale energy storage applications. However, challenges persist due to their high operating temperatures, including corrosion issues and low energy efficiency [14]. In 1994, orthorhombic $Na_xMnO_2$ was employed as a cathode material in alkali metal polymer electrolyte batteries, displaying impressive ion intercalation capacities. Cells using this configuration exhibit excellent capacity retention after extensive cycling at 85 ℃ [15]. The resurgence of interest in room-temperature SIBs was triggered by Stevens and Dahn's discovery of sodium intercalation in hard carbon in 2000. Hard carbon anodes in SIBs offer a high gravimetric capacity of 300 mAh $g^{-1}$ [16,17]. Barker et al. (2002) demonstrated the first working rocking-chair-style sodium-ion battery. A hard carbon anode, 1 M $NaClO_4$ in EC:DMC liquid electrolyte, and $NaVPO_4F$ cathode were used in this groundbreaking investigation. The study revealed encouraging performance parameters, such as a cathode-specific capacity of around 82 mA h $g^{-1}$ and a high average discharge voltage of 3.7 V, like modern lithium-ion batteries [18]. While this discovery reinvigorated interest in SIB research, it did not lead to immediate commercialization due to the lack of incentives to replace lithium. Since 2010, noteworthy progress has been made in SIB cathode materials, with the total number of reported materials between 2010 and 2013 almost equaling the total number before that period [19]. In 2015, the French network for electrochemical energy storage developed the first cylindrical SIB cells with dimensions of "18650" (18 mm diameter, 65 mm height) [20]. The high gravimetric and volumetric energy density of various cathode materials distinguishes them from other available SIB chemistries. These materials are already employed in commercial battery products across different application domains in the current SIB market. Over recent years, there has been a growing focus on Na battery materials, particularly in advanced cathode materials like Na-rich layered and disordered rocksalt (DRX) cathodes. These materials have been pivotal in advancing sodium-ion battery technology and deserve special attention for a thorough grasp of the field [21–23]. Conversely, anodes function as low-potential electrochemical electrode materials within a cell. Improving the total energy density of SIBs requires the development of an anode material with high specific capacity and theoretically low potential. Fig. 1 provides a short representation of the historical trajectory related to the technological progression of SIBs.

In general, the performance of a battery relies on the quality of its cathode and anode. The anode is crucial for battery operation, affecting capacity and energy density through various storage mechanisms. Stability, safety, and environmental impact are vital considerations for anode materials, which are crucial for efficient and sustainable battery development. Carbonaceous compounds like soft/hard carbons and graphite are promising candidates among alkali metal ion anode materials. As graphite, the conventional material used in LIBs demonstrates limited capacity, the optimal selection for SIB anodes resides in hard carbons, especially those derived from biomass. These hard carbons emerge as the most promising choice for progressing SIB technology, owing to their superior performance and cost-effectiveness [24].

This review study has three primary objectives: (1) to concentrate on identifying the most promising cathode materials for SIBs, (2) to offer a comprehensive update on the latest advancements in technology for recycling spent SIBs, and (3) to examine and analyze the current global insights and market trends within the SIB industry.

## 2. Cathode materials

Cathode materials are crucial to sodium-ion batteries, providing active sodium ions and determining the operating voltage. Research is underway to enhance performance and reduce costs, making SIBs a more viable alternative to lithium-ion batteries [25]. Layered metal oxides, polyanionic compounds, Prussian blue analogues (PBAs), and organic compounds can be used as cathode materials for SIBs. Each category shows distinct advantages and limits regarding electrochemical performance, structural stability, and capacity retention. While polyanionic compounds and analogues of Prussian blue exhibit remarkable structural stability and capacity retention, their discharge capabilities fall short of expectations. Organic materials perform well electrochemically but are prone to electrolyte dissolution. Due to their theoretical capacity and high average working voltage, layered transition metal oxides have emerged as the most promising cathode materials among these types. In the SIB research community, layered metal oxides have demonstrated outstanding promise for real-world applications. Nonetheless, more investigation is needed to enhance their stability and cycle life for prolonged utilization in SIBs [26–29]. Most Na cathode materials have a layered or spinel structure that can support Na ions in a 6-coordinated environment with little volume change, as sodium ions prefer more significant coordination numbers than lithium ions.

The cathode materials employed in liquid electrolyte SIBs are also suitable for use in solid-state batteries. Solid-state batteries are proposed as alternatives to organic liquid systems because of their superior safety and high energy density. However, they face several challenges, including limited types of solid electrolytes, low ionic conductivity, and interfacial problems. Ensuring compatibility between the cathode and solid electrolyte is essential for the overall performance of the battery system [30,31]. In solid-state sodium batteries, oxide layer materials such as $Na_{0.66}Ni0_{.33}Mn_{0.67}O_2$ [32], $Na_{0.67}Ni0_{.23}Mg0_{.1}Mn_{0.67}O_2$ [33], or polyanionic $NaTi_2(PO_4)_3$ [34], $Na_3V_2O_2(PO_4)_2F$ [35], and PB analouge $Na_2FeFe(CN)_6$ [36] can be used. To reduce resistance and improve stability, it's crucial to ensure the cathode and solid electrolyte are compatible to boost the performance and lifespan of solid-state batteries. Some strategies include reducing particle size, pressing, sintering, and modifying the composition of the cathode material to optimize the cathode/solid electrolyte interface. Surface coating on electrode particles, interface wetting with ionic liquids, and the introduction of interfacial interlayers have been proposed to enhance the interface with

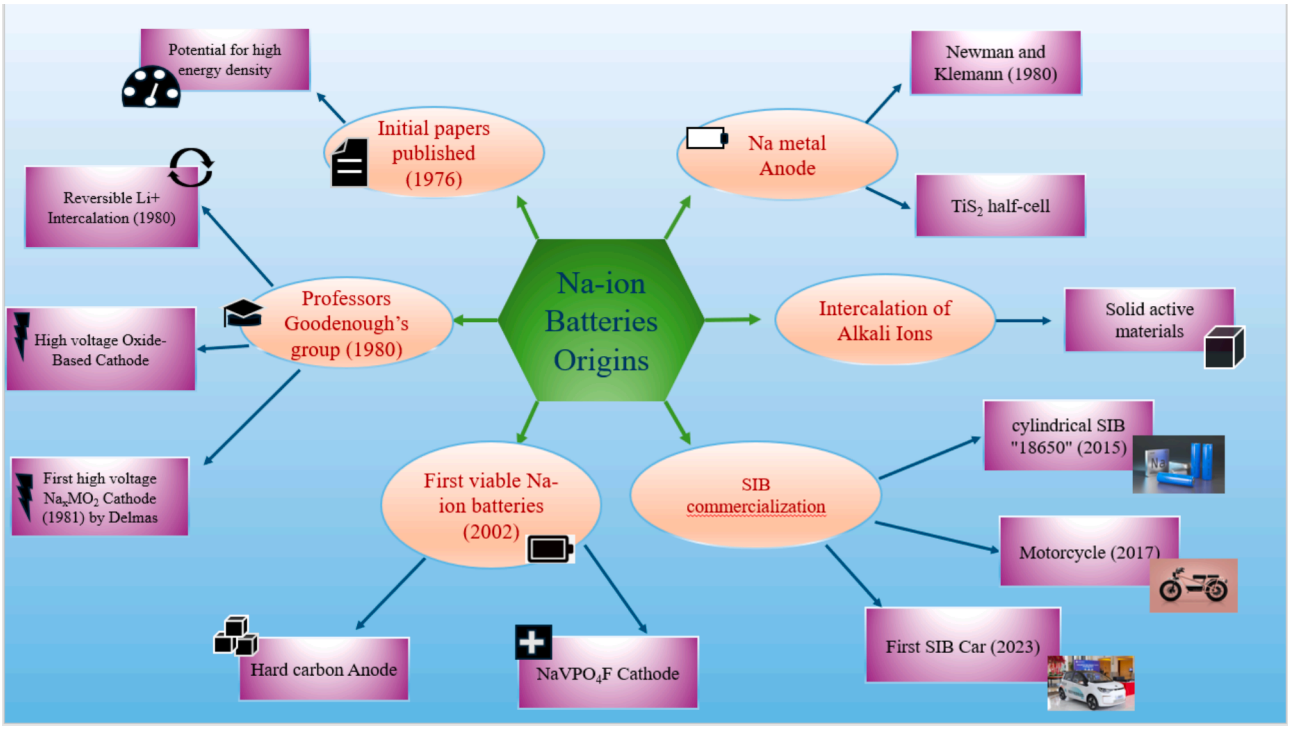


**Fig. 1.** A short schematic representation of the historical trajectory related to the technological progression of SIBs.

reduced impedance and improved stability. Additionally, innovative cathode materials with moderate redox potentials and mechanical compliance, such as organic quinone cathodes, have shown promise in forming favorable electrode–electrolyte interfaces and improving battery performance. The development and enhancement of sodium-ion battery cathodes, particularly those with liquid electrolytes, is the main emphasis of this research. This section examines the development of cathode materials for Na-ion battery cathodes in SIBs, focusing on recent developments. We highlight various cathodes that have the potential to be used in real-world high-energy or high-power SIB applications.

### 2.1. Metal oxide cathodes

Positive electrode materials, particularly layered oxides, have been the subject of extensive study in the SIBs industry. During the early 1980 s, Delmas et al. were the primary contributors to the study of layered oxides for the SIBs, producing most of the early research in this area

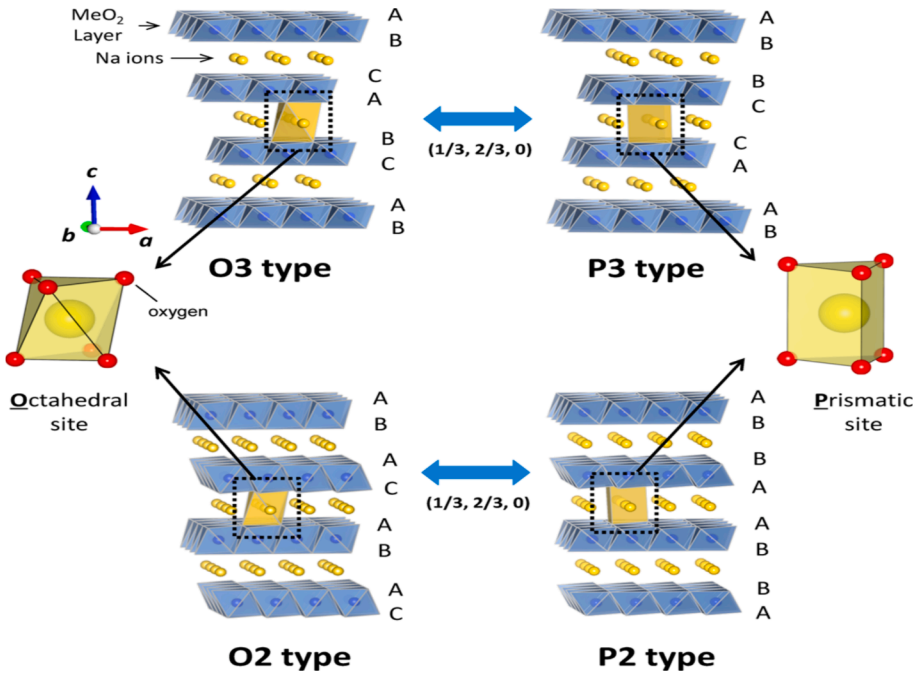


**Fig. 2.** Classification of $Na_xMO_2$ layered materials with sheets of edge-sharing $MO_6$ octahedra and phase change processes brought on by sodium extraction [38]; Copyright © 2014, American Chemical Society.

[37]. Layered oxides with the general formula $Na_xMO_2$ consist of sheets of repeating $MO_6$ layers with Na ions sandwiched between them. These Na-layered oxides can be synthesized in phases: $O_3$, $P_2$, and $P_3$, depending on the number of unique oxide layer packings and the surrounding Na environment. The letter "O" represents the octahedral environment where Na is located, and "P" represents the prismatic environment, while the number represents the number of unique interlayers surrounded by different oxide layers. The prime (') is used to indicate a distorted phase. In the $O_3$ phase, which occurs when $0.7 \leq x \leq 1$, the oxide layer stacking follows the ABCABC pattern, and all Na shares one edge and one face. In the $P_2$-phase, which mainly occurs when $x \approx 0.7$, the oxide layer stacking follows the ABBA pattern, and all Na shares either an edge or face. In the $P_3$-phase, which occurs when $x \approx 0.5$, the oxide layer stacking follows the ABBCCA pattern, and all Na shares one face with a $MO_6$ octahedron and three edges with three $MO_6$ octahedra (Fig. 2). Overall, the classification of $Na_xMO_2$ layered materials and their phase change processes are essential for understanding their electronic and magnetic properties, which are relevant for their potential applications in various fields [38,39].

The specific capacities, cycle stability, and average operating voltage of $Na_xMO_2$ can be altered by the incorporation of metal components. To enhance the performance of $Na_xMO_2$, which is a crucial material for diverse energy storage applications, metal substitution, and doping methods are used. The addition of different metal components to its structure can enhance $Na_xMO_2$'s potential for use in high-performance systems. Various techniques involving metal doping and replacement have been employed to enhance the cycle stability, long-term performance, and output voltage of $Na_xMO_2$.

### 2.1.1. Single metal oxides

$Na_xCoO_2$ has received significant attention in research due to its close resemblance to the commercially utilized $LiCoO_2$, its lithium counterpart. Na layers are sandwiched between cobalt oxide layers in the structure of $Na_xCoO_2$. A reversible capacity is produced due to the ability of the sodium ions to be introduced into and removed from the Na layers. $Na_xCoO_2$ is a potential cathode material for sodium-ion batteries despite its drawbacks because of abundant sodium availability, and relatively high capacity [40]. However, $P_2$-type oxides offer better cycling performance than $O_3$-type oxides due to their framework's open pathways with lower diffusion barriers, leading to more stabilized

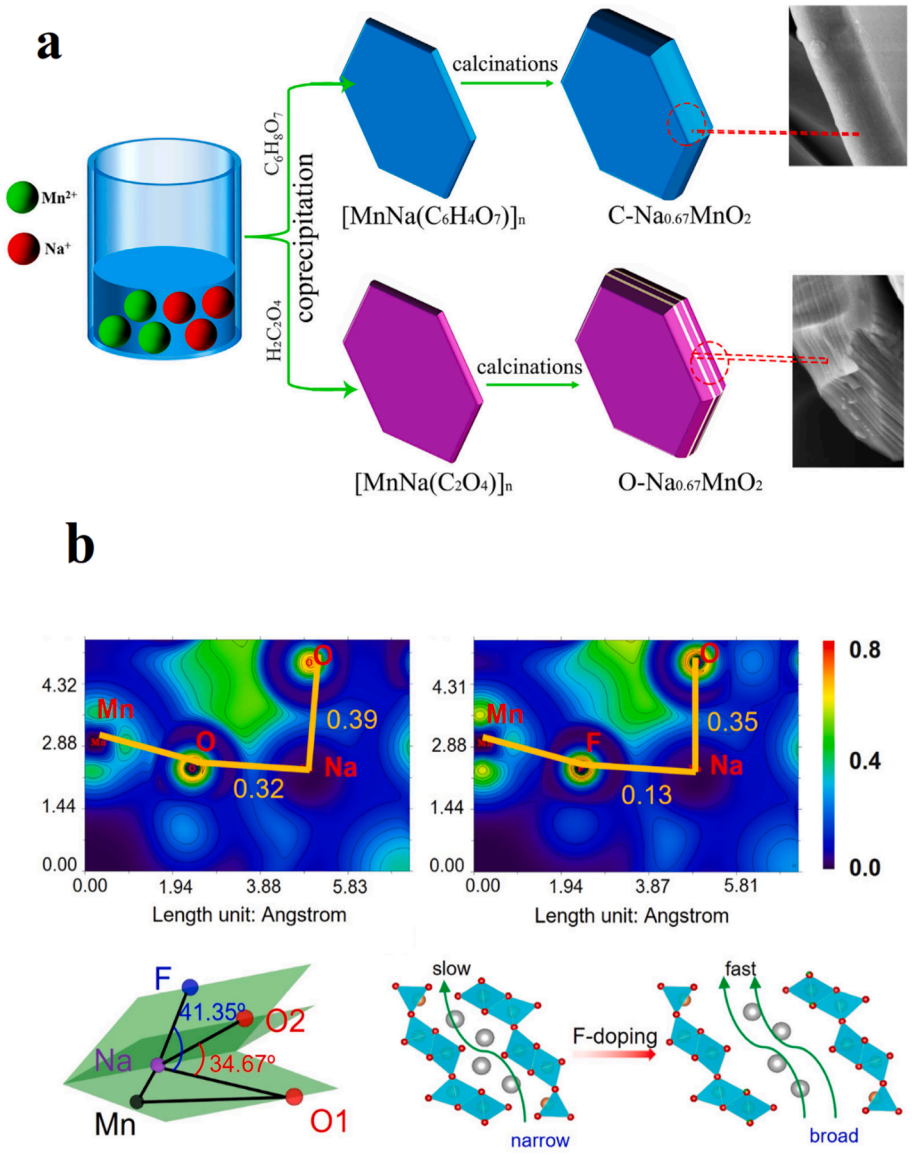


**Fig. 3.** (a) C-$Na_{0.67}MnO_2$ derived from the precursor of $Mn^{2+}$ six coordination sites and O-$Na_{0.67}MnO_2$ cathode prepared by the precursor of $Mn^{2+}$ four coordination sites [47]. Copyright © 2022 Elsevier. (b) The localized orbital locator analysis of $NaMnO_2$ and anion-cation co-doping in $NaMnO_2$ [48]. Copyright © 2023 Elsevier.

cycling. [41]. It has been confirmed that the preparation technique significantly impacts the characteristics of $Na_xCoO_2$ and that developing a practical and affordable approach is essential for maximizing the properties of $Na_xCoO_2$ [42]. Despite its advantages, $P_2$-$Na_xCoO_2$ still needs to be practical due to its limited specific capacity and cycle life. It can be attributed to the formation of $Na^+$/vacancy superstructures due to the electrostatic interaction between Na-Na and Na-Co during the charge–discharge process [43].

The $Na_xMnO_2$ system is another subclass of $Na_xMO_2$ that has been studied. Currently, layered bulk metal oxides like $NaMnO_2$, $NaMn_3O_5$, and $Na_2Mn_3O_7$ with stable $MnO_2$ having 1 T structure are extensively used in commercial SIBs [44]. $NaMnO_2$ demonstrated good cycling capabilities and a capacity (around 140 mAh $g^{-1}$), while $NaMn_3O_5$ demonstrated significant capacity (219 mAh $g^{-1}$) and capacity retention of 70 % after 20 cycles [45]. Also, $Na_2Mn_3O_7$ showed a reversible capacity of 160 mA h $g^{-1}$ [46]. Each cathode material exhibited distinctive electrochemical behavior, which may be linked to the structural alterations they undergo during charging and discharging. To manage and regulate the electrochemical performance of monoclinic layered bulk metal oxides, it is necessary to comprehend the motivation behind the structural changes that occur during de-sodiation. Compared to the O-$Na_{0.67}MnO_2$ cathode, the C- $Na_{0.67}MnO_2$ cathode has more stable sodium-ion diffusion channels and a lamellar structure (Fig. 3a). The potential for creating high-performance sodium-ion batteries is shown by an initial capacity of 106.8 mAh/g and capacity retention of 94.8 % after 150 cycles at 80 mA/g [47].

The low cost, non-toxic, eco-friendly, and abundant nature of Mn-based $P_2$-layered oxide cathodes have resulted in a highly competitive market. However, the $P_2$-type $NaMnO_2$ cathode faces several obstacles, including irreversible phase transitions due to $P_2$-$OP_4$ and $P_2$-$P_2$ structural transitions during cycling, the loss of active materials on the electrode from cracked particles reacting with electrolytes, and poor air stability. The effect of $Cu^{2+}$ and $F^-$ was studied into the standard tunnel material $Na_{0.44}MnO_2$ to address the abovementioned shortcomings [48]. It was found that replacing oxygen with fluorine near sodium decreases the electron density overlap between them due to fluorine's weak electrophilic nature. Although Na-O and Na-F bonds have similar lengths, Na-O bonds have higher bond orders than Na-F bonds. This difference allows fluorine to create larger spaces between nearby atoms, accommodating sodium better. Geometrically, this provides larger channels for sodium ion delivery than $NaMnO_2$ (Fig. 3b). Substituting $Cu^{2+}$ and $F^-$ together improves cell performance: $Cu^{2+}$ enhances cycling stability by reducing phase transitions, while F boosts sodium diffusion rates by providing larger spaces for sodium movement, thanks to Na-F's shorter bond order than Na-O [48].

$NaFeO_2$, or $O_3$-type $NaFeO_2$, is a cathode material with a layered rock-salt structure that allows for Na-ions' movement. According to Yabuuchi's group, $O_3$-type $NaFeO_2$ demonstrated a reversible capacity of 80 mAh $g^{-1}$ at 3.3 V attributed to the $Fe^{3+/}Fe^{4+}$ redox couple when the charging voltage was set to 3.4 V [49]. The findings of calculations using density functional theory on the phase stability of $NaFeO_2$ (Fig. 4) indicated that in oxidizing conditions, the α-phase remains stable over the competing β and γ phases throughout the high-oxygen chemical potential region and annealing as-milled α-$NaFeO_2$ at 700 ℃ can enhance electrochemical performance [50].

The carbon coating on the surface of $NaFeO_2$ delivered a high reversible specific capacity and increased its structural constancy, resulting in capacity retention after 100 cycles [51,52]. Because of its high working voltage and theoretical capacity, nickel-based $O_3$-type $NaNiO_2$ has drawn the most attention from these materials. Despite these benefits, $NaNiO_2$'s use in sodium-ion batteries is limited because of its low reversible capacity and poor cycle stability [53]. Several other layered oxides ($NaMO_2$, M = Ti, Cr, V, Mo, Re, W, etc.), as well as chalcogenides, were investigated for their ability to intercalate with sodium during the original development of electrode materials for sodium-ion batteries. $NaCrO_2$ holds promise as a cathode for Na-ion batteries but faces challenges like capacity fade and short cycle life due to phase transitions and chemical instabilities. Researchers used digital image correlation (DIC) to study the strain in the cathode during cycling [54]. They found significant irreversible deformations initially, decreasing over cycles. During charging and discharging, the electrode contracts at low states of charge and expands at higher ones. These changes correlate with phase transitions, indicating their role in deformations. Additionally, the formation of cathode-electrolyte interphase layers contributes to irreversible strains. Understanding these mechanisms is crucial for developing robust cathodes for Na-ion batteries.

### 2.1.2. *Binary metal oxides systems: $Na_xMM'O_2$*

Although $Na_xMO_2$ cathode materials made of a single metal have their benefits, they often encounter issues such as low capacity or rapid capacity decay caused by structural changes and phase transitions during the sodium extraction-insertion processes. Researchers have examined binary transition metal oxide layers that use synergistic interactions between various metals to address these problems. During the battery's charge and discharge cycles, Na ions are injected between the oxide layers of the compound $Na_xMM'O_2$, where M and M′ refer to two different transition metals. These cathode materials have been investigated for their potential use in lithium-ion and sodium-ion batteries, and they demonstrate desirable qualities like high operating voltage, high theoretical capacity, and relatively low cost compared to other cathode materials, making them a promising choice for battery technology. Among electrochemically active transition metals, the combination of Fe, Mn, and Ti has garnered attention for their

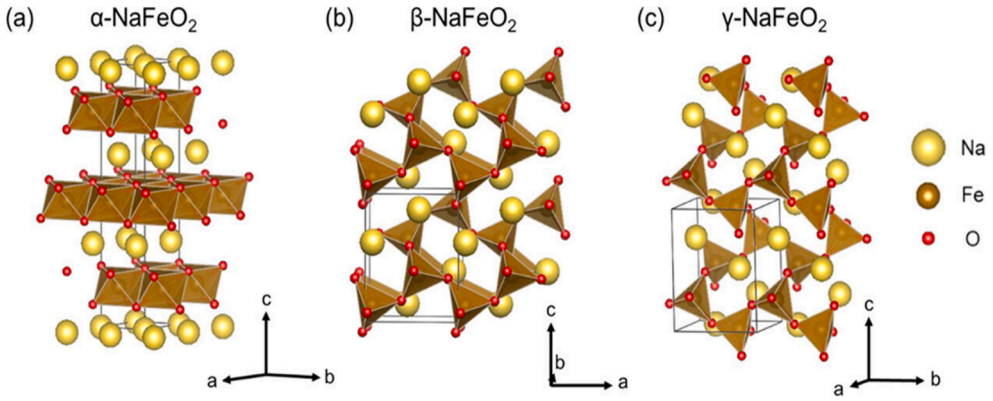


**Fig. 4.** Collinear antiferromagnetic orderings identified from magnetic ordering workflow for (a) α-$NaFeO_2$, (b) β-$NaFeO_2$, and (c) γ- [50]. Copyright © 2023 American Chemical Society.

electrochemical properties, such as obtaining the maximum reversible capacity, a reasonably flat voltage profile, and a higher working voltage. Furthermore, replacing non-electrochemically active materials in the oxide layer has also been shown to enhance cycle performance and capacity retention.

*2.1.2.1. Mn-based oxide.* Numerous research groups have examined Na $[Ni_xMn_{1-x}]O_2$ and categorized it as a typical material with an ordered structure. The electrochemical extraction and insertion of Na in $P_2$-$Na_{2/3}[Ni_{1/3}Mn_{2/3}]O_2$ was studied by in situ X-ray diffraction. Results showed that all Na can be extracted and reinserted, and for x values greater than 1/3, the structure is $P_2$. At x = 1/3, the structure becomes ($P_2 + O_3$), and for x values less than 1/3, the structure becomes ($P_2$ + minor $O_2$ + $Ni_{1/3}Mn_{2/3}O_2$) [55]. The electrochemical properties of $NaNi_{0.5}Mn_{0.5}O_2$ are investigated in a sodium cell at room temperature. The material showed good reversible capacity and retained 75 % of its capacity after 50 charge/discharge cycles. X-ray diffraction and absorption spectroscopy show that nickel ions are oxidized to the trivalent state, while manganese ions remain inactive in the tetravalent state [56]. $O_3$–$NaNi_{0.5}Mn_{0.5}O_2$ was Synthesized using a combination of spray pyrolysis and high-temperature solid-phase sintering to address the poor kinetics and irreversible phase transitions that result in degraded cyclic performance. This material showed good cyclic and rate performance, with a specific capacity of 98.4 mAh $g^{-1}$ at 1C between 2.0 and 4.0 V and a capacity retention of 89.1 % after 100 cycles [57]. Some studies have shown that P2- $Na[Ni_xMn_{1-x}]O_2$ exhibits high specific capacity and voltage but faces challenges, including phase transition and crack formation during high-voltage charging, prompting exploration of solutions like coating, topography optimization, and cation doping [58,59]. It was found that adding $K^+$ and $Cu^{2+}$ improves the stability of the layered structure and raises the threshold voltage [58,59].

The co-precipitation method followed by heat treatment at 950 ℃ produced a single phase of layered $Na_{2/3}Co_{2/3}Mn_{1/3}O_2$ with a $P_2$-type structure [60]. The $P_2$-$Na_{2/3}Co_{2/3}Mn_{1/3}O_2$ phase exhibited excellent reversibility for the intercalation of $Na^+$. The process of sodium intercalation and deintercalation takes place as a solid solution process, except for when x = 0.5, in which case a unique feature is observed on the cycling curves, possibly associated with the formation of an ordered $P_2$- $Na_{2/3}Co_{2/3}Mn_{1/3}O_2$ phase. Wang and colleagues examined the electrochemical properties of $P_2$-$Na_xMn_yCo_{1-y}O_2$, and it was found that Mn reduces the ordered state at x = 2/3 while it has little effect on the ordered state at x = 1/2 due to Coulombic interactions between Na-ions. Replacing Co with Mn increases specific capacity but reduces cycle stability. Charge-discharge cycles lead to the formation of a passivating layer on the electrode surface, which results in capacity loss and suggests the need to optimize the electrode composition to prevent its formation [61]. In another study, the synthesis of $P_2$-type $Na_xMnO_2$ and $Na_xCo_{0.1}Mn_{0.9}O_2$ with hexagonal flake and hollow sphere morphologies resulted in a phase transition in $Na_xMnO_2$ flakes and suppressed transformation in $Na_xCo_{0.1}Mn_{0.9}O_2$. This allowed for higher capacity retention in the doped $Na_xCo_{0.1}Mn_{0.9}O_2$ due to suppressed $Na^+$ ordering and enhanced $Na^+$ kinetics. The hollow sphere morphology resulted in superior cycling stability, and combining the two strategies resulted in the best battery performance in Co-doped $Na_xCo_{0.1}Mn_{0.9}O_2$ spheres [62].

The combination of Fe and Mn is a favorable electrode option as it demonstrates a high specific capacity and retains its capacity well, showing promise for its use. In 2012, Yabuuchi et al., based on experimental findings and the availability of chemical elements, attempted to synthesize $P_2$-type $Na_xFeO_2$ for application in sodium cells. However, their efforts were unsuccessful because it is difficult to stabilize $Fe^{4+}$ in the oxide-ion structure under normal conditions. Finally, they reported a new electrode material, $P_2$-$Na_{2/3}[Fe_{1/2}Mn_{1/2}]O_2$. This material provided a reversible capacity of 190 mAh $g^{-1}$ in sodium cells, where the $Fe^{3+}/Fe^{4+}$ redox is electrochemically active [63]. The researchers, Delmas and colleagues, examined four distinct phases of $Na_x(Mn, Fe)O_2$, which were $P_2$-$Na_{0.67}Mn_{2/3}Fe_{1/3}O_2$, $P_2$-$Na_{0.71}Mn_{1/2}Fe_{1/2}O_2$, $O_3$-$Na_{0.8}Mn_{1/2}Fe_{1/2}O_2$, and $O_3$-$Na_{0.82}Mn_{1/3}Fe_{2/3}O_2$. These phases exhibited discharge capacities ranging from 135 to 155 mAh $g^{-1}$ between 1.5 to 3.8 V. The $O_3$ phases exhibit discharge capacities (around 135–140 mAh $g^{-1}$) only slightly below one of the $P_2$ ones (145–150 mAh $g^{-1}$) because it takes more energy to remove $Na^+$ ions from the interlayer in the $O_3$ oxygen stacking [64]. In another study, focused on the $P_2$-$Na_{2/3}Fe_{0.4}Mn_{0.6}O_2$ phase and compared it to the more frequently studied $P_2$-$Na_{2/3}Fe_{1/2}Mn_{1/2}O_2$ and $P_2$-$Na_{2/3}Fe_{2/3}Mn_{1/3}O_2$ phases. The research highlighted the importance of the Mn:Fe ratio in determining the structural evolution and phase transitions and suggested that altering the composition could assist in optimizing the electrode and battery [65]. Currently, an in-situ solid-state reactions technique is used to produce Fe/Mn-based binary hexacyanoferrates/carbon composites. The resulting material exhibits improved rate performance and cycling stability, with 80.5 % capacity retention over 1000 cycles, as shown in Fig. 5b [66].

To investigate the impact of Mg doping on the structural stability and electrochemical performance of $P_2$-$Na_{2/3}MnO_2$, three compositions of $Na_{2/3}Mn_{1-y}Mg_yO_2$ (with y values of 0.0, 0.05, and 0.1) were compared. Adding Mg resulted in a stable P2 phase with minor electrochemical changes, increasing capacity retention and rate performance. The substitution of Mg for Mn in the cathode material of Na-ion batteries has led to improvements in the performance of $Na_{0.67}MnO_2$. Specifically, this modification has resulted in a more consistent charge/discharge pattern, reduced polarization, and increased capacity retention. As a result, the discharge capacity of $Na_{0.67}Mn_{0.95}Mg_{0.05}O_2$ was 175 mAh $g^{-1}$. Cycle stability could be improved by adding more Mg, but this would result in a decrease in discharge capacity [67]. A study conducted by Buchholz et al. showed that [68] a Mg content as low as 11 % in the $MO_2$ layer results in a smoother potential profile, high coulombic efficiencies of over 99.5 % at 12 mA $g^{-1}$, and stable long-term cycling behavior.

*2.1.2.2. Ti-based oxide.* Titanium-based binary layered oxides have been studied for their potential use as cathode materials in SIBs. $TiO_2$, in particular, has exhibited exceptional electrochemical performance when employed as a cathode material in SIBs. For example, a stable symmetric sodium-ion battery using bipolar active material $NaNi_{0.5}Ti_{0.5}O_2$ showed a reversible capacity of 121 mA h $g^{-1}$ at 0.2C with smooth charge–discharge curves. It exhibited excellent cycling stability and good rate capability [69]. The XRD patterns and Rietveld refinements showed the presence of a unique $O_3$ phase with a small amount of NiO impurities. As the quantity of titanium is raised, these impurities are anticipated to decrease. Nickel and titanium ions are randomly distributed inside the $TMO_2$ layers at the octahedral locations [69]. Zhao et al. have developed a stable symmetric sodium-ion battery using bipolar active material $Na_{0.8}Ni_{0.4}Ti_{0.6}O_2$, which has a high voltage of 2.8 V, a reversible discharge capacity of 85 mAh $g^{-1}$, 75 % capacity retention after 150 cycles, and good rate capability [70]. In another study, the crystal structure, electrical properties, and diffusion barriers of $NaNi_{1-x}Ti_xO_2$ phases (where x = 0, 0.037, 0.056, 0.083, and 0.167) were investigated using first-principles computational methods [71]. Ti doping increased the average intercalation voltage, improving the electrode material's energy density and electrical conductivity. $NaNi_{0.917}$-$Ti_{0.083}O_2$ exhibited the best performance, with a 4 % reduction in unit cell volume change during desodiation. The Na diffusion kinetics of $NaNi_{0.917}$-$Ti_{0.083}O_2$ were also studied, revealing higher ion mobility.

Li and coworkers examined the effects of Ti doping on the composition and electrochemical efficiency of $Na_{1-x}Cr_{1-x}Ti_xO_2$ cathodes. The cathodes with varying x values (x = 0, 0.03, 0.05, and [72] conducted at 900C. X-ray diffraction analysis showed that Ti doping resulted in an increased $NaO_2$ interlayer gap and delayed the phase transition during the Na ion de-intercalation process. The electrochemical performance of the cathodes was evaluated based on charge/discharge profiles and

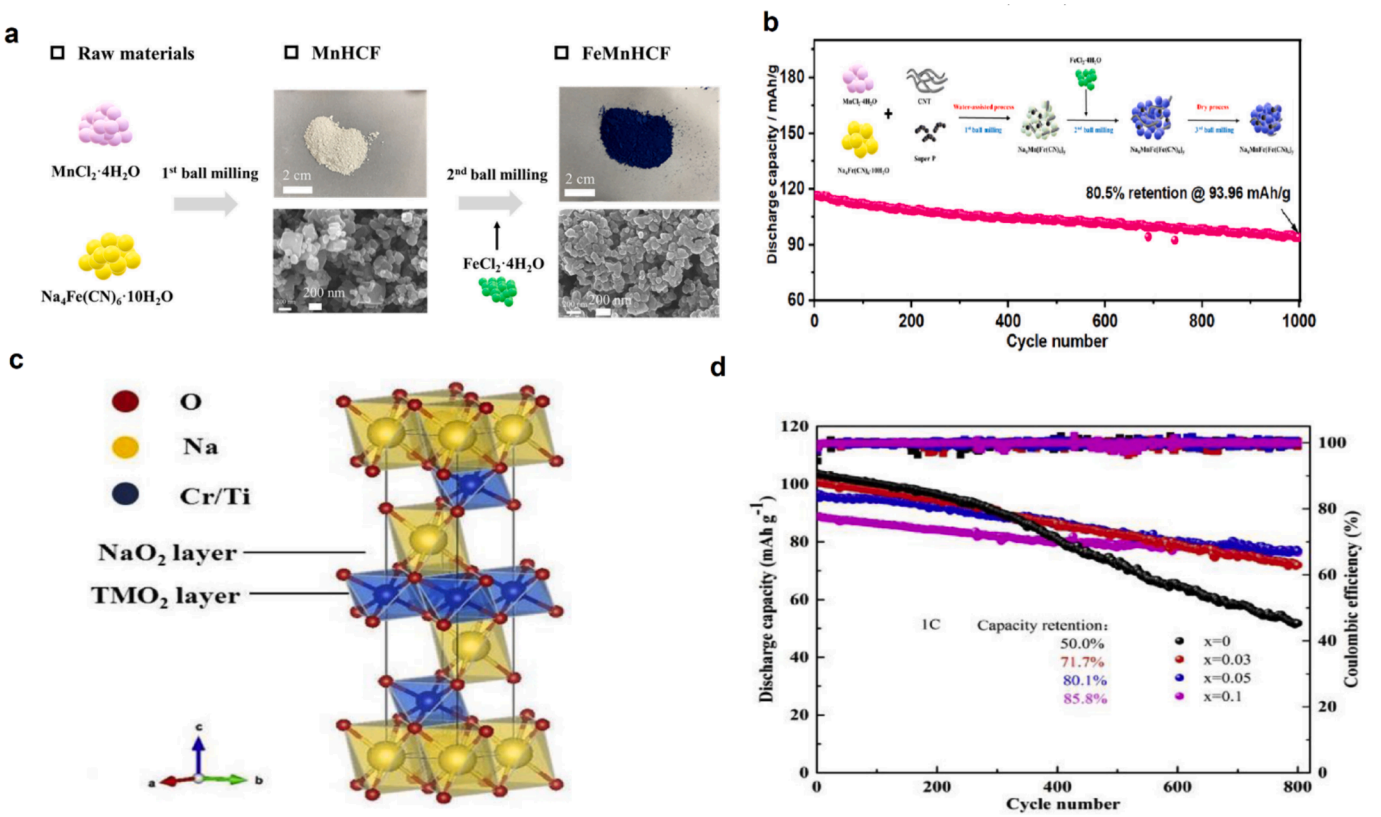


**Fig. 5.** (a) Schematic synthesis and (b) electrochemical performances of Fe-Mn based cathodes [66]. Copyright © 2023 Elsevier. (c) Schematic illustrations of $O_3$ layer-type $Na_{1-x}Cr_{1-x}Ti_xO_2$ cathodes crystal structure and (d) Cycle performance of $Na_{1-x}Cr_{1-x}Ti_xO_2$ at 1C [72]. Copyright © 2018 Elsevier.

capacity retention after cycles. The $Na_{0.95}Cr_{0.95}Ti_{0.05}O_2$ cathode exhibited the highest electrochemical performance, with an initial capacity of 104 mAh $g^{-1}$ at 0.1C, 96.7 mAh $g^{-1}$ at 1C, and 80.1 % capacity retention after 800 cycles. These findings suggest that Ti doping could be a promising approach for enhancing the electrochemical performance of $Na_{1-x}Cr_{1-x}Ti_xO_2$ cathodes and may have implications for developing more advanced sodium-ion batteries (Fig. 5 c and 5d).

A solid-state method was used to synthesize $P_2$-$Na_{2/3}Co_{1/2}Ti_{1/2}O_2$, a cathode material for sodium-ion batteries [73]. This material was compared to the $Na_xCoO_2$ and $Na_xTiO_2$ end-phases, and it was discovered that the presence of Co and Ti transition metal ions enhanced the performance of the electrode. The material demonstrated advantageous electrochemical activity when cycled between 2.0 and 4.2 V. In comparison to $Na_{2/3}CoO_2$, the cathode material $Na_{2/3}Co_{1/2}Ti_{1/2}O_2$ displayed improved stability with a capacity retention rate of 98 % and a discharge capacity of 100 mAh $g^{-1}$ [73].

$NaTiO_2$-$NaMnO_2$ cathodes, in contrast to certain other cathode materials, do not include any poisonous or risky substances, making them a safer alternative for use in batteries. However, the behavior of a novel material with a tunnel structure, $Na_{0.61}Ti_{0.48}Mn_{0.52}O_2$, was thoroughly examined in terms of sodium extraction and insertion. The material was discovered to have a discharge capacity of 86 mA h $g^{-1}$, which is made possible by the tunnel structure. Additionally, it can discharge at a high rate of 5C and has a capacity of 31 mA h $g^{-1}$ with good capacity retention of 81 % after 100 cycles [74]. Wang et al. [75] investigated Ti-substituted $Na_{0.44}MnO_2$, which has a tunnel structure, and found that it has excellent cyclability without requiring additional oxygen removal from the solution. Atomic-scale analysis and ab initio computations provided precise details on the Ti substitution sites and sodium storage mechanism. Ti substitution improved the material's charge ordering and reaction pathway, leading to smoother discharge/charge profiles and lower storage voltage. DFT calculations discussed the use of spectroscopy techniques to study electrochemically-prepared and chemically-prepared samples of sodium manganese oxide and sodium titanium-substituted manganese oxide. The results show that the manganese ions on the sample surface were reduced after Na insertion. The reduced manganese oxidation state observed in spectroscopy is due to surface catalytic reactions, which are enhanced by the large surface area of the nanoparticles. In particular, the $Mn^{2+}$ concentration in $Na_{0.66}[Mn_{0.44}Ti_{0.56}]O_2$ reached as high as 60 %, supported by DFT calculations [75].

*2.1.2.3. Fe-based oxide.* Two of the most studied cathodes for SIBs are $NaCoO_2$ and $NaFeO_2$, but they both have issues. To address this, the combination of Fe with Co or Ni can be an interesting mix due to the desirable high flat voltage nature of $NaFeO_2$, which makes it a preferred material for battery cathodes. The $O_3$-phase $NaFe_{0.5}Co_{0.5}O_2$ demonstrated a reversible capacity of 160 mA h $g^{-1}$ between 4.0 and 2.5 V when exposed to a current density of 12 mA $g^{-1}$. This material has a higher average voltage and smoother charge–discharge behavior at lower voltages than $NaFeO_2$ and $NaCoO_2$. Also, $NaFe_{0.5}Co_{0.5}O_2$ exhibited exceptional rate capability with minimal polarization, maintaining over 75 % of its discharge capacity even when discharged at a rate of 10C [76]. In addition, researchers conducted a combined computational and experimental study on $NaFe_{0.5}Co_{0.5}O_2$ as a potential cathode material [77]. According to the survey, $NaFe_{0.5}Co_{0.5}O_2$ found superior electrical characteristics and exhibits excellent cycling stability after 4000 cycles with a decent initial specific capacity retention.

The electrochemical characteristics are improved when Ni partially replace Fe in $O_3$-$NaFeO_2$. Hence, the solid-state reaction was used to successfully synthesize solid solution compounds in $O_3$-$NaFe_{1-y}Ni_yO_2$ ($0.5 \leq y \leq 0.7$) [78]. These compounds exhibit significantly higher capacity and improved cycle stability compared to $O_3$-$NaFeO_2$. The increased cycle stability results from the $Ni^{4+/3+}$ redox couple's

substantial contribution to the total capacity, which inhibits the synthesis of unstable Jahn-Teller $Fe^{4+}$.

Since cathode materials suffered from quick capacity deterioration resulting in inferior cyclic functioning, which is caused by the secondary reactions that mostly happen at the interface between the cathode and the electrolyte, Chung and coworkers developed an artificial cathode-electrolyte interphase layer on $O_3$-$NaFe_{0.5}Ni_{0.5}O_2$ through a simple electrochemical pre-discharge step, which effectively minimized electrolyte decomposition and prevented transition metal dissolution, improving the interfacial stability of the cathode [79]. The cyclability of pre-sodiated $O_3$-$NaFe_{0.5}Ni_{0.5}O_2$ was improved to 86 % after 50 cycles compared to the pristine $O_3$-$NaFe_{0.5}Ni_{0.5}O_2$ (66 %), demonstrating that pre-sedation is a promising and straightforward approach to enhance the stability and capacity retention of cathode materials for SIBs.

### 2.1.3. Multi-metal oxides

Numerous investigations have been conducted on ternary and multi-metal oxide cathodes for sodium-ion batteries. These materials offer advantages such as elevated specific capacities, excellent cycle life, and remarkable rate capability. Nevertheless, multi-metal oxide cathodes have the potential to serve as cathode materials for sodium-ion batteries. However, further research is needed to refine their electrochemical properties and enhance their performance in practical battery systems.

$P_2$-$Na_{0.67}Mn_{0.65}Ni_{0.1}Co_{0.15}O_2$, synthesized as a new cathode material by a sol–gel method for sodium-ion batteries [80]. The material demonstrated high-rate capability and long-term cycling performance with a wide voltage range of 1.5–4.2 V for charging and discharging. Even at high current densities, it showed a reversible capacity that is noticeably higher than earlier described materials. Even after 100 cycles, the material still retains its capacity quite well. The discharge diffusion coefficient is somewhat higher than the charge diffusion coefficient, and the Na-ion diffusion coefficient is around 10–14 $cm^2\ s^{-1}$. According to the researchers, $Mn^{4+}$ activation at low voltages plays a part in the material's increased capacity. Recently, co-precipitation was used to create samples $P_2$-$Na_{0.7}Co_{0.5}Mn_{0.33}Ni_{0.16}O_2$, $P_2$-$Na_{0.7}Co_{0.4}Mn_{0.43}Ni_{0.16}O_2$, $P_2$-$Na_{0.7}Co_{0.3}Mn_{0.53}Ni_{0.16}O_2$, $P_2/P_3$-$Na_{0.7}Co_{0.4}Mn_{0.33}Ni_{0.26}O_2$ and $P_2/P_3$-$Na_{0.7}Co_{0.3}Mn_{0.33}Ni_{0.36}O_2$ [81]. The findings demonstrated that increasing manganese content did not affect the $P_2$-type structure, while increasing nickel content led to the co-existence of $P_2$ and $P_3$ phases. According to electrochemical measurements, the increase in manganese concentration resulted in lower discharge capacities but better capacity retention after 100 cycles. As a result of their increased charge transfer resistance, nickel-rich electrodes with a high $P_3/P_2$ content ratio displayed better discharge capacities but worse cycle performance.

Because of its inherent structural instability and the highly reactive nature of $Ni^{4+}$ ions, the ternary $O_3$-type $Na[Ni_xCo_yMn_z]O_2$cathode still has limits in terms of capacity and cycling. Li et al. developed a quaternary $O_3$-type layered compound, $Na[Mn_{0.25}Fe_{0.25}Co_{0.25}Ni_{0.25}]O_2$, to address both problems simultaneously. This compound has a high initial capacity of 180 mAh $g^{-1}$ and runs at an average working potential of 3.21 V [82]. In addition, more research on $Na[Ni_{0.32}Fe_{0.13}Co_{0.15}Mn_{0.40}]O_2$ indicated that the addition of Fe to the CoNiMn composition increased the discharge capacity and caused rapid capacity loss due to Fe-ion migration during cycling. This material [83] combined the advantages of $Fe^{3+/4+}$ redox couples and minimized detrimental Fe-ion migration, resulting in high discharge capacities of 182 mAh $g^{-1}$ at 0.2C-rate and 137.4 mAh $g^{-1}$ at 5C-rate. Moreover, the cathode displayed good cycling stability at various temperatures.

Copper can stabilize the structure and maintain the rechargeable capacity due to its similarity in ionic radius and valence states to Nickel. The electrochemical activity of $Cu^{2+}/Cu^{3+}$ redox during the charge/discharge cycles is favorable and able to provide a high potential, making copper-substituted cathodes better than electrochemically inert substitutes. The researchers added copper to the cathode material to improve its ability to store sodium ions and to prevent phase transitions and degradation at high potentials (Fig. 6). The $P_2$-type $Na_{0.67}Ni_{0.1}Cu_{0.2}Mn_{0.7}O_2$ cathode exhibited improved performance, with higher reversible capacity and better capacity retention, attributed to the presence of Cu contributing to its rechargeable capacity [84].

Kouthaman et al. have provided the results of their Rietveld refinement for several cathode materials, including $O_3$-$Na_{0.9}Mn_{0.60}Ni_{0.30}Cu_{0.05}Ti_{0.05}O_2$ (MNCT), $O_3$– $Na_{0.9}Mn_{0.60}Ni_{0.30}Mg_{0.05}Ti_{0.05}O_2$ (MNTM), $O_3$– $Na_{0.9}Mn_{0.60}Ni_{0.30}Cu_{0.05}Mg_{0.05}O_2$ (MNMC), and bare $O_3$–$Na_{0.9}Mn_{0.60}Ni_{0.40}O_2$ (MN) as shown in Fig. 7a and 7b [85]. The capacity retention of $O_3$-$Na_{0.9}Mn_{0.60}Ni_{0.30}Cu_{0.05}Ti_{0.05}O_2$ at 0.1C rate was 92 % after 100th cycle, which indicates worthy electrochemical performance than $Na_{0.9}Mn_{0.60}Ni_{0.30}Mg_{0.05}Ti_{0.05}O_2$ (90 %), $Na_{0.9}Mn_{0.60}Ni_{0.30}Cu_{0.05}Mg_{0.05}O_2$ (89 %) and bare $Na_{0.9}Mn_{0.60}Ni_{0.40}O_2$ (59 %). It suggests that the co-substitution led to an increase in the interlayer distance between the $TMO_2$ layers and an improvement in the bond strength between O and TM, resulting in improved performance of the layered $O_3$-$Na_{0.9}Mn_{0.60}Ni_{0.30}Cu_{0.05}Ti_{0.05}O_2$ cathode material compared to the others. Therefore, this material could be a suitable option for SIBs.

Titanium can be added to materials to reduce irreversible phase transitions, improve structural stability, and increase discharge capacity. In a study by Zhou et al., it was observed that doping the $Na_{0.67}Co_{0.67}Mn_{0.33}O_2$ sample with Ti had beneficial effects [86]. The cathode material $Na_{0.67}Co_{0.67}Mn_{0.23}Ti_{0.1}O_2$ had a discharge capacity of 91.2 mAh $g^{-1}$ at 1C, and additionally, it showed a high-capacity retention of 81.02 % after 1000 charge/discharge cycles at 20C. It was reported [87] that managing the $P_2$-$O_2$ transition at higher voltages is essential, which can be achieved through optimized cut-off voltages. The electrodes made of $Na_{0.67}Ni_{0.25}Ti_{0.08}Mn_{0.67}O_2$ material experience a reduction of only 12 % in their initial capacity after 50 cycles when cycled up to a maximum voltage of 4.3. Deng et al. [88] $P_2$-$Na_{0.59}Co_{0.1}0Mn_{0.85}(Ti_2V)_{0.05}O_2$ oxide by Ti, V co-doping technique using the solid-phase method (Fig. 7c-e). The successful introduction of Ti and V into the Mn sites significantly improved cycle stability and better kinetic characteristics in the Ti and V co-doped material. Also, $NaNi_{1/2}Mn_{1/4}Ti_{1/4}O_2$ as a novel cathode material was used for sodium-ion batteries and showed impressive electrochemical performance, including high-capacity retention and stability, attributed to its distinct composition [89]. A remarkable $O_3$-type layered $NaNi_{0.45}Mn_{0.3}Ti_{0.2}Zr_{0.05}O_2$ exhibited an initial reversible capacity of 141.4 mAh $g^{-1}$ with a coulombic efficiency of 98.8 % and remarkable capacity retention of 70 % after 200 cycles at 0.05C as cathode material for sodium-ion batteries [90].

### 2.1.4. High-entropy metal oxides

The high-entropy (HE) structure has garnered significant scientific interest in recent years due to its inclusion of multiple components (five or more elements), high configurational entropy, pronounced chemical disorder, and substantial lattice distortion [91–93]. These materials offer the potential to transform energy storage, improving battery performance and safety. Thus, they could promote renewable energy adoption and technological advancements while overcoming the limitations of conventional low-entropy materials [94]. It was shown that it is possible to integrate five different metals into a single lattice site within a unified oxide phase. The term "entropy-stabilized oxide" was coined to describe this phenomenon, as it became clear that entropy played a crucial role in stabilizing the structure [95]. For example, Zhao et al. prepared a high-entropy cathode containing nine metals within $TMO_6$ slabs. It exhibited outstanding capacity retention, with 83 % after 500 cycles [96]. It was demonstrated that incorporating a high-entropy component reduced Jahn-Teller distortion and Na/vacancy ordering. However, there is still a limited understanding of structural evolution, air stability, and mechanical behaviors [97].

### 2.1.5. Synthesis methods for transition metal oxide cathode materials

Hydrothermal methods and coprecipitation are widely employed for the synthesis of transition metal oxide cathode materials, each offering

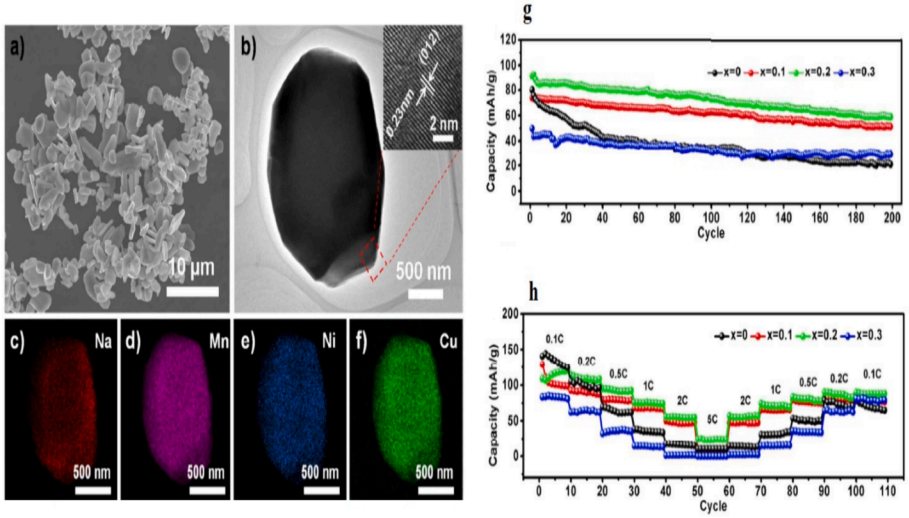


**Fig. 6.** A) the sem, b) tem, c-f) EDS elemental maps of the $P_2$-type $Na_{0.67}Ni_{0.3-x}Cu_xMn_{0.7}O_2$. g) The cycling performance of the as-prepared $Na_{0.67}Ni_{0.3-x}Cu_xMn_{0.7}O_2$ (x = 0, 0.1,0.2 and 0.3) electrodes at 1C; h) The rate capabilities of $Na_{0.67}Ni_{0.3-x}Cu_xMn_{0.7}O_2$ (x = 0, 0.1, 0.2 and 0.3) electrodes between 0.1C and 5C [84]. Copyright 2012, Royal Society of Chemistry.

distinct advantages in producing various nanostructures and compositions.

In hydrothermal synthesis, $O_3$-$NaFeO_2$ nanoflakes are produced by adding nanosized $Fe_2O_3$ and NaOH to ethanol and strongly stirred for 2 h. The mixed solution heated at 200 ℃ for 36 h to obtain the product [52]. For $Mn_3O_5$, a mixed solution of NaOH and $H_2O_2$ was added to Mn $(NO_3)_2$, stirred, and transferred to an autoclave at 150 ℃ for 16 h, yielding $NaMn_3O_5{\cdot}nH_2O$. To remove lattice water effects, a portion was thermally treated at 200 ℃ for 2 h [45]. $VO_2$ nanomaterial is synthesized using $V_2O_5$ and $H_2C_2O_4$ in a Teflon-lined autoclave at 180 ℃, where graphene addition results in graphene nanodots on the $VO_2$ surface [98].

Coprecipitation methods offer scalability and control over particle size and distribution. For instance, $Na_{0.66}Co_{0.66}Mn_{0.44}O_2$ was prepared via a co-precipitation method. A solution containing transition metal nitrates (2/3 $Co(NO_3)_2{\cdot}6H_2O$ and 1/3 $Mn(NO_3)_2{\cdot}4H_2O$) was gradually added to a solution of NaOH (1 M)–$NH_4OH$ (3 M) with a 5 % excess of sodium. The resulting powder was dried at 110 ℃ and heat treatment at 950 ℃ for 12 h under $O_2$ was conducted, followed by sample quenching [60]. Ni-rich O3-type $Na[Ni_{0.60}Fe_{0.25}Mn_{0.15}]O_2$ cathode is synthesized via hydroxide coprecipitation and high-temperature calcination. By reducing the charge voltage, the electrode exhibited excellent performance, including high reversible capacity and superior capacity retention over cycles [99]. A high entropy $Na_{0.75}Co_{0.125}Cu_{0.125}Fe_{0.125}Ni_{0.125}Mn_{0.5}O_2$ was synthesized through co-precipitation using salt solutions of salt sulphates at 50 ℃ and 800 rpm stirring. A NaOH base solution was used to precipitate the salt sulfates into a mixed transition-metal hydroxide ($Co_{0.125}Cu_{0.125}Fe_{0.125}$-$Ni_{0.125}Mn_{0.5}$ $(OH)_2$). After filtration and drying, nanosized $Na_2CO_3$ was mixed with the precursor, then calcined at 850 ℃ for 10 h to obtain the final electroactive material [100].

Solid-state reactions at high temperatures (around 900 ℃) using sodium carbonate and metal oxide powders are the common method for synthesizing layered sodium-inserted metal oxide cathodes. Layered sodium-inserted metal oxide cathodes, such as P2-$Na_{2/3}(Mn_{1/2}Fe_{1/4}Co_{1/4})O_2$ and $Na_{0.44}MnO_2$, are synthesized via high-temperature solid-state reactions using sodium carbonate and metal oxide powders [101,102].

### 2.2. Polyanion cathodes

Polyanion-type electrode materials are a specific type of compound that have an open structure composed of tetrahedral anionic units $(XO_4)^{n-}$ or their derivatives $(X_mO_{3m+1})^{n-}$ (X = S, P, Si, As, Mo, or W) connected to transition metals. This allows for quick ion movement and maintains the stability of transition metals' redox potentials, even when sodium ions are added or removed.

Compared to other compounds, polyanion-type electrode materials have stronger covalent bonding between X and O. This creates ionicity in the bonding between M and O, resulting in weaker M−O bonding and a wider gap between its antibonding orbitals. As a result, the redox potential is increased, referred to as the "inductive effect" in polyanion-type electrode materials. The strong X-O covalent bonds found in polyanion-type electrode materials also improve oxygen stability within the structure, making them safer for use in rechargeable batteries. As a result of this advantage, they are a preferred choice for battery applications.

#### 2.2.1. Phosphate polyanions

Phosphate framework-based materials are a promising choice for Na storage electrodes due to their versatile structure and exceptional electrochemical performance. The stable P-O bond in phosphate frameworks provides high structural stability, ensuring long-term cycling and increased safety content while reducing the risk of oxygen release. Additionally, phosphate or other substituent groups induce higher redox potential values on the redox couple.

Phosphate-based polyanionic frameworks can be formed through various methods, including edge/corner sharing coordination, the formation of metaphosphates and pyrophosphates, and the combination of mixed polyanions. Olivine-type $NaMPO_4$ is not thermodynamically stable and instead crystallizes in the maricite phase. Pyrophosphate-structured compounds like $Na_2MP_2O_7$ and NASICON-structured $Na_xM_2(PO_4)_3$ are some of the most studied compounds in SIBs [103–105].

*2.2.1.1. Orthophosphates.* $NaMPO_4$ (where M stands for a transition metal) is a chemical formula that describes the class of polyanionic substances. $NaFePO_4$ illustrates this substance and was one of the first polyanionic substances to be researched. For example, $NaFePO_4$ electrode obtained by electrochemical Li-Na exchange of $LiFePO_4$ olivine displayed impressive cyclability and a reasonable rate capability [106]. Based on theoretical calculations and confirmed by neutron diffraction maximum entropy methods, it has been predicted that $Li^+$ migration pathways in $LiFePO_4$ follow a zigzag path along the [0 1 0] direction (path B of Fig. 8). This zigzag path has also been found to be followed by $Na^+$ migration in olivine-type $NaFePO_4$. The migration barrier for $Na^+$ is

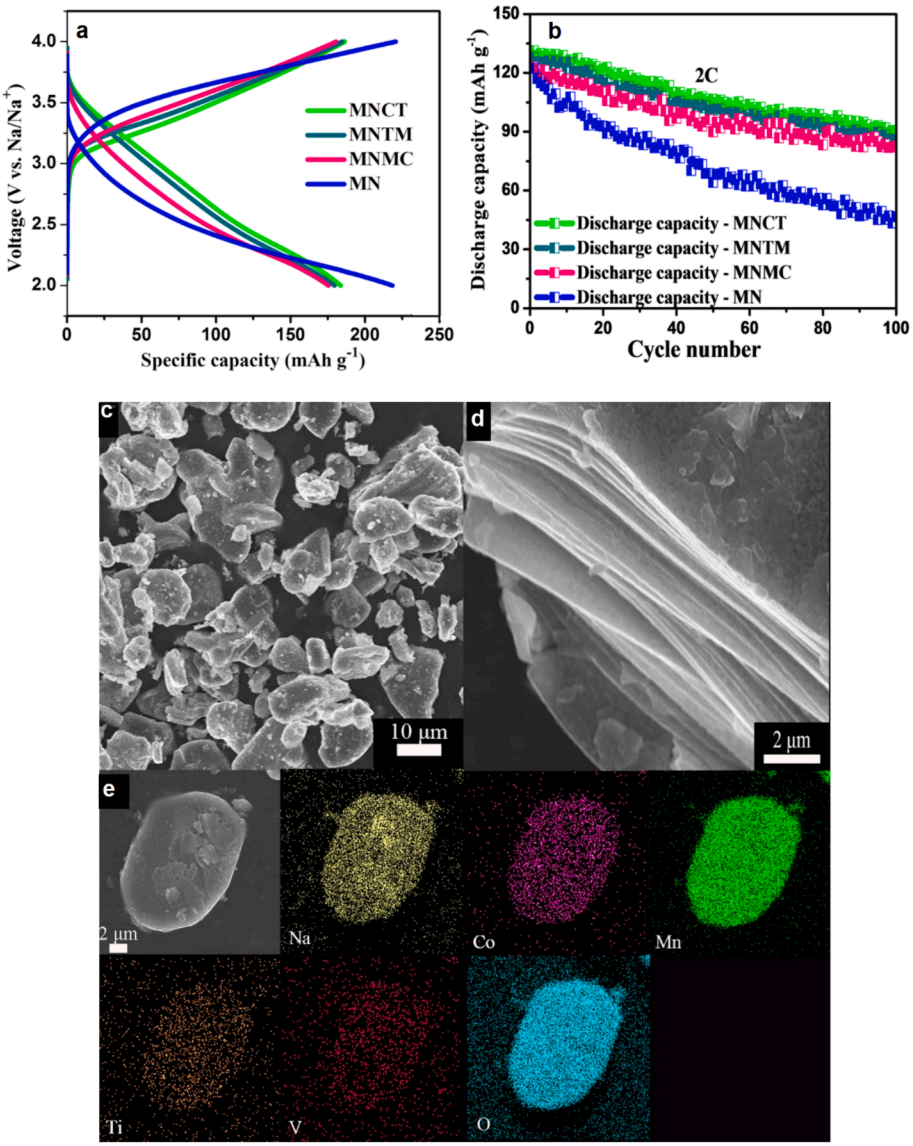


**Fig. 7.** (a) Initial discharge and charge profile, and (b) cycling performance at 2C of the MNCT, MNTM, MNMC, and MN [85]. Copyright © 2022 Elsevier. (c-d) FESEM images and (e) EDS elementary mapping images of $Na_{0.59}Co_{0.1}0Mn_{0.85}(Ti_2V)_{0.05}O_2$ [88]. Copyright © 2024 Elsevier.

lower compared to the Li analogue, with a value of 0.31 eV compared to 0.55 eV for $Li^+$ [107].

Maricite $NaFePO_4$ [108] showed impressive durability with only a slight reduction in capacity after 200 cycles (retaining 95 % of its initial capacity). During the first cycle, it achieved a capacity of 142 mAh $g^{-1}$, 92 % of its theoretical capacity. $FePO_4$ still faces challenges like low operating voltage and insufficient cycling performance at high rates. To overcome these limitations, the synthesis of Ni-doped, Mn-doped, and Ni, Mn co-doped $FePO_4$@C is proposed, offering a non-toxic, cost-effective solution with promising potential for various applications [109].

*2.2.1.2. NASICON.* A remarkable group of electrode materials known as sodium superionic conductors (NASICON) have outstanding ionic conductivity and strong structural stability. The standard formula for them is $Na_xM_2(XO_4)_3$, where x can have a value between 1 and 4, and M can be any of the elements V, Fe, Ni, Mn, Ti, Cr, Zr and X can be any of the components P, S, Si, Se, Mo. In 1975 [110], Goodenough et al. proposed the NASICON structure, $Na_{1+x}Zr_2P_{3x}Si_xO_{12}$. For example, in a single-step solid-state process, carbon layer was uniformly coated onto $Na_3V_2(PO_4)_3$ to test as a cathode material in SIB [111]. It displayed a favorable initial charge capacity of 98.6 mAh $g^{-1}$ and a discharge capacity of 93 mAh $g^{-1}$. The electrode also demonstrated good cycle performance, maintaining 99 % of its capacity after 10 cycles, moderate rate performance. Li et al. [112] prepared $Na_3V_2(PO_4)_3$/C using glucose-assisted carbon-thermal reduction. The resulting material displayed a 3.4 V voltage plateau when tested against Na, with a capacity of around 98 mAh $g^{-1}$. Zhu et al. showed that carbon, especially N-doped carbon modification, is the most effective method and strategy to improve the conductivity of $Na_3V_2(PO_4)_3$ [113]. The research demonstrated that the electrophoretically deposited technique could efficiently synthesize firmly adhered and porous $Na_3V_2(PO_4)_3$ carbonaceous material (Fig. 8b). Incorporation rGO or CNT further enhances performance, resulting in excellent rate performance and significant capacitive contributions [114].

Also, various ions have been utilized to partially substitute V in NVP, resulting in high-performance NVP-based solid solutions, such as Mn, Sn, and Ga. For example, using the sol–gel method [115], researchers synthesized a new compound $Na_2VSn(PO_4)_3$. This material was tested as a cathode in a Na half-cell, the discharge curve showed a plateau at approximately 3.4 V, and the capacity retention after 100 cycles at 0.5C was over 90 %. The crystal structure (Fig. 8c) of a single unit cell of

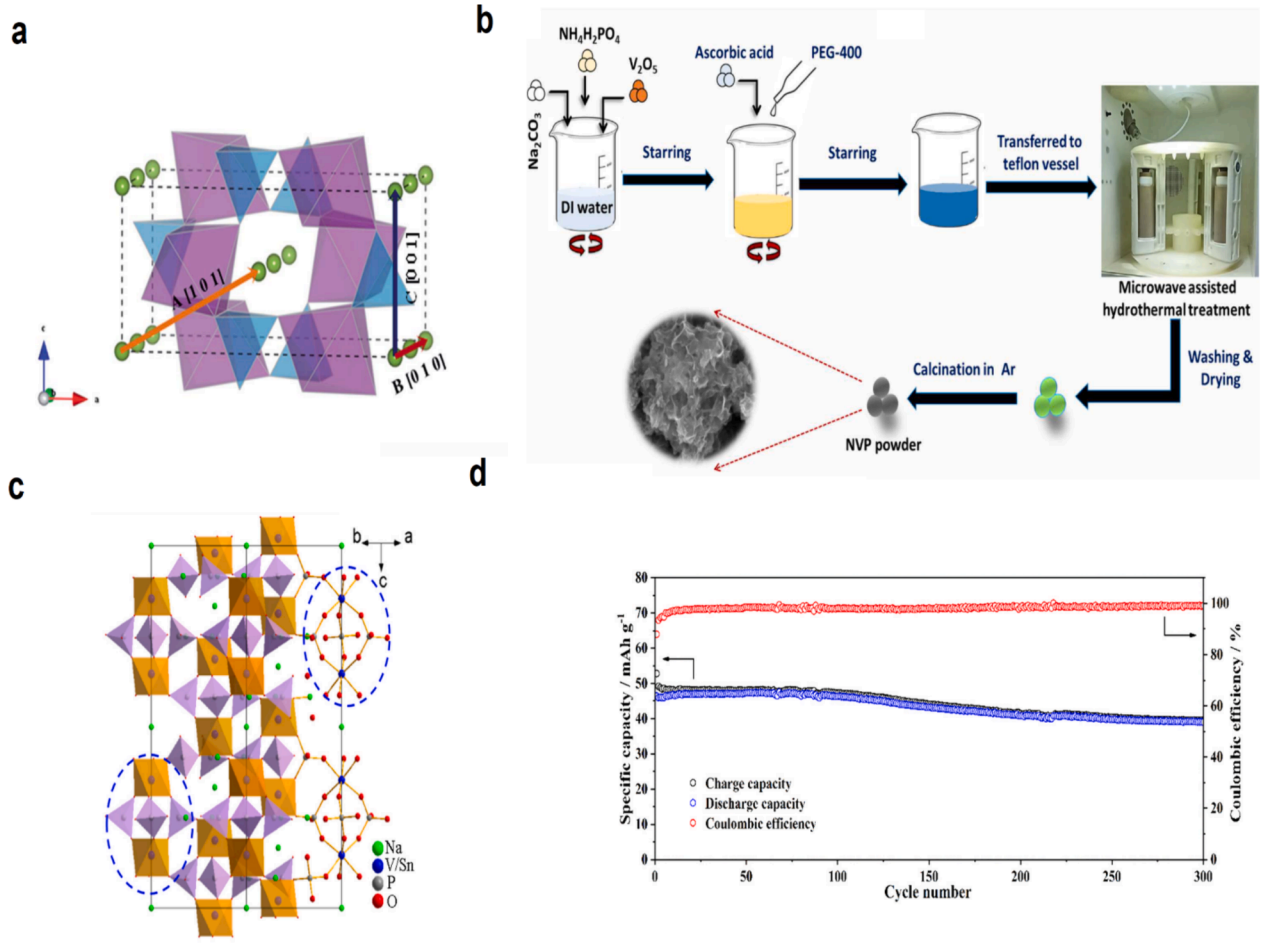


**Fig. 8.** (a) Schematic representation of the migration routes in olivine-type $AFePO_4$, where A can be either $Li^+$ or $Na^+$. Blue: $PO_4$ tetrahedra; purple: $FeO_6$ octahedra; green: Li/Na [107]. Copyright 2012, Royal Society of Chemistry. (b) Schematic representation of synthesis of $Na_3V_2(PO_4)_3$ [114]. Copyright © 2023, Elsevier. (c) Crystal structure of one unit cell $Na_2VSn(PO_4)_3$ [115]. Copyright © 2023, Elsevier. (d) Long cycling performance of $Na_{3.4}Mn_{1.2}Ti_{0.8}(PO_4)_3$ at 10C [119]. Copyright © 2022, Elsevier. (For interpretation of the references to colour in this figure legend, the reader is referred to the web version of this article.)

$Na_2VSn(PO_4)_3$, revealing a strong three-dimensional framework consisting of $V/SnO_6$ octahedra and $PO_4$ tetrahedra that are linked together via corner-sharing. Na ions occupy the cavities in this structure. The image clearly shows "lantern" units, the distinctive features of NASICONs.

Ga is added to $Na_3V_2(PO_4)_3$ to activate the $V^{4+}/V^{5+}$ redox couple, enhancing energy density. The resulting $Na_3V_{1.25}Ga_{0.75}(PO_4)_3$ cathodes exhibit excellent electrochemical performance and stability, offering a promising strategy for improving NASICON-structured polyanionic phosphates [116]. At the same, a NASICON-type $Na_4MnV(PO_4)_3/C$ compound is used as a high-performance cathode material for SIBs [117].

Alongside $Na_3V_2(PO_4)_3$, $NaTi_2(PO_4)_3$ can also serve as a cathode material in SIBs. However, despite its promising theoretical capacity, safety, and stability in seawater, $NaTi_2(PO_4)_3$-based materials suffer from challenges such as structural collapse over extended cycles, inadequate electronic conductivity, and slow ionic diffusion kinetics, which impede their electrochemical performance [118]. Wu and colleagues reported using a variety of cathodes with NASICON structure based on manganese as $Na_{1+2x}Mn_xTi_{2-x}(PO_4)_3$ (x = 1, 1.2, 1.4, denoted as NMTP, $NM_{1.2}T_{0.8}P$ and $NM_{1.4}T_{0.6}P$) for application in aqueous SIBs [119]. Among the samples, $Na_{3.4}Mn_{1.2}Ti_{0.8}(PO_4)_3$ exhibited the most favorable electrochemical performance with a discharge capacity of 39.1 mAh $g^{-1}$ after 300 cycles at 10C and a capacity retention ratio of 84.3 % as shown in Fig. 8d.

*2.2.1.3. Pyrophosphates.* Pyrophosphates are a different group of polyanionic phosphate compounds with a general $Na_xMy(P_2O_7)_z$ formula, where M is a transition metal and x, y, and z are integers. At high temperatures, pyrophosphates are more energetically stable than orthophosphates. These materials can be used as pigments, catalysts, and electrical devices [120]. For instance, the modification of $Na_2MnP_2O_7$ with graphene delivered 95.4 % of its theoretical capacity with almost 90 % initial Coulombic efficiency and had a high-energy density exceeding 300 Wh $kg^{-1}$ at 0.2C [121]. Furthermore, it demonstrated an impressive capacity retention of 83 % after 600 cycles at 2C, indicating the potential of this modified material for various applications requiring high-performance energy storage. Barpanda et al. [122] synthesized a polymorph of Mn-based pyrophosphate called b-$Na_2MnP_2O_7$, making it a new member of a small group of Mn-based cathodes for SIBs. The electrochemical activity of b-$Na_2MnP_2O_7$ was investigated at an average potential of 3.6 V, and a reversible capacity of approximately 80 mA h $g^{-1}$ was found, consistent with DFT calculations. It also showed the highest $Mn^{3+}/Mn^{2+}$ redox potential compared to all other reported Mn-based cathodes, confirming that pyrophosphate chemistry can be used to design high-voltage cathode materials. The researchers [123] conducted a structural analysis on $Na_7V_3(P_2O_7)_4$ and realized that the crystal structure had vacancies that may eventually allow for the insertion of more $Na^+$ ions. The electrochemical measurements used a wider voltage range of 1.3–4.8 vs. $Na^+/Na$ indicating that three redox couples ($V^{3+}/V^{4+}$, $V^{4+}/V^{5+}$, and $V^{3+}/V^{2+}$) allowed the cathode active material to display a reversible capacity of about 118 mA h $g^{-1}$ during these

experiments. This allowed the transmission of several electrons per transition metal ion during the electrochemical process.

A type of inorganic compound known as mixed phosphates, or $Na_4M_3(PO_4)_2P_2O_7$, includes both phosphate ($PO_4$) and pyrophosphate ($P_2O_7$) ions as part of its structure. Mixed phosphates are used in various industrial processes, such as water treatment additives, fertilizers, and corrosion inhibitors. Mixed *ortho*-pyrophosphates are more advantageous for ion storage and transportation. Some examples of such compounds include $Na_7V_4(P_2O_7)_4(PO_4)$ [124], and $Na_4M_3(P_2O_7)(PO_4)_2$ (where M can be Fe, V, Ti, Mn, Co, or Ni) [125]. Gezovic et al. showed that $Na_2FeP_2O_7$ forms predominantly due to phosphate to pyrophosphate decomposition without pH adjustment. However, increasing the fraction of pyrophosphate and adjusting the suspension pH to neutral alters the reaction path. It results in the formation of a mixed polyanion phase with promising sodium storage performance in an aqueous medium, surpassing $Na_4M_3(PO_4)_2P_2O_7$ heterostructure performance and achieving theoretical capacity even at high currents of 1 A $g^{-1}$ [126].

*2.2.1.4. Fluorophosphates.* First suggested by Barker et al. [18], $NaVPO_4F$ has a tetragonal symmetry structure, an average discharge voltage of 3.7 V, an initial capacity of 82 mAh $g^{-1}$, and less than 50 % of the capacitance is still present after 30 cycles. To improve this electrochemical activity, Lu et al. [127] synthesized $NaVPO_4F$/carbon using a high-temperature solid-state reaction technique. The results reveal that the modified material had a maximum capacity of 97.8 mAh $g^{-1}$, and 89 % of the capacity could be maintained even after 20 cycles. More studies by adding carbon nanotubes to $Na_3V_2(PO_4)_2F_3$ exhibited an impressive capacity retention of 97.5 % at 1C over 100 cycles and a high coulombic efficiency of 99.4 % [128]. Morais et al. [129] developed sodium vanadium fluorophosphates doped with $Ti^{4+}$ and $Nb^{5+}$ via an original low-temperature synthesis. The results showed that doping $Ti^{4+}$ into the material improved access to electrode sites and led to higher capacities at high current densities, and $Nb^{5+}$ doping provided a remarkable 91.7 % capacity retention between the 20th and 200th cycle suggestion that the $Ti^{4+}$ and $Nb^{5+}$ doping strategies have positive impacts on the electrochemical properties of the material. In addition, Co-doping with Fe and Cr enhances the electrochemical performance of $NaVPO_4F$, with $Na_3V_{1.9}Fe_{0.095}Cr_{0.005}(PO_4)_2F_3$ displaying high initial capacity and excellent capacity retention over 500 cycles [130]. DFT calculations [131] were performed on $NaAlPO_4F$ and $Na_3Al_2(PO_4)_2F_3$, which belong to the same crystal series as $NaVPO_4F$, indicating that the formation energy of monoclinic $NaVPO_4F$ was found to be much lower than that of the tetragonal phase, suggesting that monoclinic $NaVPO_4F$ is more stable (Fig. 9a). It explains the irreversible phase transition from the tetragonal to the monoclinic phase at high temperatures. Additionally, the monoclinic and tetragonal phases exhibit different morphologies. The incorporation of high-entropy elements improves the stability of $Na_2$ sites, effectively inhibiting intermediate reactions between the $Na_3V_2(PO_4)_2F_3$ and $Na_{3-x}V_2(PO_4)_2F_3$ phases in the low potential region. It is demonstrated in a high-entropy carbon-coated $Na_3V_{1.9}$(Mg, Cr, Al,

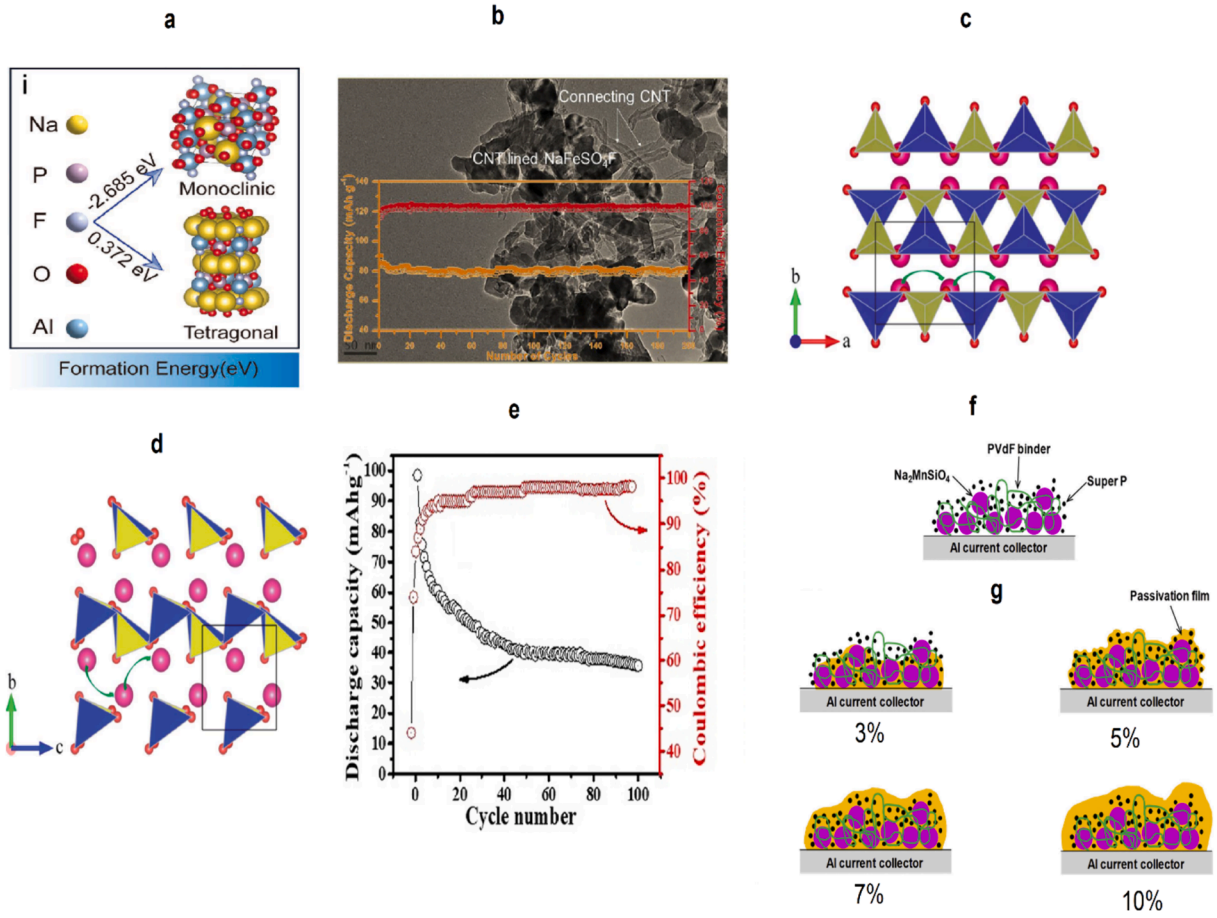


**Fig. 9.** (a) The formation energy calculated by DFT [131]. Copyright © 2021 Wiley. (b) TEM image and cycling stability curves of the $NaFeSO_4F$ and $NaFeSO_4F$-CNT (red line) at 1C [135]. Copyright © 2018 Elsevier. (c and d) Crystal structure of $A_2MSiO_4$ (A = Li and Na; M = Fe, Mn, Co and Ni) from two different viewpoints: along the c-axis (c) and along the a-axis (d), Pink atoms: Li, red atoms: O, yellow tetrahedrons: $SiO_4$, and blue: $MO_4$ tetrahedrons. Green arrows indicate the Li/Na ion migration pathways [140]. Copyright © 2016 Royal Society of Chemistry. (e) Cycling performance of as-synthesized NFS over 100 cycles [143]. Copyright © 2022 Elsevier. Schematic illustrations of formation of the passivation layer (f) without and (g) with different vol% vinylene carbonate [145]. Copyright © 2017 Elsevier. (For interpretation of the references to colour in this figure legend, the reader is referred to the web version of this article.)

Mo, Nb)$_{0.1}(PO_4)_2F_3$ cathode, which exhibits superior performance in sodium-ion batteries [132].

### 2.2.2. Sulfates polyanions

Sulfates are crucial in producing high-voltage materials because $SO_4$ has a higher electronegativity than other polyanion groups. The alluaudite-type mineral $Na_2M(SO_4)_2n{\cdot}H_2O$, where m refers to transition metals Mg, Fe, Co, Ni, Cu, Cr, and Mn, is a vast source of minerals for SIBs. $Na_2M(SO_4)_2n{\cdot}H_2O$ compounds with alluaudite phase, such as $Na_2Fe(SO_4)_2$, $Na_2Co(SO_4)_2$, $Na_2Mn(SO_4)_2$, $Na_2Mg(SO_4)_2$, and others, have been extensively researched. In particular, $Na_2Fe(SO_4)_2$cathode materials show potential for use in rechargeable batteries because they have high operating voltages and are composed of abundant elements found on Earth. $Na_2Fe(SO_4)_2$ exhibited a high $Fe^{2+}/Fe^{3+}$ redox potential at 3.6 V, which allows it to deliver a specific capacity of 82 mAh $g^{-1}$ at 0.1C, and it retains over 60 % of its capacity even when discharged at a higher rate of 2C [133]. Song et al. used a mixed polyanionic molecule termed $Na_2Fe(C_2O_4)SO_4H_2O$ [134] as cathode for SIBs via experimental and simulation methods. It demonstrated the ability to reversibly insert and remove Na ions over 500 cycles, with coulombic efficiencies exceeding 99 % and average discharge voltages of 3.5 and 3.1 V due to the redox reactions of $Fe^{2+}/Fe^{3+}$ helped to compensate for electrons during the insertion and desertion of $Na^+$ ions.

In another research [135], a novel system consisting of $NaFeSO_4F$-CNT was created using the solid-state technique, and it has been found to have a very stable $Fe^{2+}/Fe^{3+}$ redox couple. A capacity of around 110 mAh $g^{-1}$ at a discharge rate of 0.1C was achieved while retaining more than 91 % of its capacity after 200 cycles discharged at a rate of 1C (Fig. 9b).

$Na_{2.44}Mn_{1.79}(SO_4)_3$ as a high-voltage cathode material was used for sodium-ion batteries [136]. It is shown that this compound provided large tunnels for possible $Na^+$ transport and can facilitate efficient $Na^+$ (de)insertion when $Mn^{3+}/Mn^{2+}$ redox activity is centered at 4.4 V. Also, the alluaudite phase $Na_{2+2x}Co_{2x}(SO_4)_3$ showed a high platform of 4.76 V, which is attributed to the $Co^{3+}/Co^{2+}$ redox reaction [137].

In summary, metals-based sulfate polyanions are a promising but challenging material for commercial applications due to poor thermal stability, high moisture sensitivity, and inadequate electronic conductivity. Various approaches, including morphology design, metal ion doping, and conductive carbon coating, have been used to improve their properties, but further development is still needed [138,139].

### 2.2.3. Silicate polyanions

The polyanionic orthosilicate compounds $Na_2MSiO_4$ (M = Fe, Mn, Co, and Ni) have drawn more interest in study as potential sodium-ion battery materials because of their high theoretical specific capacity, stable structure, and low cost. Li et al. The exceptional thermodynamic stability of $Na_2MSiO_4$ at temperatures exceeding 1000 °C can be ascribed to the high bond strength of Si-O [140]. They used the experimental crystal structure of $Li_2FeSiO_4$ as the starting point for their calculations to study the crystal structure and electrochemical properties of $A_2MSiO_4$ (A = Li and Na; M = Fe, Mn, Co, and Ni). The relaxed structures of $A_2MSiO_4$ (A = Li and Na; M = Fe, Mn, Co, and Ni) were found to have orthorhombic structures. This indicates that the crystal structure of these compounds has a unique arrangement of atoms in three dimensions and symmetry elements that belong to the orthorhombic crystal system (Fig. 9c and 9d).

Due to the abundance of resources for the Na-Fe-Si system on the earth, $Na_2FeSiO_4$ is the most well-known example of sodium orthosilicate minerals. $Na_2FeSiO_4$ was synthesized for the first time using solvothermal synthesis, with two unavoidable impurities, $Na_2SiO_3$ and $Fe_3O_4$ [141]. The initial discharge capacity of sodium iron silicate during the galvanostatic charge/discharge experiments was 126 mAh $g^{-1}$ at a voltage range of 1.0–4.1 V; however, after the initial charge, the sodium iron silicate crystal lattice permanently broke down, resulting in an amorphous phase. The text suggests that $Na_2FeSiO_4$ synthesized via the solid-state method and sol–gel [142], showed better cycling performance, indicating the high stability of the structure and its zero-strain characteristics. Recently, the synthesis of the monoclinic phase of $Na_2FeSiO_4$ using a polymer-assisted technique exhibited an initial charge capacity of 225 mAhg$^{-1}$ at 0.1C [143]. However, the study finds that this phase of $Na_2FeSiO_4$ was not cyclable for long-term cycling due to the continuous growth of interfacial resistance during the initial cycle (Fig. 9e).

$Na_2MnSiO_4$ is also highly desirable due to its high theoretical capacity of 278 mAh $g^{-1}$ and increased redox potential. Carbon-coated $Na_2MnSiO_4$ synthesized by a sol–gel method displayed a reversible capacity of 125 mAh $g^{-1}$ with an acceptably high-rate capability achieved at 363 K [144]. Dissolution of $Mn^{2+}$ into the electrolyte caused irreversible capacity decay of $Na_2MnSiO_4$ performance. To address this issue, Law et al. [145] the effect of varying concentrations of vinylene carbonate additive in the electrolyte on the electrochemical performance of $Na_2MnSiO_4$. As illustrated in Fig. 9 f and 9 g, they found that increasing the vinylene carbonate concentration from 0 to 5 vol% resulted in an improvement in discharge capacity, and vinylene carbonate also played a crucial role in forming a surface-stabilizing layer on cathodes that prevented the dissolution of $Mn^{2+}$. However, a higher concentration of vinylene carbonate led to lower capacity delivery. The study confirmed that the high specific capacity of $Na_2MnSiO_4$ resulted from the consecutive redox of $Mn^{2+}/Mn^{3+}$ and $Mn^{3+}/Mn^{4+}$ species. In addition to Fe/Mn-based orthosilicate electrodes, a $Na_2CoSiO_4$ cathode has also been reported. $Na_2CoSiO_4$ is a promising cathode material for sodium-ion batteries due to its high voltage (3.3 V vs. Na/$Na^+$). The performance of $Na_2CoSiO_4$ as a cathode material showed that $Na_2CoSiO_4$ has a reversible capacity greater than 100 mAh $g^{-1}$ when tested at a rate of 5 mA $g^{-1}$ [146].

## 2.3. Synthesis methods for polyanionic compounds

Solid-state reactions are commonly employed for the synthesis of $NaFePO_4$ and $Na_3V_2(PO_4)_3$. Maricite $NaFePO_4$ can be obtained through a simple solid-state method followed by ball-milling with conductive carbon [108]. Similarly, $Na_3V_2(PO_4)_3$ can be synthesized by dissolving $V_2O_5$ in $H_2O_2$, followed by sequential dissolution of $NaC_2H_3O_2$, $NH_4H_2PO_4$, and PVP, then heating the dried powder at 700–800 ℃ for 8 h under a 5 % $H_2$/Ar atmosphere [147]. Also, $Na_4MnV(PO_4)_3$ [148], $Na_2CoP_2O_7$ [149], $Na_2MnP_2O_7$ [150] and $NaVPO_4F$/C [127] composites were synthesized using simple solid-state reduction methods. Mixed polyanion compounds like $Na_4Fe_3(PO_4)_2(P_2O_7)$ were successfully synthesized using a similar solid-state method [151].

Hydrothermal methods have been widely utilized for synthesizing various small and large single crystals, as well as nanomaterials, resulting in diverse morphologies and sizes on a nanoscale. $Na_3(VPO_4)_2F_3$ nanoparticles were synthesized in a single step at low temperatures (60–120 ℃) using $H_3PO_4$ as the phosphate source without any additional organic ligands or extractants. The nanoparticles had sizes ranging from 50 to 100 nm [152]. $Na_3V_2O_2(PO_4)_2F$ nanowires coated with $RuO_2$ using a microemulsion-mediated hydrothermal synthesis when employed as a cathode material for Na-ion batteries, achieve a reversible capacity of 120 mAh/g at 1C and 95 mAh/g at 20C after 1000 charge–discharge cycles [153]. Various polyanionic compounds like; $Na_3MnPO_4CO_3$ [154], $Na_7V_4(P_2O_7)_4(PO_4)$ [155] have also been reported using the hydrothermal method.

Many nanosizing polyanion-type cathode materials can be obtained using sol–gel method. For example, the precursor of $NaFePO_4$ was prepared via a sol–gel method by adding, $NH_4H_2PO_4{\cdot}2H_2O$, $NaNO_3$, citric acid, and $FeC_2O_4{\cdot}2H_2O$ to a mixed solvent of distilled water and ethylene glycol. The solution was dried at 80 ℃ to obtain a solid gel precursor. This precursor was then treated at 300 C for 8 h under an argon atmosphere, followed by calcination at 500 ℃ for 12 h in a $H_2$/Ar mixed gas to obtain the Carbon encapsulated maricite NaFePO4 nanoparticles [156]. A $Na_3V_2(PO_4)_2F_3$@C nanocomposite was prepared via a

sol–gel method using $NH_4VO_3$, NaF, and $NH_4H_2PO_4$ with a molar ratio of 2:3:2 [157]. Another study by S. J. Lim et al. synthesized $Na_{3-x}K_xV_2(PO_4)_3/C$ (x = 0, 0.05, 0.10, 0.15) using $V_2O_5$, $C_2H_2O_4{\cdot}2H_2O$, $NaH_2PO_4{\cdot}2H_2O$, and $KH_2PO_4$ as precursors [158].

Scalable preparation of polyanionic materials is achieved through innovative methods. Multi-shelled $Na_3(VOPO_4)_2F$ microspheres are produced using in situ generated bubbles as soft templates at room temperature, showing outstanding rate capacity and cycling stability [159]. Similarly, $Na_3V_2(PO_4)_2O_2F$ is rapidly synthesized using a solvent-free room-temperature solid-phase mechanochemical method, demonstrating high initial capacity, superior rate capability, and remarkable cyclability. The successful kilogram-scale production confirms the feasibility of large-scale synthesis, paving the way for commercialization of SIBs [160].

### 2.4. Prussian blue analogues

Prussian blue analogues (PBAs) have a perovskite composition, which can be represented by the formula $Na_xM_a[M_b(CN)_y]{\cdot}nH_2O$. This structure is formed by the alternating connection of $M_a$ and $M_b$ through CN to create a sturdy and open framework [161]. Their excellent electrochemical performance as SIB cathodes is due to their crystal structures, which contain a rigid open framework and large interstitial sites that facilitate the fast transfer of sodium ions during intercalation and extraction. In the perfectly formed face-centered cubic PBAs, shown in Fig. 10a, the metals M and Fe are positioned at the cube's corners, while the (C-N) anions are located on the edges. This arrangement contributes to the stability of the crystal structure and the production of porosity on a nanometer scale [162,163]. In the defective framework (Fig. 10b), rapid precipitation reaction rates that lead to the loss of $Fe(CN)_6$ ion groups might arbitrarily result in vacancies in the $Fe(CN)_6$ group. Due to the presence of water during material synthesis, vacancies created by the loss of $Fe(CN)_6$ ion groups in a defective framework will be occupied by water molecules, which will coordinate with the framework.

According to previous research, the poor electrochemical performance of PBAs as insertion cathodes for $Li^+$ and $Na^+$ is due to the structural irregularity of their lattices. PBA samples prepared by chemical precipitation methods contain $Fe(CN)_6$ vacancies and coordinated water in the crystal framework. The vacancies introduce more water molecules into the lattice, reducing available sites for $Na^+$ ions and lowering capacity utilization. Water molecules also compete with $Na^+$ ions for interstitial spaces and can cause electrolyte decomposition. The vacancies can also break down the lattice structure, increasing the material's ohmic polarization [164]. Hence, researchers have tried to eliminate the adverse effects of structural irregularity in PBAs and attempted to create high-performance $Na^+$ insertion cathodes. For instance, Na-rich PBAs where M = Mn, Fe, Co, and Ni [165] were obtained by precipitation method, and a comparative study was conducted on the electrochemical properties of these samples. The results clarified that the PBA with Mn showed a high reversible capacity of 126 mAh $g^{-1}$ in the 2.0 – 4.2 V because of the high redox potentials of Mn and the large Na content. However, the cycle performance of Na-rich $Na_xMn[Fe(CN)_6]{\cdot}nH_2O$ was not as good as that of $Na_xFe[Fe(CN)_6]{\cdot}nH_2O$ among them. In addition, the PBA with Ni demonstrated the best cyclability and rate performance, even though it only delivered 66 mAh $g^{-1}$. In a recent study by Qiao et al. [161], PBA materials were synthesized as cathode materials for SIB by adjusting the electronic state of Fe-ion with different structural defects. As shown in Fig. 11a, the study confirms that Na-ion can undergo reversible phase transformation in $Fe^{III}[Fe^{III}(CN)_6]$, with a cubic ↔ cubic/rhombohedral ↔ rhombohedral mechanism, leading to excellent electrochemical reversibility and structural stability [161]. $Fe^{III}[Fe^{III}(CN)_6]$ demonstrated the highest discharge capacity of 121.4 mAh $g^{-1}$ at 10 mA $g^{-1}$ with a working voltage of 2.94 V and superior cyclability at both 10 and 50 mA $g^{-1}$ (Fig. 11b) [161].

In summary, among different kinds of cathodes, Mn and Fe-based PBAs are the most promising candidates for practical SIBs due to their material cost, environmental friendliness, and electrochemical performance. However, due to their low gravimetric densities, PBA frameworks are not suitable for high-specific energy batteries. Nevertheless, they are an attractive option for low-cost SIBs in large-scale stationary energy storage applications.

#### 2.4.1. Synthesis methods for PBAs compounds

The synthesis methods for PBAs are generally classified into three main types: precipitation, hydrothermal, and electrodeposition. Various PBAs have been synthesized using the precipitation method, where metal-ion salts are mixed with ferrocyanide ligands, resulting in random morphologies due to fast reactions [166–172]. For example, The MnFeNi-PB compound with the formula $Na_2Mn_{0.6}Fe_{0.2}Ni_{0.2}(CN)_6$ was synthesized via a coprecipitation method using citrate sodium as a chelating agent to control crystallization. Metal salts ($MnSO_4{\cdot}H_2O$, $NiSO_4{\cdot}6H_2O$, $FeSO_4{\cdot}7H_2O$) and $Na_3C_6H_5O_7{\cdot}2H_2O$ were dissolved in saturated sodium sulfate solution, then a 0.1 M $Na_4Fe(CN)_6$ solution was slowly added under magnetic stirring. After aging at 60 ℃ for 3 h, the precipitate was obtained by centrifugation, washed, and dried [166]. To control morphology, coordination agents are used, such as trisodium citrate dehydrate, leading to the formation of 2D $Ni[Ni(CN)_4]$ nanoflakes and 3D $Na_2CoFe(CN)_6$ nanocubes. Acid/photon-assisted precipitation methods have also been developed, where metal ions are indirectly provided with acid or photon assistance. Flexible electrodes of Prussian Blue on Xuan paper were synthesized using a photosensitizer solution as the precursor, allowing for improved crystallinity and dispersion of PB particles due to controlled crystal nucleation and growth [173].

The hydrothermal method is widely employed for synthesizing PB microparticles by utilizing the decomposition of $Fe(CN)_6^{4-}$ into $Fe^{3+}$/$Fe^{2+}$ in acid solution. $Co_3[Co(CN)_6]_2$ PBAs with various nanostructures are prepared under different conditions, utilizing $K_3[Co(CN)_6]$ as the

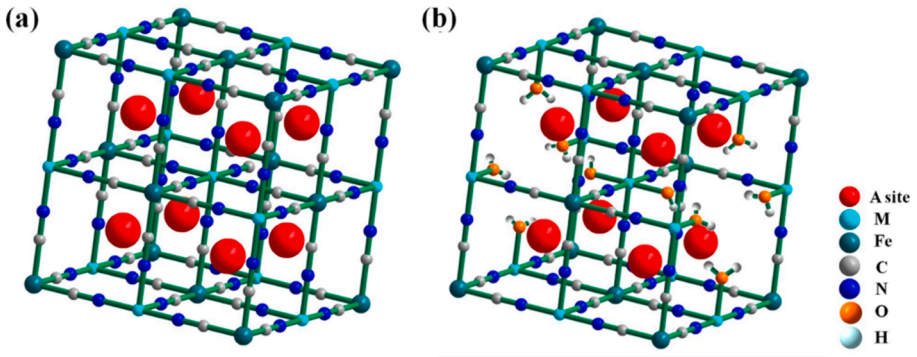


**Fig. 10.** (a) Crystal structures of PBAs without any structural defects, and (b) an ideally defective framework for $Na_2M^{II}[Fe^{II}(CN)_6]$ includes 25% $Fe(CN)_6$ vacancies within each unit cell [163]. Copyright © 2016 American Chemical Society.

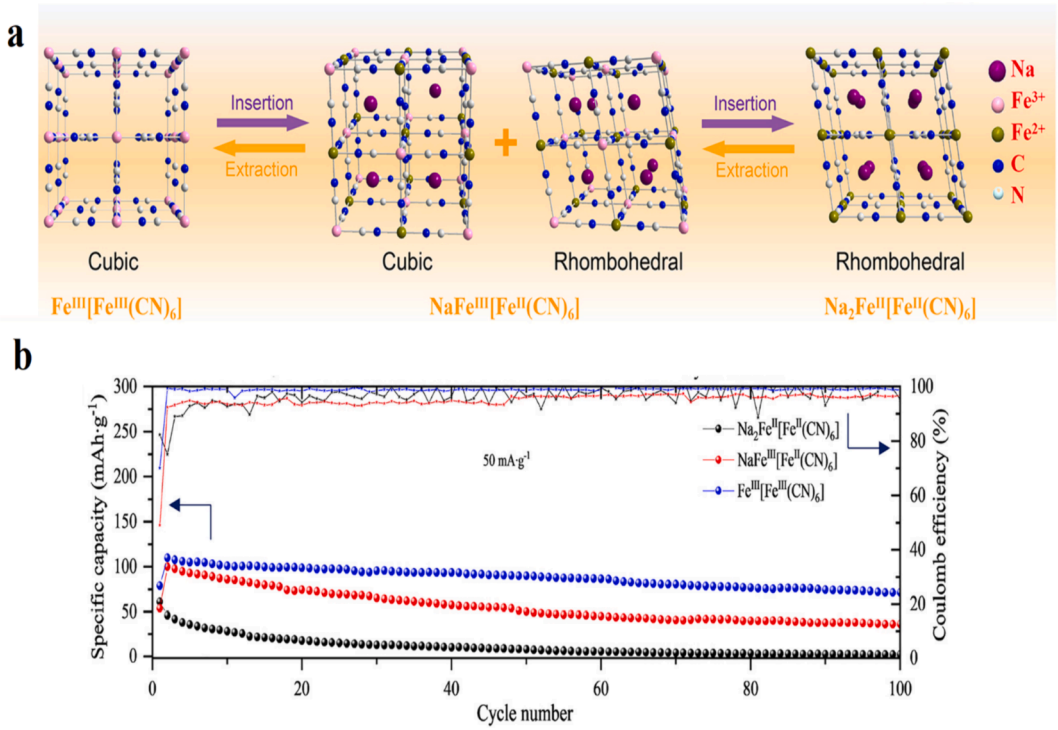


**Fig. 11.** (a) Schematic illustration of Na-ion storage mechanism of $Fe^{III}[Fe^{III}(CN)_6]$ and (b) cycling performance of different cathodes in SIBs at 50 mA $g^{-1}$ [161]. Copyright © 2023 Elsevier.

precursor. Acid not only initiates the chemical reaction but also acts as an etching reagent, allowing for the control of morphology, leading to the formation of PB microcubes, rough PB cubes, and porous PB spheres [174]. Additionally, PB-carbon composites like PB/rGO and PB/CNT are synthesized using a two-step method, where PB particles are initially synthesized via the hydrothermal method and then coated with rGO or CNTs [175–177].

Prussian blue can be directly deposited by electrochemical reaction from an $Fe^{3+}$ and $[Fe(CN)_6]^{4-}$ acidic solution. $Fe_4[Fe(CN)_6]_3{\cdot}xH_2O$ nanowires and nanotubes have been synthesized through electrodeposition on various substrates, including polycarbonate membranes and anodized porous aluminum foil, followed by selective etching to obtain PB nanotubes [178].

### 2.5. Organic molecules

Due to their many advantages, organic cathode materials have become a potential choice for organic sodium-ion batteries. They have a highly customizable molecular structure that makes functionalization simple. Furthermore, if some organic tiny molecules undergo multi-electron redox processes, their low atomic weights can result in substantial gravimetric capacities. Also, the flexible molecular structure of organic cathode allows for practical methods to fabricate electrodes, which facilitates the reversible acceptance of large sodium ions with low resistance [179].

Suitable combinations of organic materials with appropriate anodes can form full batteries in organic sodium-ion batteries. Fig. 12 shows different configurations of organic materials used in organic sodium-ion batteries. In Fig. 12a, n-type materials, such as carbonyls, are matched with Na-rich anodes, while in Fig. 12b, p-type materials are paired with hard carbon anodes. These configurations ensure a large output voltage. Fig. 12c shows an all-organic battery configuration that is entirely eco-friendly, using an organic compound derived from 2,5-dihydroxyterephthalic acid that can reversibly transform to $Na_6C_8H_2O_6$ or $Na_2C_8H_2O_6$ by storing or removing sodium ions [179].

Small and polymer molecules are two types of organic materials

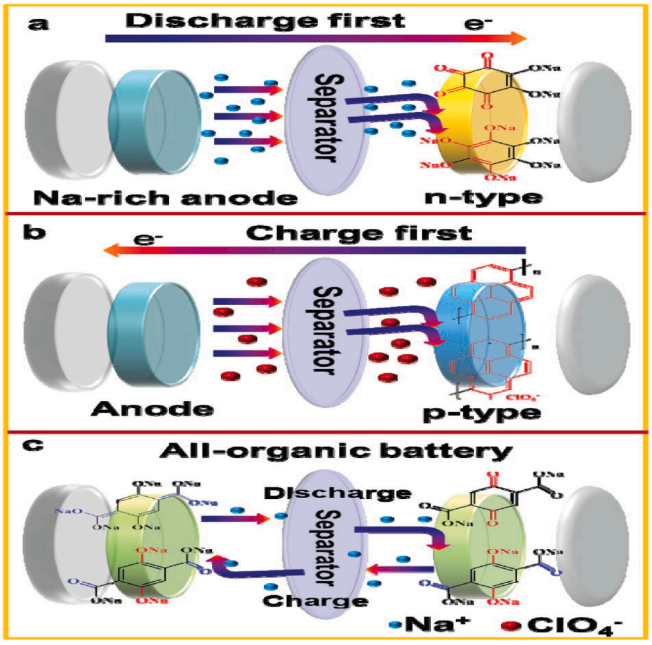


**Fig. 12.** A–c) configurations for organic materials as cathodes in sibs[179]. Copyright © 2021 Wiley.

commonly used in organic sodium-ion batteries. As electroactive electrode materials for sodium-ion batteries (SIBs), organic small molecules with various functional groups, including C = O (such as quinones and ketones, carboxylates, anhydrides, and imides derivatives), C = N (such as Schiff and pteridine derivatives), and N = N (such as azo derivatives), have been demonstrated. Among them, carbonyl compounds with C = O bonds have drawn the most interest as organic electrode materials for SIBs because of their distinctive multielectron redox reactions, extensive

theoretical capabilities, and wide structural variety.

Redox-active polymers are a promising option for electrode-active materials in organic sodium-ion batteries due to their flexibility, structural diversity, and sustainability. Organic polymers can accommodate larger sodium ions and have fast kinetics for $Na^+$ insertion and extraction reactions. They are also low-cost, environmentally friendly, and potentially accessible from biomass resources. However, despite considerable work on developing polymeric electrode materials for Li-ion batteries and electrochemical supercapacitors, only some have been devoted to Na-ion batteries [180]. Although organic materials have benefits; they have poor conductivity, solubility, and low-voltage platform shortcomings. To tackle these challenges, researchers are employing various strategies. One approach involves boosting intrinsic electronic conductivity and combining highly conductive materials with organics. Additionally, they are exploring atomic layer deposition (ALD) coatings of metal oxides to enhance the stability and kinetics of organic electrodes. ALD allows for the application of ultrathin coatings at low temperatures, improving performance while preserving the properties of organic materials [181]. Currently, satisfactory organic electrode materials for SIBs are still needed due to the complex requirements that need to be balanced.

#### 2.5.1. Synthesis methods for organic compounds

Some organic cathodes or anode materials for sodium-ion batteries can be prepared using traditional organic synthesis methods such as refluxing at various temperatures. Additionally, chemical modifications can be incorporated to introduce desired functional groups or alter the molecular structure of the organic compound. [182]. For example, to enhance stability, atomic layer deposition (ALD) is used to coat thin films on the surface of organic compounds [181]. These compounds are also mixed with carbon materials (CNT, rGO) using techniques such as ultrasound, stirring, hydrothermal, and solvothermal methods. Subsequent calcination is then performed to strengthen the bond between organic compounds and carbon materials, thereby improving conductivity and stability. These techniques address issues such as low conductivity and solubility in organic electrolytes, ensuring the stable and efficient performance of organic electrode materials in sodium-ion batteries [183].

### 2.6. Comparing the characteristics of different cathode types in Na-ion batteries

Table 1 shows the average operating potentials, discharge capacities, and cycling performance of the principal cathode material families for SIBs, allowing for a comparative analysis of their electrochemical characteristics.

Investigations into various cathode materials cover a broad spectrum, including metal oxides, polyanions, derivatives derived from Prussian blue, and organic compounds. Research into sodium-containing layered transition metal oxides, such as $Na_{1-x}FeO_2$ possessing an $O_3$-type structure, has indicated that their electrochemical behavior is primarily linked to the redox processes involving $Fe^{3+}/Fe^{4+}$. In contrast, lithium-based counterparts with an $O_3$-type structure employ the same layered transition metal oxides. Substituting Co or Mn for Fe at transition metal sites has been shown as a practical approach to address the challenge of irreversible capacity due to the migration of iron ions in $Na_{1-x}FeO_2$. However, the issue of insufficient cycle stability still needs to be solved. Some of these materials exhibit high reversible capacity, reaching around 200 mAh $g^{-1}$, achieving attractive specific energies of around 600 mWh $g^{-1}$ or even more. However, a frequent drawback of large capacity is poor cycle stability, primarily related to significant interlayer expansion. New research has revealed that the original MnNi system had issues with structural stability. However, this problem was addressed by incorporating substitutions, specifically by introducing Cu and Ti into the composition (resulting in $(Na_{0.9}Mn_{0.60}Ni_{0.30}Cu_{0.05}Ti_{0.05}O_2)$. This modified material exhibits a discharge capacity of 184 mAh $g^{-1}$ and maintains 92 % of its capacity after 100 cycles.

Polyanion compounds have better thermal stability than oxides due to P-O covalent bonds in their crystal structure. They operate at similar voltage levels as lithium-based systems. Studies on $NaFePO_4$ have revealed that the diffusion of $Na^+$ ions is slightly slower compared to $Li^+$ ions, contrary to earlier research suggesting faster diffusion of $Li^+$ ions. NASICON-type compounds were considered promising for solid $Na^+$ ion electrolytes due to their robust three-dimensional open structure, which allows for efficient $Na^+$ ionic conductivity. These compounds can also serve as electrode materials when transition metals are incorporated into their structure. For example, $Na_3V_2(PO_4)_3$ exhibited improved performance in higher and lower voltage ranges after surface modification with carbon.

Prussian blue and its analogues have garnered significant interest because of their impressive energy storage capabilities, high power density, and favorable electrochemical characteristics. However, a notable hurdle in their practical application is their restricted ability to withstand high temperatures, which challenges their thermal stability. Furthermore, while hexacyanometalates offer exceptional specific energy levels, achieving such high energy comes at the expense of their cycling durability. In other words, these materials may provide substantial energy storage potential, but their ability to maintain this performance over numerous charge and discharge cycles is compromised. Organic compounds demonstrate redox reactions, enabling the simultaneous release and uptake of $Na^+$ ions or electrolyte anions to prevent expansion issues. These compounds possess noteworthy specific capacities and operate at moderate potentials thanks to their substantial redox energy. Nevertheless, practical application encounter hurdles such as slow reaction rates and material dissolution. Employing a combination of material encapsulation and electrolyte optimization can enhance Coulombic efficiency and extend cycling life. Nonetheless, adding conductive carbon still requires a compromise, which results in a reduction in the specific capacities of organic materials.

In conclusion, metal oxides have become the most appealing cathode options for SIBs due to their high specific energy and ability to improve cycling durability and rate performance significantly. The fundamental properties, advantages, and drawbacks of typical cathode materials are outlined in Table 2. However, as capacity increases, safety concerns such as poor structural and thermal stability become more significant and require further refinement for practical use.

## 3. Sibs as a next-generation alternative to LIBs

LIBs have long been the front-runners in the search for sustainable energy solutions, but SIBs are now beginning to make headway. With a focus on essential factors like cost, resource accessibility, and recycling procedures for both battery types, this report conducts comparison research to acquire insights into the possible benefits and difficulties SIBs pose in their function as next-generation LIB substitutes by looking at these characteristics.

### 3.1. Comparing electrodes for SIB and LIB

Transitioning from LIBs to SIBs is not straightforward, as significant differences in their chemical properties and performance. For example, sodium needs to integrate more effectively within graphite despite graphite being a frequently employed anode substance in LIBs. Previously, graphite materials demonstrated limited capacity (35 mAh $g^{-1}$) and unsatisfactory cycling performance when utilized as an anode material for SIBs. It is attributed to the narrow interlayer spacing of graphite, which cannot adequately accommodate the larger sodium ions [218]. Non-graphitic carbon materials, particularly hard carbons, are favored anodes for SIBs due to their cost-effectiveness, easy accessibility, sustainability, and stable electrochemical performance. Hard carbons typically show good capacity values and stable cycling properties over

**Table 1**
Comparing the electrochemical properties of cathode materials.

| Structure | | Compositions | Voltages (V) | Practical capacity [mAh/g] | Capacity retention | Ref |
|---|---|---|---|---|---|---|
| Metal oxides cathodes | Single metal oxide cathodes | $Na_{0.74}\ CoO_2$ | 2.0–3.8 | 125 (at 5 mA $g^{-1}$) | 86 % (300 cycles) | [184] |
| | | $Na_{0.7}MnO_2$ | 2.0–4.5 | 163 (at 0.1C) | 77 % (50 cycles) | [185] |
| | | $Na_{0.44}MnO_2$ | 2.0–4.0 | 112 (at 0.1C) | 97.8 % (100 cycles) | [186] |
| | | $NaFeO_2$ | 2.5–3.5 | 100 (at 0.05C) | 50 % (30 cycles) | [49] |
| | | $NaNiO_2$ | 1.2–3.7 | 123 (at 0.1C) | 91.6 % (20 cycles) | [187] |
| | | $NaMn_3O_5$ | 1.5–4.7 | 219 (at 0.1C) | 70 (20 cycles) | [45] |
| | **Binary metal oxide cathodes** | $NaNi_{0.5}Mn_{0.5}O_2$ | 2.0–4.0 | 98.4 (at 1C) | 89.1 % (100 cycles) | [57] |
| | | $Na_{2/3}Ni_{1/3}Mn_{2/3}O_2$ | 2.0–4.5 | 165 (at 0.05C) | 80 % (50 cycles) | [188] |
| | | $Na_{2/3}Fe_{0.2}Mn_{0.8}O_2$ | 1.5–4.2 | 189.8 (at 0.1C) | 71.6 % (50 cycles) | [189] |
| | | $NaFe_{0.4}Mn_{0.6}O_2$ | 1.5–4.2 | 175 (at 0.1C) | 65 % (20 cycles) | [65] |
| | | $NaFe_{0.5}Mn_{0.5}O_2$ | 1.5–4.3 | 190 (at 0.1C) | 82 % (30 cycles) | [63] |
| | | $Na_{0.67}Mn_{0.85}Al_{0.15}O_2$ | 2.0–4.0 | 104 (at 0.05C) | 81 % (100 cycles) | [190] |
| | | $NaMg_{0.28}Mn_{0.72}O_2$ | 1.5–4.4 | 200 (at 0.1C) | 50 % (30 cycles) | [191] |
| | | $Na_{0.61}Ti_{0.48}Mn_{0.52}O_2$ | 1.5–4 | 86 (at 0.1C) | 81 % (100 cycles) | [74] |
| | | $Na_{9/10}Cr_{1/2}Fe_{1/2}O_2$ | 2.0–4.0 | 129 (at 0.1C) | 69.3 % (100 cycles) | [192] |
| | **Multi-metal oxide cathodes** | $NaNi_{1/3}Mn_{1/3}Co_{1/3}O_2$ | 2.0–3.75 | 120 (at 0.1C) | 100 % (50 cycles) | [193] |
| | | $NaNi_{0.2}Mn_{0.65}Co_{0.15}O_2$ | 1.5–4.2 | 144 (at 0.1C) | 78 % (100 cycles) | [80] |
| | | $NaNi_{0.6}Mn_{0.35}Co_{0.05}O_2$ | 1.5–4.1 | 157 (at 0.05C) | 80 % (100 cycles) | [81] |
| | | $NaNi_{0.25}Fe_{0.5}Mn_{0.25}O_2$ | 2.1–3.9 | 140 (at 0.1C) | 93 % (50 cycles) | [28] |
| | | $NaNi_{0.4}Fe_{0.2}Mn_{0.4}O_2$ | 2.0–4.0 | 131 (at 0.05C) | 95 % (30 cycles) | [194] |
| | | $Na_{1.0}Li_{0.2}Mn_{0.7}Ti_{0.1}O_2$ | 1.5–4.0 | 163 (at 0.05C) | 97 (50 cycles) | [195] |
| | | $Na_{0.75}Fe_{0.25}Cu_{0.25}Mn_{0.5}O_2$ | 2.5–4.1 | 108 (at 0.1C) | 91 % (50 cycles) | [196] |
| | | $Na_{0.8}Mn_{0.6}Ni_{0.2}Cu_{0.1}Mg_{0.1}O_2$ | 1.5–4.0 | 161 (at 20 mA $g^{-1}$) | 82.6 % (500 cycles) | [197] |
| | | $NaNi_{0.45}Mn_{0.3}Ti_{0.2}Cr_{0.05}O_2$ | 1.5–4.3 | 185 (at 12 mA $g^{-1}$) | 67 % (100 cycles) | [198] |
| | | $Na_{0.9}Mn_{0.60}Ni_{0.30}Cu_{0.05}Ti_{0.05}O_2$ | 2.0–4.0 | 184 (at 0.1C) | 92 (100 cycles) | [85] |
| | | $Na_{0.67}Ni_{0.17}Co_{0.17}Mn_{0.66}Mg_{0.1}O_2$ | 2.0–4.5 | 111 (at 100 mA/g) | 90.6 % (100 cycles) | [199] |
| | **HE metal oxide cathodes** | $NaMn_{0.2}Fe_{0.2}Co_{0.2}Ni_{0.2}Sn_{0.1}Al_{0.05}Mg_{0.05}O_2$ | 1.5–4.2 | 152 (at 0.1C) | 47 % (150 cycles) | [92] |
| | | $Na_{1.0}Mn_{0.2}Fe_{0.2}Co_{0.2}Ni_{0.2}Ti_{0.2}O_2$ | 1.5–4.2 | 180 (at 0.1C) | 97 % (100 cycles) | [200] |
| | | $Na_{0.65}Mn_{0.65}Cu_{0.2}Li_{0.06}Mg_{0.015}Ti_{0.015}Al_{0.015}Zr_{0.015}Y_{0.015}La_{0.015}O_2$ | 2.0–4.5 | 115 (at 0.1C) | 87 % (500 cycles) | [91] |
| | | $NaNi_{0.12}Cu_{0.12}Mg_{0.12}Fe_{0.15}Co_{0.15}Mn_{0.1}Ti_{0.1}Sn_{0.1}Sb_{0.04}O_2$ | 2.0–3.9 | 110 (at 0.1C) | 83 % (500 cycles) | [96] |
| | | $Na_{0.94}Ni_{0.29}Cu_{0.1}Fe_{0.16}Mn_{0.3}Ti_{0.15}O_2$ | 2.0–4.0 | 125 (at 0.1C) | 79 % (300 cycles) | [201] |
| **Polyanion cathodes** | **Ortho phosphate** | $NaFePO_4$ | 1.5–4.2 | 142 (0.05C) | 95 % (200 cycles) | [108] |
| | | $NaMnFePO_4$ | 2.0–4.0 | 137.8 (at 0.1C) | 26.6 % (150 cycles) | [109] |
| | | $NaFePO_4$ | 2.0–4.0 | 157.4 (at 0.1C) | 62.9 % (150 cycles) | [109] |
| | | NaNi-$MnFePO_4$ | 2.0–4.0 | 154.8 (at 0.1C) | 74.3 % (150 cycles) | [109] |
| | **Nasicon** | $Na_3V_2(PO_4)_3$ | 2.5–3.8 | 98.2 (at 0.1C) | 94.5 % (50 cycles) | [112] |
| | | $Na_2VSn(PO_4)_3$ | 2.0–4.0 | 53.4 (at 0.1C) | 90 % (100 cycles) | [115] |

(*continued on next page*)

**Table 1** (*continued*)

| Structure | | Compositions | Voltages (V) | Practical capacity [mAh/g] | Capacity retention | Ref |
|---|---|---|---|---|---|---|
| | | $Na_3V_{1.25}Ga_{0.75}(PO_4)_3$ | 2.2–4.2 | 105 (at 1.0C) | 92.3 % (400 cycles) | [116] |
| | | $Na_4MnV(PO_4)_3/C$ | 2.5–3.8 | 106.7 (at 0.1C) | 87 % (100 cycles) | [117] |
| | | $NaTi_{1.5}Mn_{0.5}(PO_4)_3$ | 2.0–4.0 | 69.6 (at 0.1C) | 92 % (100 cycles) | [118] |
| | **Fluorophosphates** | $Na_3V_2(PO_4)_2F_3$ | 2.0–4.3 | 132 (at 0. 5C) | 70 % (1000 cycles) | [157] |
| | | $NaVPO_4F$ | 2.0–4.3 | 143 (at 0.1C) | 95.5 % (500 cycles) | [131] |
| | | $Na_2FePO_4F$ | 2.0–3.8 | 110 (at 0.05C) | 75 % (20 cycles) | [104] |
| | | $Na_2CoPO_4F$ | 2.0–5.0 | 100 (at 0.02C) | 85 % (5 cycles) | [202] |
| | **Pyrophosphate** | $Na_2FeP_2O_7$ | 2.0–4.5 | 92 (at 0.02C) | 100 % (80 cycles) | [103] |
| | | $Na_2CoP_2O_7$ | 1.5–4.5 | 80 (at 0.02C) | 100 % (10 cycles) | [203] |
| | | $Na_2MnP_2O_7$ | 1.5–4.2 | 100 (at 0.1C) | 91.7 % (100 cycles) | [121] |
| | | $Na_7V_3(P_2O_7)_4$ | 3.4–5.0 | 110 (at 0.1C) | – | [123] |
| | | $Na_4\ Fe_3(PO_4)_2\ P_2O_7$ | 1.7–4.3 | 112 (at 0.05C) | 100 % (15cycles) | [126] |
| | | $Na_4\ Co_3(PO_4)_2\ P_2O_7$ | 3.0–4.7 | 95 (at 1.0C) | 100 % (100cycles) | [125] |
| | **Sulphates** | $Na_2Fe(C_2O_4)SO_4{\cdot}H_2O$ | 1.7–4.3 | 88 (at 1.0C) | 85 % (500 cycles) | [134] |
| | | $NaFeSO_4F$-CNT | 1.5–4.2 | 110 (at 0.1C) | 91 % (200 cycles) | [135] |
| | | $NaFeSO_4F$ | 1.5–4.2 | 82 (at 0.1C) | 60 % (100 cycles) | [133] |
| | **Silicates** | $Na_2MnSiO_4$/graphene | 1.5–4.3 | 182 (at 0.1C) | 64.4 % (30 cycles) | [204] |
| | | $Na_2FeSiO_4$ | 1.5–4.2 | 225 (at 0.1C) | – | [143] |
| | | $Na_2MnSiO_4$ | 2.0–4.3 | 216 (at 0.1C) | 89.5 % (100 cycles) | [145] |
| **Prussian blue analogues** | | $Fe^{III}[Fe^{III}(CN)_6]$ | 2.5–4.0 | 121 (at 10 mA $g^{-1}$) | 96.5 (100 cycles) | [161] |
| | | $Na_2CoFe(CN)_6$ | 2.0–4.0 | 150 (at 20 mA $g^{-1}$) | 90 % (200 cycles) | [163] |
| | | $Na_{1.92}Fe[Fe(CN)_6])$ | 2.0–3.8 | 160 (at 10 mA $g^{-1}$) | 80 % (750 cycles) | [205] |
| | | $Na_{0.64}Fe[Fe(CN)_6]_{0{\cdot}93}6H_2O$ | 1.3–4.0 | 130 (at 50 mA $g^{-1}$) | 90 % (2000 cycles) | [206] |
| | | $Na_{1.04}Fe_{0.83}Ni_{0.17}[Fe(CN)_6]_{0.76}$ 0.2.36$H_2O$ | 2.0–4.0 | 114 (at 100 mA $g^{-1}$) | 90 % (1000 cycles) | [207] |
| | | $Na_{1.92}Mn[Fe(CN)_6]_{0.98}$ | 2.0–4.0 | 152 (at 10 mA $g^{-1}$) | 82 % (500 cycles) | [208] |
| | | $Na_{1.11}Ni[Fe(CN)_6]_{0{\cdot}8}0.71H_2O$ | 2.0–4.0 | 90 (at 1.1C) | 83 % (5000 cycles) | [209] |
| **Organic Compounds** | | $Na_2C_6O_6$ | 1.5–2.8 | 250 (at 18 mA $g^{-1}$) | 60 % (40 cycles) | [210] |
| | | $Na_4C_8H_2O_6$ | 1.0–3.0 | 183 (at 0.1C) | 83 % (100 cycles) | [211] |
| | | PPy-Fe | 1.5–3.8 | 135 (at 0.2C) | 85 % (100 cycles) | [212] |
| | | Aniline–nitroaniline | 2.2–4.0 | 180 (at 0.2C) | 96 % (50 cycles) | [213] |
| | | PTPAn | 2.7–3.9 | 98 (at 50 mA $g^{-1}$) | 97 % (200 cycles) | [180] |
| | | graphene/polyimide | 1.5–3.5 | 240 (at 450 mA $g^{-1}$) | 81.2 % (600 cycles) | [214] |
| | | PTCDI-DAQ | 1–3.5 | 195 (at 100 mA $g^{-1}$) | 90 % (2500 cycles) | [215] |
| | | MWCNT/$C_5O_5Na_2$ | 3.2–3.8 | 123 (at 1.0C) | 57 % (30 cycles) | [216] |
| | | TDT | 1.5–3.0 | 293 (at 500 mA $g^{-1}$) | 73 % (3500 cycles) | [217] |

**Table 2**
A comparative analysis of the advantages and disadvantages of Na-ion cathode materials.

| Material | Structure | Advantages | Disadvantages |
|---|---|---|---|
| **Layered oxide** | | Efficient $Na^+$ transport; High working voltage | Limited air stability; $Na^+$/vacancy ordering, $P_2$–$O_2$ phase transition |
| | | High theoretical capacity; High initialcapacity | Limited air stability; Complex phase transition, Poor cycle performance |
| | | Good rate performance; High stability in water and air, Low cost | Low initial charge-specific capacity, Insufficient sodium in a full battery |
| **Polyanion compounds** | orthogonal, or tetragonal | Low cost, Excellentcycle performance, High specific capacity | Lower electronic conductivity, Low theoretical capacity, Toxic, Limited charge–discharge performance at high rates |
| **Prussian blue analogs** | or rhombohedral | Low cost, Good structural stability and rate capability, High material design flexibility, Variable operating voltage | Unstable cycle performance, Limited conductivity, Low coulombic efficiency, Dissolution of metal ions |
| **Organic Compounds** | Diverse structures | Potential for high specific capacity, good flexibility, stable redox potential, Environmental friendliness; Low cost | Limited conductivity, Complex synthesis processes, Dissolvability in the electrolyte |

250 mAh $g^{-1}$. Hard carbons are versatile materials from diverse origins, like corn stalk waste, providing efficient negative-electrode options for SIBs without chemical additives. Moreover, hard carbon microfibers can be derived from recycled paper through a straightforward carbonization process [219].

SIBs require cathode materials with solid and enduring cycling performance and a high capacity for storing sodium. Currently, cathode materials such as polyanion compounds, PBAs, and layered transition metal oxides are in use. These materials include open framework structures, easy integration of $Na^+$ ions, and limited structural wear during cycling. Challenges arise from the tendency of these materials to reassemble after numerous cycles, necessitating the inclusion of supporting elements within the layers. Deepening our understanding of electrochemical processes through further research will greatly improve the usefulness and commercial feasibility of Sodium-ion batteries. Techniques like surface coating, electron doping, and structural design can enhance cycling durability and energy density [220].

Layered oxide cathodes in LIBs necessitate expensive cobalt and nickel to maintain their structured layers. In contrast, SIBs can employ more affordable Mn and Fe in cathode materials due to the favorable formation of sodium-based layered transition-metal oxides with various transition metals. This results in a significant reduction in material costs. The structural formula for layered metal oxides used in sodium-ion batteries is $Na_xTMO_2$, where TM stands for a transition metal like Mn, Fe, Ni, Cu, or Ti. Their structure can be tailored with target structures, allowing for transition between $P_2$- and $O_3$-type structures. The main challenges faced by $O_3$-type and $P_2$-type layered transition metal oxide cathode materials are poor air stability, multiple phase transitions, and subpar electrochemical performance. Various strategies have been suggested, such as substituting cations (like $Cu^{2+}$ and $Ti^{4+}$), applying protective coatings (like MgO-Coating and $Al_2O_3$-Coating) to the surface, optimizing the microstructure (using materials with micro-rod shapes), and creating mixed O-/P-type phases to solve these issues. Future research on layered cathode materials for SIBs should prioritize enhancing energy density, achieving consistent sodium storage across a wider voltage range, and improving the efficiency of initial charging and discharging. Additionally, efforts should focus on designing cathode materials that are both cost-effective and high-performing, such as those found in the Ni-Fe-Mn and Cu-Fe-Mn systems [221].

The practical application of SIBs with polyanionic compound cathodes faces challenges in achieving uniform compositions. NASICON-type compounds were considered promising for solid Na + ion electrolytes due to their robust three-dimensional open structure, which allows for efficient Na + ionic conductivity. These compounds can also serve as electrode materials when transition metals are incorporated into their structure. For example, $Na_3V_2(PO_4)_3$ exhibited good performance in SIBs after carbon surface modification. Prussian blue analogues have low capacity and stability issues.

Future studies need to delve deeper into mechanisms and explore novel materials. Due to their comparable reaction mechanisms to LIBs, inexpensive elements such as Mn, and Fe are good candidates. Even though cobalt is expensive, a good performance may be obtained with only a little usage.

### 3.2. Comparing cost and resource aspects: SIB and LIB

In terms of price, the study showed that when compared to lithium-ion batteries, sodium-ion batteries might show lower expenditures in terms of cell materials. As shown in Fig. 13, When comparing the costs of LIBs and SIBs, cathode materials are the most critical component [222]. The cost of the cell components is less than that of a typical lithium-ion battery in sodium-ion battery that uses aluminum and sodium instead of copper and lithium. However, it is critical to recognize that the whole cost of a battery, which includes additional fees for things like casings, management systems, and personnel, is far more than just the cost of the cell ingredients. Therefore, the cost-benefit seen in sodium-ion batteries at the level of the cell components may not always convert into a comparable benefit at the battery level [223].

Because sodium is more plentiful than lithium and is less vulnerable to supply threats, sodium-ion batteries have an advantage over lithium-ion batteries in terms of resources. Lithium and cobalt, the two primary raw materials utilized in lithium-ion cathodes, were also examined for possible supply vulnerabilities. Lithium-ion battery costs might increase due to supply-related problems with these materials [224]. In conclusion, because sodium-ion batteries use more accessible and inexpensive raw materials, they may offer a cost advantage. However, it is critical to consider the whole cost of batteries and any potential supply risks for lithium-ion battery components.

### 3.3. Comparing safety Aspects: SIB and LIB

The safety of SIBs and LIBs can vary due to several factors. One significant distinction lies in the electrolyte employed in these batteries. The type of electrolyte used greatly influences the safety of the battery. Using highly flammable carbonate-based compounds as electrolyte solvents in batteries, such as ethylene carbonate and propylene carbonate, enables high energy density but poses a significant risk due to their flammability and volatility. In elevated temperatures, even a minor leakage can lead to a catastrophic failure of the entire battery system, triggering a series of reactions that may result in thermal runaway, where the solvents evaporate, causing cell swelling and potentially leading to fire or explosion [225]. Recent research indicates that sodium-ion electrolytes can employing a high proportion of heat-resistant solvents tend to generate heat at lower rates or have higher thresholds before potentially hazardous self-heating reactions occur [225,226].

One notable difference is the state of charge during transportation and storage. Due to safety concerns, lithium-ion batteries must be shipped and stored at 30 % SOC or lower. In contrast, sodium-ion cells can be discharged safely down to 0 V and even into negative voltages

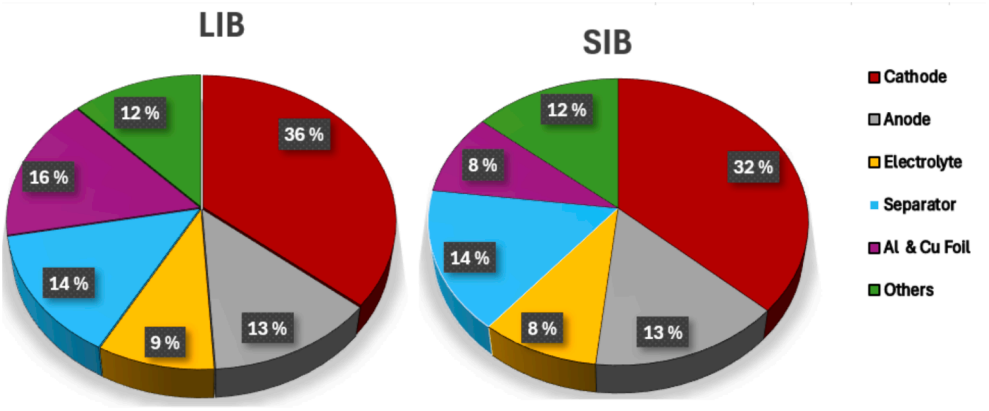


**Fig. 13.** Comparison of the manufacturing costs for LIB and SIB.

[226]. Furthermore, the choice of materials in the batteries can impact their safety. Lithium-ion batteries utilizing a carbon-based anode may face complications when discharged to 0 V, such as copper dissolution, which can negatively affect cycling performance and cell safety. In contrast, sodium-ion cells can utilize a lighter and more affordable aluminum current collector on the anode, avoiding these issues [227].

### 3.4. Comparing future climate impacts of LIBs and SIBs

According to World Bank statistics, there is a notable upswing in worldwide waste production, anticipated to grow by 70 % by 2050 if no action is taken (Fig. 14)[228]. The global market research institute SNE Research forecasted that the global used battery market will increase by over 100 times by the year 2050. It suggests the used battery market is on track for significant expansion in the coming decades. Hence, the used battery market provides companies with a sustainable opportunity for cost reduction, new business ventures, and meeting carbon neutrality demands. The sustainability of SIBs presents a complex and intricate challenge with multifaceted dimensions. As the inevitable trend towards electrification gains momentum, innovative post-lithium-ion technologies such as SIBs are steadily emerging alongside other robust alternatives. Despite the current dominance of LIBs, a potential paradigm shift is on the horizon. The success of replacing LIBs depends on the ability of these alternatives to not only match the performance of LIBs but also enhance their sustainability features.

As we delve into the environmental impacts of SIBs and LIBs, it is essential to consider a range of factors, including battery cycle lifetime, safety, operating temperature range, resource availability, and cost-effectiveness. SIBs have shown remarkable potential in cycle lifetime, safety, and a wider operating temperature range compared to LIBs. Furthermore, SIBs leverage abundant and low-cost sodium resources, positioning them as a cost-effective solution for stationary storage and specific EV applications. While LIBs have gained traction due to their higher energy density and established supply chains, the advancements in SIB technology and potential cost savings paint a promising picture. SIBs could emerge as a competitive alternative to LIBs, particularly in applications where high energy density is not the primary requirement [229,230]. Recent research underscores a positive trend in the environmental impacts of SIBs compared to LIBs from 2020 to 2050, underscoring the potential of SIBs as a more environmentally friendly choice for energy storage. The research articles reveal that from 2020 to 2050, the environmental impacts of SIBs decreased significantly by 43–57 % compared to LIBs under optimal performance scenarios [231].

### 3.5. Comparative life cycle assessment of LIBs and SIBs

Life cycle assessment (LCA) is a powerful method used to assess the environmental impacts of a process or product throughout its entire life

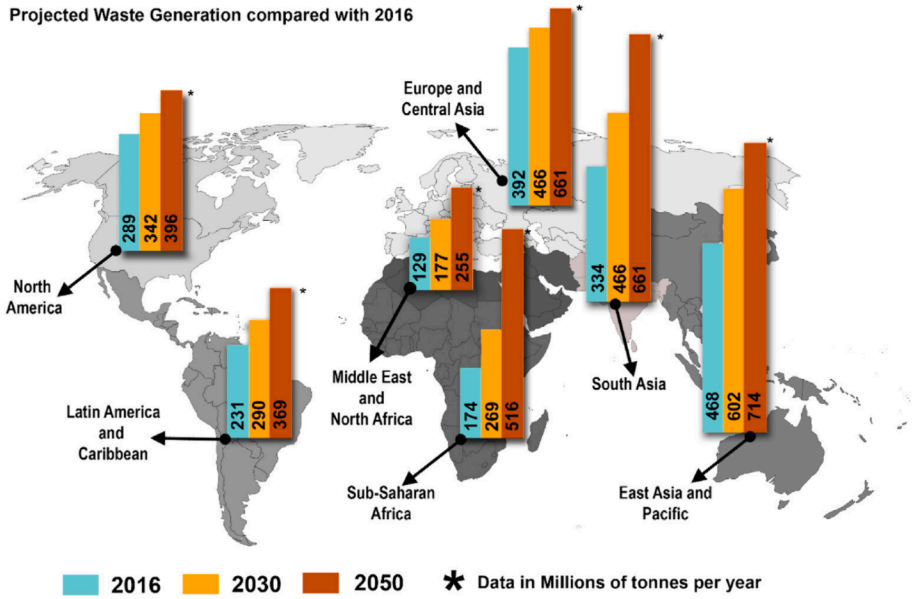


**Fig. 14.** waste produced annually in various global regions and its projected trends in the near future [228] (License: CC BY 4.0).

cycle or a portion thereof. By providing a comprehensive understanding of environmental effects, LCA aids researchers, industries, societies, and policymakers in developing environmentally friendly and sustainable products and processes [232]. The assessed research on the SIB, based on 1 kWh storage capacity and 3000 cycles, showed promising results compared to existing LIBs. Optimization potential exists, especially in cathode composition and reducing hard carbon impacts. Despite SIBs' technical immaturity, they offer potential environmental advantages over LIBs due to the use of more abundant raw materials, potentially reducing costs [233]. Another research comparing the LCA of the environmental impacts of 1 kWh SIB and LFP batteries, focusing on their recycling effects in China's automotive industry, showed that while LFP demonstrates superior environmental performance during production, SIB exhibits greater potential over the entire life cycle as a promising replacement. During usage, SIB demonstrates higher energy conversion efficiency and lower energy losses compared to LFP, but both experience significant power losses during second use [234]. Currently, research on SIB cells using abundant elements suggested better mineral scarcity performance than LIB cells within the cradle-to-gate system boundary. in this study, models SIB cells with Prussian white cathodes and hard carbon anodes based on abundant elements, showed lower mineral resources scarcity impacts compared to NMC-type LIB cells, while their global warming impacts are similar [235]. While LIBs have held sway in the market, SIBs offer a promising alternative that enhances performance and reduces environmental impacts over time. Predictions and early-stage research hint at SIBs achieving specific energy levels comparable to LFP batteries, making them suitable for applications such as stationary storage and short- or medium-range EVs. Several LCA studies have evaluated the environmental impacts of SIBs, including analyses of their anode or cathode materials. However, more research is needed regarding the future climate impacts of SIBs, especially as society rapidly transitions towards decarbonization, particularly in high energy-intensive sectors.

## 4. Significance of SIBs recycling in sustainability

It is important to note that while sustainability lacks a universally agreed-upon definition, it generally encompasses environmental, economic, and societal aspects. Within this framework, critical elements of sustainability include recycling and repurposing, which are particularly relevant for batteries. When comparing the environmental sustainability of LIBs and SIBs, various factors come into play, such as resource costs, recycling efficiency, social interactions' effects, and broader ecological implications. Both these battery archetypes are poised to exert pivotal roles in engendering a more sustainable society, mainly as technological progress transcends the realm of conventional lithium-ion technologies [236].

The practice of recycling plays a pivotal role in sustainability. The efficacy of lead-acid batteries in this regard, achieving approximately 96 % recycling efficiency attributed to their manageable constituents, serves as an illustrative model. By contrast, the intricate chemical compositions and diverse packaging configurations of LIBs engender complications in their recycling procedures [237]. Although LIB recycling confronts challenges stemming from its intricate composition, sustainability encompasses a broader spectrum encompassing the minimization of environmental detriments during the recycling process. Consequently, the strategic development of batteries conducive to recycling or optimizing disposal mechanisms where recovery is unviable assumes pivotal importance. Moreover, the tenets of social sustainability, encapsulating the repercussions on stakeholders and society at large, exert a discernible influence on the holistic assessment [238].

Meanwhile, SIBs are emerging as a more amenable option for recycling due to their simplified packaging structures. Thus, sustainability becomes intricately intertwined with recyclability, technological advancements, and economic viability.

Concurrently, pursuing sustainability objectives embraces the aspiration to devise solutions grounded in ecological prudence, factoring in the environmental costs inherent in production and deployment. In this context, the deployment of life cycle assessments emerges as an indispensable tool, facilitating a systematic dissection of the ecological ramifications spanning battery manufacturing through to ultimate disposal. The intricacy of this evaluative process rests in its consideration of variables such as energy efficiency, lifecycle durability, and the potential for material reclamation [239].

### 4.1. Recycling technologies

Consideration of the most efficient and environmentally responsible recycling techniques is crucial since both types of batteries perform essential tasks in various sectors and applications. There are several important aspects of recycling for both SIBs and LIBs. Firstly, it is crucial to note that both types of batteries pose safety risks, such as flammable electrolytes and potential explosions, especially as they age and undergo incomplete discharges. It necessitates the implementation of rigorous safety protocols to mitigate these potential hazards effectively [240]. The initial steps in preparing SIBs and LIBs for recycling are similar from a technical standpoint. It involves discharging the batteries and then pulverizing them. However, SIBs usually require a complete discharge due to the high reactivity of sodium metal and sodiated carbon materials. Regarding recycling methods, pyro techniques are considered more favorable for SIBs than LIBs [241]. This is largely because sodium is less likely to evaporate under heat treatment, and its recycling is less critical due to its natural abundance. Additionally, physically separating SIBs is easier since only aluminum needs to be recovered from the current collectors, shells, and tabs. Also, the processes after treatment for cathode and anode materials are generally less complicated for SIBs than for LIBs. This is because there are fewer impurities and elements to extract. In terms of resources, during LIB recycling, valuable metals such as lithium, cobalt, nickel, and copper are typically recovered and subsequently utilized in the manufacturing of new batteries or other applications. Nevertheless, the utilization of harsh chemicals in LIB recycling procedures frequently leads to challenges such as low recovery rates and environmental issues. On the other hand, SIB recycling technologies may offer some advantages in terms of resource utilization. As SIBs are based on more abundant elements, such as sodium and carbon, the recycling process may be less reliant on scarce or environmentally damaging materials. Additionally, SIB recycling processes may be simpler and more energy-efficient compared to LIB recycling, as they do not involve complex separation processes for rare materials. It should be noted that SIB recycling may benefit from cutting-edge strategies like direct recycling or cascading, which might enhance resource efficiency and lessen negative environmental effects. It is crucial to remember that the specifics of SIB recycling technologies and how they use resources might change based on the techniques and tools used. To properly comprehend and improve SIB recycling procedures, further study in this field is required. However, specialized methods will need to be developed to handle the unique chemistries of SIBs, particularly those using polyanionic and Prussian blue analogue cathode materials [241].

The recycling of cathode materials brings about both environmental and economic advantages. This recycling process involves two main steps: (1) Pretreatment is carried out to separate the active cathode materials from other components within the battery and, (2) the hydrometallurgy or pyrometallurgy or direct regeneration process is then employed to recover the valuable metal components from the cathode (Fig. 15) [242].

Direct recycling maintains the structure of cathodes and facilitates the complete retrieval of valuable components. Nonetheless, it necessitates sorting batteries by type and may exhibit performance disparities. Separating electrodes presents difficulties due to the toxicity of solvents and the potential release of hazardous gases. Hydrometallurgy provides better energy efficiency, diminished toxic emissions, and enhanced material retrieval. However, additional preparatory steps and various

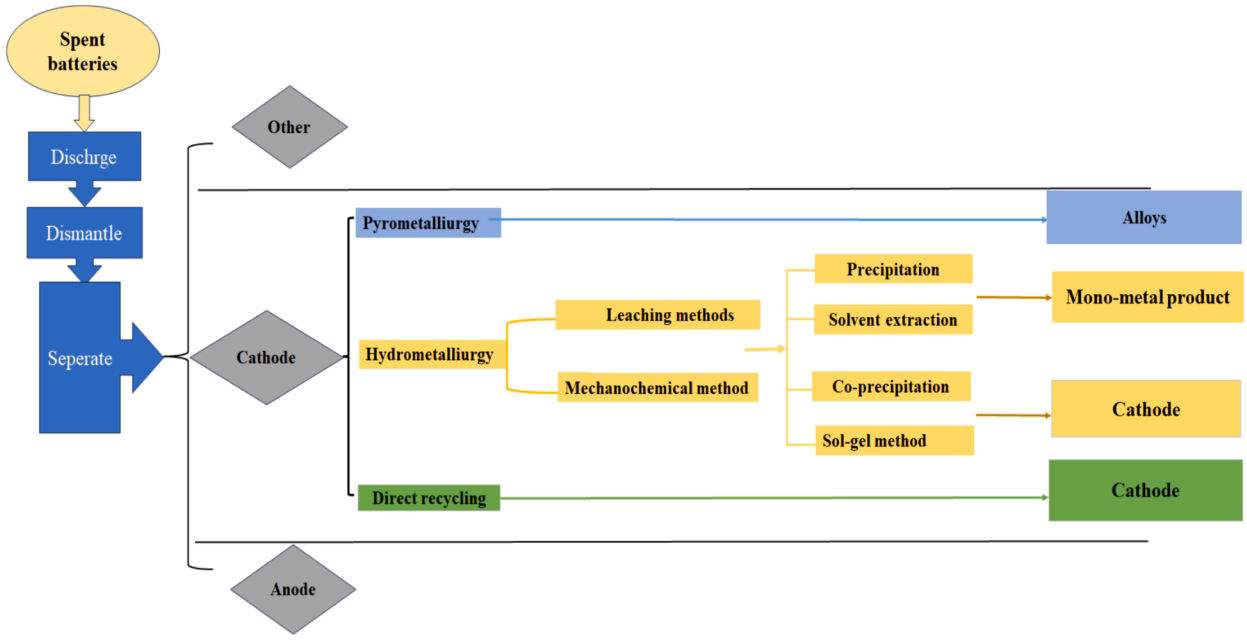


**Fig. 15.** Schematic illustration of typical recycling processes.

chemical agents are needed. On the other hand, pyrometallurgy can process batteries of any type, yet it demands substantial energy [243]. It is a favorable choice for SIBs due to the lower probability of sodium evaporation following heat treatment and the decreased need for urgent recycling.

The reclamation of valuable constituents from spent SIBs can be achieved through integrated processes. Following initial steps such as disassembly and discharge, recycling high-purity crusts and organic separators becomes notably efficient. The extraction of cathodes and hard carbon from aluminum foils can be accomplished using thermal, physical, or mechanical methods. Subsequently, metallic foils can be designated for recycling. After this phase, the quality of the cathode can be improved by utilizing techniques such as hydrometallurgy, thermal treatment, and ultrasonic hydrothermal rejuvenation. The segregation and retrieval of each precious component from spent SIBs substantially contribute to mitigating environmental risks, ensuring resource sustainability, and fostering overall economic progress. An array of approaches, including leaching and extraction, can separate valuable metal constituents from SIB batteries.

### 4.2. Reclaiming resources

Unlike Li-ion batteries, cathodic systems in SIBs are composed of economically viable materials, often without Li and Co. Furthermore, it is worth noting that Na ions exhibit minimal reactivity with Al metal, affirming that Al serves as the sole metal source required for SIBs within their typical operational constraints. This distinctive characteristic underscores the substantial potential for an eco-friendly and economically efficient battery technology [223].

The same recognized techniques used to recycle the electrolytes in LIBs may also be applied to the recycling of electrolytes in SIBs. In general, electrolytes containing high-grade salts are dissolved in a dipolar organic solvent in a dipolar organic solvent. Different methods have been developed to recover the electrolytes' organic solvents and lithium salts, including vacuum pyrolysis, organic solvent extraction, and liquid $CO_2$ extraction. Several companies have made efforts to recover electrolyte from spent LIBs alongside electrode recycling. Methods involve organic solvent extraction (AEA Technology Batteries), supercritical $CO_2$ (OnTo Technology), and pyro-hydro-metallurgical processes (IME and Accurec). While progress has been made, greater emphasis is needed on lab-scale and industrial-scale electrolyte recycling to mitigate environmental and health risks [244].

In the context of recycling Na and Al recycling, Liu et al. identified two standout methods for reclaiming Na and Al from used SIBs [245]. The first involves subjecting active materials to a water-based system, resulting in NaOH production and the Al foil's simultaneous corrosion.

$$Na(s) + H_2O(l) \rightarrow NaOH(aq) + H_2(g) \quad (1)$$

$$NaOH(aq) + Al(s) \rightarrow NaAlO_2(aq) + H_2(g) \quad (2)$$

$$NaAlO_2(aq) + HCl(aq) \rightarrow NaCl(aq) + Al(OH)_3(s) \quad (3)$$

The production of hydrogen gas can raise safety concerns during recycling procedures, necessitating special precautions to mitigate the associated risks. Additionally, the second method involves controlled Na reactions with $O_2$ and $CO_2$; by segmenting metallic Na from waste SIBs, controlled reactions with $O_2$ and $CO_2$ lead to sodium oxide and sodium carbonate formation. This method significantly reduces the production of hydrogen, enhancing safety and efficiency.

$$Na(s) + O_2(g) \rightarrow Na_2O(s) \quad (4)$$

$$Na_2O(s) + CO_2(s) \rightarrow Na_2CO_3(s) \quad (5)$$

$$Na_2O(s) + H_2O(aq) \rightarrow NaOH(aq) \quad (6)$$

Despite advancements in cathode materials for SIB technologies, comprehensive environmental assessments and detailed inventory data for these batteries still need to be fully established. The early stage of their development currently hinders metals recycling in SIBs, and the scarcity of returned spent SIBs necessitates end-of-life treatment. Detailed and high-quality inventory data for recycling processes is scarce for Li-ion batteries and even less for emerging systems like SIBs. Nonetheless, similar technology can be applied in the metal recovery recycling process, facilitated by the high technological resemblance between LIBs and SIBs [239]. Nowadays, pyrometallurgy and hydrometallurgy are the two main methods used extensively in metal recovery. Pyrometallurgy could be a favorable option for SIBs due to the lower probability of sodium evaporation following heat treatment and the decreased need for urgent recycling.

### 4.3. Valuable metals for recycling

The valuable metals in contemporary or upcoming sodium-ion batteries primarily originate from the cathodes. Anodes comprise a carbon-based structure with hard and soft carbon and expanded graphite particles. Moreover, considerable interest is in the economic feasibility of extracting sodium from electrolytes and cathodes. The following sections outline the significant materials that have the potential for recovery in future iterations of cathodes derived from depleted sodium-ion batteries.

#### 4.3.1. Manganese

Manganese, the twelfth most abundant element in the Earth's crust, is primarily used in steelmaking due to its sulfur-fixing, deoxidizing, and alloying properties; metallurgical applications account for most of its consumption. Global reserves stand at around 620 million metric tons, distributed unevenly. Manganese is found in over 100 minerals, with significant forms of pyrolusite, braunite, psilomelane, and rhodochrosite. Smelting manganese ores, which contain iron, yields an iron-bearing ferroalloy used in steel production. High-carbon ferromanganese and silicomanganese are common manganese ferroalloys. Electrolytic manganese dioxide and electrolytic manganese metal are other commercial forms produced through a similar leaching and electrodeposition process. Non-metallurgical applications include dry cell batteries, fertilizers, animal feed, and brick colorants. In 2018, global manganese production was 18,000 tons, with negligible scrap recovery, rendering recycling manganese, especially from spent lithium-ion batteries, considered economically unviable due to low recoverable quantities and high recycling costs [246].

#### 4.3.2. Iron

Iron, ranked fourth in abundance, is vital across diverse industries due to its robustness and adaptability. Iron primarily serves the metallurgical sector, with approximately 230 billion metric tons in global reserves. It is present in various minerals such as hematite, magnetite, goethite, and siderite. Extracting iron from its ores results in the creation of iron-rich alloys, crucial for steel production. Moreover, iron finds application in construction materials, machinery, transportation infrastructure, and everyday consumer products like household appliances and automobiles. Iron-based compounds serve critical functions in pharmaceuticals and water treatment and act as catalysts in chemical reactions.

Recycled iron and steel scrap are crucial for making new steel and cast-iron products. The U.S. steel and foundry industries heavily rely on scrap, with recycling saving significant resources and energy. The scrap recycling rate has stayed between 80 % and 90 % in the past decade, with automobiles being the primary source. This practice annually recycles over 15 million tons of steel, equivalent to about 12 million cars, resulting in substantial energy savings [247].

#### 4.3.3. Nickel

According to the Nickel Institute, Brussels, nickel is the fifth most common element on Earth and occurs extensively in the Earth's crust and core, with as much as 600 million tons available on land and under the sea. Global production reached 3.3 million tons in 2022. Currently, nickel (70 %) is primarily used in producing stainless steel. A smaller portion is allocated to specialized alloys (15 %), plating (8 %), foundries, castings, and batteries (3 %), and chemicals, catalysts, and dyes (2 %). The introduction of EV batteries is expected to increase nickel demand substantially. Projections indicate an impressive 36 % annual growth rate in nickel demand for EV batteries until 2025, 14 % of the total market. Although the proportion of nickel used in batteries is smaller than in other applications, getting the quantity for EVs will be challenging [248].

Moreover, the recycling of cathode materials based on nickel is of particular significance due to potential health, environmental, or safety risks, given that nickel has also been classified as a CMR substance. Hence, nickel recycling is crucial. The Nickel Institute reports that approximately 68 percent of all nickel is now being recycled, increasing from around 63 percent since 2000 [249].

#### 4.3.4. Aluminium

The high abundance of aluminium, at approximately 8 wt%, makes it the most plentiful metal in the Earth's crust and the third most abundant element overall, following oxygen and silicon. Aluminium is the second most produced metal after steel and the foremost among non-ferrous metals. Its production surpasses that of all other non-ferrous metals combined. The US Geological Survey has reported a slight increase in global aluminum production in 2022, reaching 69 million tons, compared to 67.5 million tons of 2021. In industries like aerospace and automotive, aluminium is increasingly substituting steel components. It is reported that replacing one kilogram of mild steel, high-strength steel, or cast iron with aluminium can prevent emissions of 13 to 20 kg of greenhouse gases. Due to its widespread use in construction, packaging, automotive, aerospace, and electrical distribution, and its relative value, aluminium stands out as one of the most recycled materials. According to the Aluminium Association, 90 % of aluminium in building and automotive parts is recycled at the end of its life. Furthermore, a significant 75 % of historically produced aluminium is still in use today [250].

#### 4.3.5. Copper

Due to its unique properties, copper is a versatile metal employed in various applications, including electric and electronic devices, automobiles, and plumbing. It boasts high thermal and electrical conductivity and exhibits considerable corrosion resistance. Copper is derived from both ores and recycled scrap. The production originating from ores is commonly termed primary production, while the production sourced from recycled scrap is called secondary production [251]. In 2022, the collective global copper mine production is estimated to have reached 22 million tons. This represents a consistent upward trend over the last ten years, increasing from 16 million metric tons in 2010. Close to 70 % of copper production is dedicated to applications involving electrical conductivity and communications. Copper stands out as one of the rare materials that can undergo repeated recycling without any degradation in performance. Additionally, there is no distinction in quality between recycled copper and freshly mined copper, allowing them to be used interchangeably [252]. Over the past decade, approximately 35 % of the annual copper consumption was sourced from recycled materials.

#### 4.3.6. Sodium

Sodium is characterized by its soft, silvery-white appearance and high reactivity. In its elemental form, sodium is not naturally occurring and must be synthesized from compounds. Sodium is the sixth most abundant element in the Earth's crust, which contains 2,83 % of sodium in all its forms. It contains numerous minerals such as feldspars, sodalite, and halite (NaCl). Sodium, in its metallic state, plays a crucial role in producing esters and manufacturing organic compounds.

Additionally, sodium is utilized to enhance alloy structure in soap production, sodium vapor lamps, metal descaling, molten metal purification, and glass creation through solid sodium carbonate. Sodium is located below lithium in the far-left column of the periodic table, indicating that they share similar properties. Compared to lithium, sodium is more accessible due to its abundance in the Earth's crust. This lessens the dependence on a select few countries with considerable lithium deposits. Sodium's abundance and affordability in SIBs reduce the need for extensive recovery and recycling efforts compared to lithium.

## 5. Marketing and commercialization trends in SIBs

SIBs are in a pivotal phase of becoming commercially viable. Established companies and newcomers are competing to transition from

laboratory development to large-scale manufacturing, aiming to provide a credible substitute for LIBs, which currently dominate the electric mobility and stationary storage sectors. For the new technology to succeed, it must demonstrate clear advantages over the existing standard. SIBs appear promising, offering superior safety, lower raw material expenses, and better environmental credentials. The following examines some of key aspects of SIBs technology, along with its inherent challenges and strengths, to assess its potential as a viable option beyond traditional LIBs:

- Lower Energy Density: SIBs have at least 30 % lower energy density than LIBs because sodium is heavier and has a lower redox potential. While this makes them less suitable for high-energy tasks like vehicle propulsion, they are well-suited for cost-effective applications such as medium and low-speed electric vehicles. However, SIB technology's research and development progress has advanced significantly in 10 years, compared to more than 30 years of Li-ion development.
- Power Rate Capability: SIBs excel in fast charging, regenerative braking, and grid applications. For instance, Tiamat's NVPF/C 18,650 SIB offer competitive power rates and higher voltage at lower costs per kWh and kW compared to some lithium-ion counterparts.
- Safety and Transport Advantages: SIBs can be safely discharged to 0 V without performance loss, unlike LIBs, which require more expensive copper collectors that can oxidize. This allows SIBs to be transported without regulatory issues and reduces safety risks like dendrites and explosions.
- Eco-Friendly Materials: Na-ion batteries use abundant, cobalt-free materials such as manganese, iron, and nickel.
- Cost-Effective Production: Large-scale production of sodium ion cells offers the potential for significant cost savings, estimated at 20 % to 30 % compared to LFP batteries, which currently dominate stationary storage. This advantage arises from the abundance of sodium and its comparatively low extraction and purification costs. Additionally, utilizing aluminum rather than copper for the anode current collector, a feature unique to SIBs, further drives down costs and reduces supply chain risks. The switch to aluminum can yield a cost reduction of approximately 10 % per kWh. Moreover, existing lithium-ion manufacturing infrastructure can be repurposed for sodium ion production, minimizing the need for additional investments. Nonetheless, it's essential to recognize that these cost savings remain speculative and contingent upon successful large-scale production and widespread market adoption.

The increasing demand for renewable energy has driven the need for energy storage solutions, particularly SIBs. The growth of renewable energy sources, such as solar and wind power, has created opportunities for SIBs in providing efficient and cost-effective energy storage. Despite challenges such as initial investment requirements and performance limitations at low temperatures, SIBs offer a promising solution for grid-scale energy storage and support the expansion of renewable energy infrastructure. With the global push towards emissions reduction and renewable energy adoption, the market potential for SIBs is expected to continue growing [253]. The global SIBs market size was valued at $1025 million 2021, and SIBs industry is projected to reach $2665 million by 2031, growing at a CAGR of 11.2 % from 2021 to 2030 (Fig. 16) [254].

The market introduction of SIBs is anticipated to be rapid, given their similarities with LIBs in working principles and materials. Making use of existing battery manufacturing infrastructure, SIBs provide benefits such as storage and transport at 0 V, reducing costs and safety risks. Companies like Faradion, Tiamat, Altris AB, HiNa, Natron Energy, and Indi Energy are actively involved in SIB development, offering various sodium chemistry options. Recognizing the research potential, the Faraday Institution launched NEXGENNA to innovate high-performance, cost-competitive SIBs.

China's sodium-ion batteries are forecasted by SNE Research to enter mass production by 2025, targeting two-wheelers, small EVs, and energy storage, with costs expected to undercut lithium iron phosphate batteries by 11 % to 24 % by 2035, creating a $14 billion annual market. These batteries are characterized by lower energy density but higher electrochemical stability and cold resistance, promising a complementary role alongside lithium batteries. BYD's construction of a sodium-ion battery plant in Xuzhou, aiming to produce 30 GWh annually starting in January 2024, signifies a major breakthrough in the sector. Other key

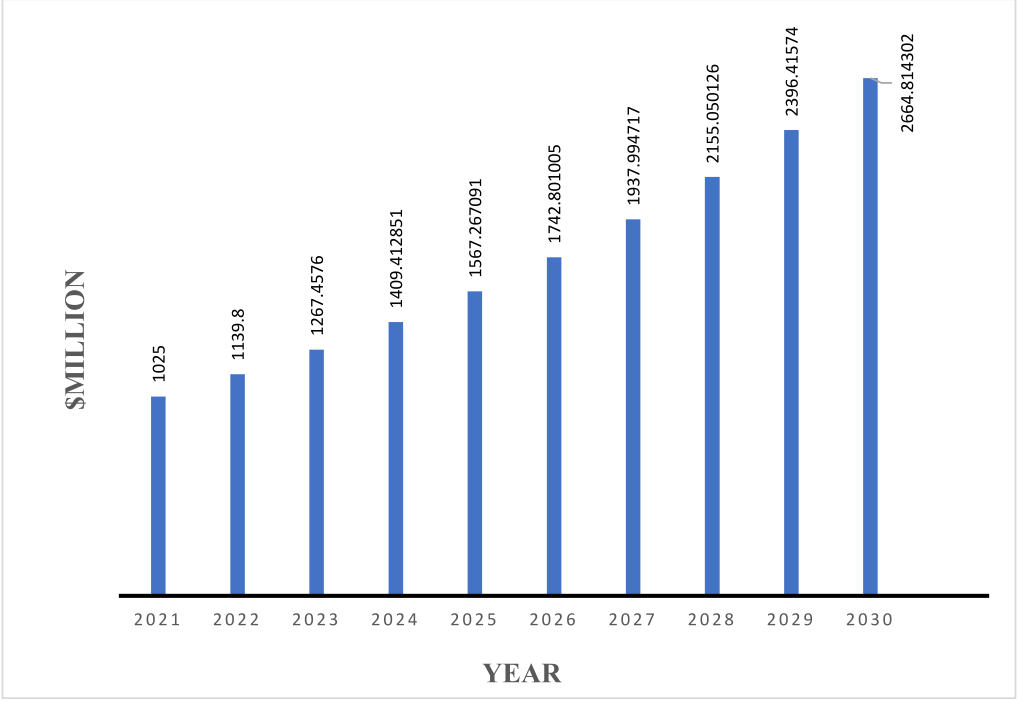


**Fig. 16.** The estimated global sodium ion battery market size by 2031.

players such as JAC Yiwei, Jiangling Motors, CATL, and Chery Auto's iCar brand are also actively contributing to the adoption and production of sodium-ion batteries.

North America stands out as a prime market for SIBs, with a projected growth rate of 15.9 %. Collaborations between companies like Natron Energy and Clarion are driving SIB production, with a Michigan facility poised to become the world's largest SIB manufacturing plant by 2023. In India, as the shift to EVs gains momentum, there is a rising need for battery recycling and repurposing. Despite reduced performance in EVs, retired EV batteries offer potential for second-life applications or recycling, supporting environmental sustainability. Emerging technologies like lithium-ion batteries are gaining prominence, highlighting the importance of proper disposal and recycling practices for environmental protection and a secure supply chain for battery manufacturers. Segmented by application (residential, commercial, industrial) and end-use (stationary energy storage, transportation), the sodium ion battery market is thriving in North America, followed by Europe and Asia-Pacific [255].

Commercialization of SIBs requires overcoming technological hurdles and reducing expenses. Improving SIB performance to meet the requirements of extensive energy storage systems is a key aspect of the global commercialization strategy. Companies are actively engaged in developing SIB technologies to offer low cost, high-rate capability, and cycle stability, crucial for large-scale energy storage applications [20]. Progress towards commercializing SIBs has been led by startup companies, with over ten emerging in the field. CATL, Faradion Limited, Tiamat, Novasis Energies, and HiNa are spearheading efforts in SIB commercialization. Founded 2011 in the UK, Faradion is the world's first non-aqueous sodium-ion battery company. Their batteries utilize a layered nickelate oxides cathode, hard carbon anode, and non-aqueous liquid electrolyte, ensuring optimal performance. In 2017, Faradion introduced an electric bicycle prototype powered by a 418 Wh SIB. This SIB demonstrated the potential to exceed the energy densities of LiFePO4/graphite, featuring rapid cycle life convergence, comparable rate performance, and charge acceptance [256]. Also, Faradion focuses on pouch cells with proprietary cathode $Na_{1.1}Ni_{0.3}Mn_{0.5}Mg_{0.05}Ti_{0.05}O_2$ and hard carbon anode. Faradion's SIBs offer an impressive energy density, ranging from 140 to 160 kWh kg $^{-1}$ in a 32 Ah pouch cell at 4.2–1.0 V, with a cycling lifetime of 1000 or 3000 cycles. Faradion's SIBs serve as a viable alternative to lead-acid batteries for electric transportation. With a specific energy density of around 80 Wh $kg^{-1}$, Faradion's 3 Ah pouch cell can form a 400 W h battery pack, suitable for use as a 12 V battery for starter-lighting-ignition or as a mild hybrid EV 48 V battery [229].

Tiamat specializes in cylindrical cells with $Na_3V_2(PO_4)_2F_3$ cathode and hard carbon anode, while HiNa produces pouch cells with $Na_{0.9}[Cu_{0.22}Fe_{0.30}Mn_{0.48}]O_2$ cathode and hard carbon anode, boasting the largest SIB module to date in China [257]. Since 2011, Hu's research group has focused on developing SIB technology, drawing on over 30 years of experience with LIBs. HiNa, founded with a vision for low-cost, high-performance, eco-friendly, and safe SIBs, now holds numerous patents and is advancing battery products for the market. In 2014, the research team at HiNa discovered the electrochemical activity of the $Cu^{3+}/Cu^{2+}$ redox couple in a $P_2$-phase $Na_{0.68}Cu_{0.34}Mn_{0.66}O_2$ material. In 2019, HiNa announced the largest SIB module ever, a 100 kWh (30 kW power) installation in Jiangsu Province, China, for energy management through load shifting. Novasis Energies, founded in 2010 by academic scientists, specializes in SIBs for energy storage. Their proprietary technology includes Prussian blue analog cathodes and hard carbon anodes with a non-aqueous electrolyte. These materials offer high capacity and retention rates. The fabrication process is simple and cost-effective, using readily available chemicals without rare or hazardous substances. This approach promises significant reductions in energy consumption and manufacturing costs compared to other battery materials [20].

CATL, founded in 2011, has established ten battery manufacturing bases globally, including locations in Sichuan, Guangdong, and Germany, with subsidiaries in Paris, Japan, Yokohama, and Detroit. Using a combination of lithium-ion and sodium-ion cells in a single pack, CATL introduced its first-generation sodium-ion battery in 2021. This innovative battery features a PBA cathode and a porous hard carbon anode. Additionally, in 2023, CATL announced the launch of a compact battery with an energy density of up to 500 Wh/kg, enabling the electrification of passenger aircraft. In 2023, the first electric car powered by SIB was introduced, marking a big step forward in making this new technology widely available [258].

## 6. Conclusion and prospect

SIBs present a promising alternative to LIBs, offering advantages such as low raw material costs and good safety performance. However, current high-performance SIBs face challenges, including low cycle stability, capacity, operating potential, and electronic conductivity. Considering the current advancements in this technology, the direction for the next generation of NIBs can be established by addressing critical materials design issues and delving into essential scientific topics:

- It is possible to use SIBs as a complement, not a replacement, for LIBs, particularly in applications where energy density is less critical. They offer a sustainable alternative, reducing dependence on lithium and mitigating potential shortages.
- Cathode materials for SIBs include layered transition metal oxides, polyanionic compounds, Prussian blue analogs, and organic compounds, each with advantages and limitations. Strategies to enhance electrochemical performance, such as encapsulation, nanosizing, and doping with elements, are employed, with doping and encapsulation being the most common methods.
- The future advancements in cathode materials predominantly revolve around creating high-capacity cathode materials with superior performance. In the context of SIBs, layered oxides exhibit notable capacity and charge–discharge potential. However, their structure often collapses over extended cycling periods due to numerous phase transitions during charge and discharge operations. Polyanionic compounds, characterized by robust frameworks, offer stable electrochemical performance and high thermal safety. Nonetheless, their larger anionic groups typically result in diminished capacity and inadequate electronic conductivity. Prussian blue materials, featuring a spacious tunnel structure, demonstrate relatively stable cycling behavior. Yet, they possess low tap density and pose challenges in removing crystal water, potentially escalating safety risks during thermal runaway.
- Mn-based layered oxides are a good option for NIBs in transportation and storage, offering low toxicity, suitable voltage, and high capacity. Further experimental studies are needed to validate the reversible oxygen redox hypothesis and understand decomposition risks associated with intercalation compounds. Polyanionic materials, like sodium vanadium fluorophosphate, excel in high-voltage and long-life applications but face challenges due to toxic V metal. Despite lower energy density, Prussian Blue analogues are reliable for aqueous NIBs, while manganese- and iron-based compounds offer superior performance with eco-friendly metals.
- The industrial chain for sodium-ion batteries is less mature than that for lithium-ion batteries. This includes the supply chain for materials like cathodes, anodes, electrolytes, and separators, leading to higher costs and less scalable production. The similarity in manufacturing equipment for both battery types allows for easier transition and adaptation. As investment in sodium-ion technology grows, the industrial chain is expected to mature, reducing costs and increasing production efficiency.
- SIBs offer a sustainable alternative to Li-ion batteries due to their environmentally friendly electrodes made of elements like Mn, Fe, and Ni. They are also Co-free, which resonates with lower prices and

cost reduction of stored kWh. Additionally, Na-ion technology stands as an attractive option for greener and more sustainable batteries, contributing to the electrification of the world without creating new environmental burdens.

- Due to their specific chemistries and materials, recycling SIBs poses unique challenges, requiring efficient extraction methods for components like fluorinated compounds and electrolytes. Early commercialization efforts of SIBs should prioritize recyclability to foster a circular industry. Future research should explore new materials and develop cost-effective recycling methods to promote sustainability and economic viability. Efforts should also focus on formulating recycling standards to ensure the healthy development of the SIB industry, aiming for batteries that can be efficiently recycled with high material utilization efficiency and low cycle life energy consumption and emissions. This outlook underscores the importance of addressing recycling challenges and advancing sustainability in the SIB industry.
- The cost-effectiveness and enhanced safety of NIBs make them an appealing energy storage option for both stationary and mobile applications. While first-generation NIBs are already available, second-generation cells must reduce cost per kWh to compete with LIBs, achievable through cells reaching 210 Wh $kg^{-1}$ with specific cathode and hard carbon capacities. Individual components meet sub-targets, but further material development, especially for second-generation cells, is necessary to fully meet goals. Overall, by commercializing first-generation systems and innovating next-generation materials, NIBs will become more commercially viable. Continued research and development of Na-based technologies are crucial for advancing NIB technology in the near future.
- Despite challenges like initial investment requirements and performance limitations, SIBs offer cost-effective energy storage, especially in regions like China, North America, and India, where collaborations and EV adoption drive market growth. Startups like Faradion and established players like CATL are advancing SIB commercialization and developing high-performance batteries suitable for large-scale energy storage and transportation applications. As efforts continue to improve SIB performance and overcome technological hurdles, the industry is poised for significant growth, contributing to the global shift towards renewable energy.

## Declaration of competing interest

The authors declare that they have no known competing financial interests or personal relationships that could have appeared to influence the work reported in this paper.

## Acknowledgments

This work was supported by the Ministry of Education and Culture (Grant agreement number OKM/32/524/2022). Academy of Finland, Govermat project (grant no 346726) is acknowledged for financial support. U.L. acknowledges Finnish Research Impact Foundation for Tandem Industry Academy professorship funding in 2023-2025.

## References

[1] J.L. Holechek, H.M.E. Geli, M.N. Sawalhah, R. Valdez, A global assessment: can renewable energy replace fossil fuels by 2050? Sustainability (switzerland) 14 (2022) https://doi.org/10.3390/su14084792.
[2] Y. Liu, J. Li, Q. Shen, J. Zhang, P. He, X. Qu, Y. Liu, Advanced characterizations and measurements for sodium-ion batteries with NASICON-type cathode materials, Escience 2 (2022) 10–31, https://doi.org/10.1016/j.esci.2021.12.008.
[3] Y. Liu, X. Liu, T. Wang, L.Z. Fan, L. Jiao, Research and application progress on key materials for sodium-ion batteries, Sustain, Energy Fuels 1 (2017) 986–1006, https://doi.org/10.1039/c7se00120g.
[4] Y. Wang, Y. Liu, Y. Liu, Q. Shen, C. Chen, F. Qiu, P. Li, L. Jiao, X. Qu, Recent advances in electrospun electrode materials for sodium-ion batteries, Journal of Energy Chemistry 54 (2021) 225–241, https://doi.org/10.1016/j.jechem.2020.05.065.
[5] D.A. Winn, J.M. Shemilt, B.C.H. Steele, Titanium Disulphide: A Solid Solution Electrode for Sodium and Lithium, Pergamon Press Inc, 1976.
[6] G.H. Newman, L.P. Klemann, Ambient Temperature Cycling of an Na-TiS2 Cell, J. EZectrochem. Soc.: Electrochemical Science and Technology (1980).
[7] K. Mizushima, P.C. Jones, P.J. Wiseman, J.B. Goodenough, LixCoO 2 (0<x~l): A New Cathode Material for Batteries of High Energy Density, 1980.
[8] C. Delmas, J.-J. Braconnier, C. Fouassier, P. Hagenmuller, Electrochemical Intercalation of Sodium in NaxCoO2 Bronzes, 1981.
[9] Lawrence W. Shacklette, Linda B. Townsend, Taiguang R. Jow, Rechargeable battery cathode from P2-phase sodium cobalt dioxide, 5,011,748, 1991.
[10] S. Megahed, B. Scrosati, Lithium-ion rechargeable batteries, 1994.
[11] Toshikazu Shishikura, Masataka Takeuchi, Yoshihiko Murakoshi, Hiroshi Konuma, Mutsumi Kameyama, Secondary batteries, United States Patent 5,051,325 (1991).
[12] R.J. Gummow, A. De Kock, M.M. Thackeray ', E3 6_Solid State Improved capacity retention in rechargeable 4 V lithium/lithium-manganese oxide (spinel) cells, 1994.
[13] A.K. Padhi, K.S. Nanjundaswamy, C. Masquelier, S. Okada, J.B. Goodenough, Effect of structure on the Fe3 + / Fe2 + redox couple in iron phosphates, J Electrochem Soc 144 (1997) 1609–1613, https://doi.org/10.1149/1.1837649.
[14] K. Chayambuka, G. Mulder, D.L. Danilov, P.H.L. Notten, From Li-Ion batteries toward Na-ion chemistries: challenges and opportunities, Adv Energy Mater 10 (2020), https://doi.org/10.1002/aenm.202001310.
[15] M.M. Doeff, M.Y. Peng, Y. Ma, L.C. De Jonghe, Orthorhombic NaxMn02 as a Cathode Material for Secondary Sodium and Lithium Polymer Batteries, 1994.
[16] D.A. Stevens, J.R. Dahn, High Capacity Anode Materials for Rechargeable Sodium-Ion Batteries, 2000.
[17] D.A. Stevens, J.R. Dahn, The mechanisms of lithium and sodium insertion in carbon materials, J Electrochem Soc 148 (2001) A803, https://doi.org/10.1149/1.1379565.
[18] J. Barker, M.Y. Saidi, J.L. Swoyer, A sodium-ion cell based on the fluorophosphate compound NaVPO4F, Electrochem. Solid St. 6 (2003), https://doi.org/10.1149/1.1523691.
[19] D. Larcher, J.M. Tarascon, Towards greener and more sustainable batteries for electrical energy storage, Nat Chem 7 (2015) 19–29, https://doi.org/10.1038/nchem.2085.
[20] A. Bauer, J. Song, S. Vail, W. Pan, J. Barker, Y. Lu, The scale-up and commercialization of nonaqueous Na-ion battery technologies, Adv Energy Mater 8 (2018), https://doi.org/10.1002/aenm.201702869.
[21] B.K. Ganesan, M. Moorthy, R. Thangavel, K.W. Nam, V. Aravindan, Y.S. Lee, Fluorine substitution enabled superior performance of NaxMn2-xO1.5F0.5 (x = 1.05–1.3) type Na-rich cathode, Chem. Eng. J. 454 (2023), https://doi.org/10.1016/j.cej.2022.139876.
[22] H. Gao, J. Zeng, Z. Sun, X. Jiang, X. Wang, Advances in layered transition metal oxide cathodes for sodium-ion batteries, Mater Today Energy 42 (2024), https://doi.org/10.1016/j.mtener.2024.101551.
[23] B.K. Ganesan, R. Thangavel, Y.S. Lee, Studying Na criticality in NaxMn2−xO2 (x = 1.05–1.3) type Na-rich disordered rocksalt cathode for higher capacity, Mater Today Chem 28 (2023), https://doi.org/10.1016/j.mtchem.2022.101368.
[24] S.K. Saju, S. Chattopadhyay, J. Xu, S. Alhashim, A. Pramanik, P.M. Ajayan, Hard carbon anode for lithium-, sodium-, and potassium-ion batteries: Advancement and future perspective, Cell Rep Phys Sci (2024), https://doi.org/10.1016/j.xcrp.2024.101851.
[25] M.D. Slater, D. Kim, E. Lee, C.S. Johnson, Sodium-ion batteries, Adv Funct Mater 23 (2013) 947–958, https://doi.org/10.1002/adfm.201200691.
[26] Z.X. Huang, Z.Y. Gu, Y.L. Heng, E. Huixiang Ang, H.B. Geng, X.L. Wu, Advanced layered oxide cathodes for sodium/potassium-ion batteries: Development, challenges and prospects, Chem. Eng. J. 452 (2023), https://doi.org/10.1016/j.cej.2022.139438.
[27] W. Lee, J. Kim, S. Yun, W. Choi, H. Kim, W.S. Yoon, Multiscale factors in designing alkali-ion (Li, Na, and K) transition metal inorganic compounds for next-generation rechargeable batteries, Energy Environ Sci 13 (2020) 4406–4449, https://doi.org/10.1039/d0ee01277g.
[28] S.M. Oh, S.T. Myung, C.S. Yoon, J. Lu, J. Hassoun, B. Scrosati, K. Amine, Y.K. Sun, Advanced Na[Ni0.25Fe0.5Mn0.25]O 2/C-Fe3O4 sodium-ion batteries using EMS electrolyte for energy storage, Nano Lett 14 (2014) 1620–1626, https://doi.org/10.1021/nl500077v.
[29] X.T. Wang, Y. Yang, J.Z. Guo, Z.Y. Gu, E.H. Ang, Z.H. Sun, W.H. Li, H.J. Liang, X. L. Wu, An advanced cathode composite for co-utilization of cations and anions in lithium batteries, J Mater Sci Technol 102 (2022) 72–79, https://doi.org/10.1016/j.jmst.2021.05.074.
[30] E. Goikolea, V. Palomares, S. Wang, I.R. de Larramendi, X. Guo, G. Wang, T. Rojo, Na-ion batteries—approaching old and new challenges, Adv Energy Mater 10 (2020), https://doi.org/10.1002/aenm.202002055.
[31] H.L. Yang, B.W. Zhang, K. Konstantinov, Y.X. Wang, H.K. Liu, S.X. Dou, Progress and challenges for all-solid-state sodium batteries, Advanced Energy and Sustainability Research 2 (2021), https://doi.org/10.1002/aesr.202000057.
[32] L. Liu, X. Qi, Q. Ma, X. Rong, Y.S. Hu, Z. Zhou, H. Li, X. Huang, L. Chen, Toothpaste-like electrode: a novel approach to optimize the interface for solid-state sodium-ion batteries with ultralong cycle life, ACS Appl Mater Interfaces 8 (2016) 32631–32636, https://doi.org/10.1021/acsami.6b11773.
[33] H. Hou, Q. Xu, Y. Pang, L. Li, J. Wang, C. Zhang, C. Sun, Efficient storing energy harvested by triboelectric nanogenerators using a safe and durable all-solid-state sodium-ion battery, Adv. Sci. 4 (2017), https://doi.org/10.1002/advs.201700072.

[34] L. Chen, J. Liu, Z. Guo, Y. Wang, C. Wang, Y. Xia, Electrochemical profile of LiTi 2 (PO 4) 3 and NaTi 2 (PO 4) 3 in lithium, sodium or mixed ion aqueous solutions, J Electrochem Soc 163 (2016) A904–A910, https://doi.org/10.1149/2.0531606jes.

[35] J. Li, G. Du, T. Huang, F. Zhang, M. Xie, Y. Qi, S.J. Bao, M. Xu, Na3V2O2(PO4)2F cathode for high-performance quasi-solid-state sodium-ion batteries with a wide workable temperature range, Energ. Technol. 8 (2020), https://doi.org/10.1002/ente.202000494.

[36] Y. You, X.L. Wu, Y.X. Yin, Y.G. Guo, High-quality Prussian blue crystals as superior cathode materials for room-temperature sodium-ion batteries, Energy Environ Sci 7 (2014) 1643–1647, https://doi.org/10.1039/c3ee44004d.

[37] K. Soo Park, M. Hun Cho, S. Jang Jin, C. Hoon Song, K. Suk Nahm, Structural and Electrochemical Characteristics of Li 0.7 [Li 1/6 Mn 5/6 ]O 2 Synthesized using Sol-Gel Method, 2005.

[38] N. Yabuuchi, K. Kubota, M. Dahbi, S. Komaba, Research development on sodium-ion batteries, Chem Rev 114 (2014) 11636–11682, https://doi.org/10.1021/cr500192f.

[39] Q. Liu, Z. Hu, M. Chen, C. Zou, H. Jin, S. Wang, S.L. Chou, S.X. Dou, Recent progress of layered transition metal oxide cathodes for sodium-ion batteries, Small 15 (2019), https://doi.org/10.1002/smll.201805381.

[40] A.K. Rai, L.T. Anh, J. Gim, V. Mathew, J. Kim, Electrochemical properties of NaxCoO2 (x–0.71) cathode for rechargeable sodium-ion batteries, Ceram Int 40 (2014) 2411–2417, https://doi.org/10.1016/j.ceramint.2013.08.013.

[41] L. Gao, S. Chen, H. Hu, H. Cheng, L. Zhang, X. Yang, Hierarchical NaxCoO2 microspheres with low surface area toward high performance sodium ion batteries, Mater Lett 260 (2020), https://doi.org/10.1016/j.matlet.2019.126965.

[42] R. Akram, J. Khan, S. Rafique, M. Hussain, A. Maqsood, A. Ali Naz, Enhanced thermoelectric properties of single phase Na doped NaXCoO2 thermoelectric material, Mater Lett 300 (2021), https://doi.org/10.1016/j.matlet.2021.130180.

[43] W. Luo, F. Shen, C. Bommier, H. Zhu, X. Ji, L. Hu, Na-ion battery anodes: materials and electrochemistry, Acc Chem Res 49 (2016) 231–240, https://doi.org/10.1021/acs.accounts.5b00482.

[44] R. Zhang, Z. Lu, Y. Yang, W. Shi, First-principles investigation of the monoclinic NaMnO2 cathode material for rechargeable Na-ion batteries, Curr. Appl Phys. 18 (2018) 1431–1435, https://doi.org/10.1016/j.cap.2018.08.011.

[45] S. Guo, H. Yu, Z. Jian, P. Liu, Y. Zhu, X. Guo, M. Chen, M. Ishida, H. Zhou, A high-capacity, low-cost layered sodium manganese oxide material as cathode for sodium-ion batteries, ChemSusChem 7 (2014) 2115–2119, https://doi.org/10.1002/cssc.201402138.

[46] E.A. Raekelboom, A.L. Hector, J. Owen, G. Vitins, M.T. Weller, Syntheses, structures, and preliminary electrochemistry of the layered lithium and sodium manganese(IV) oxides, A2Mn3O7, Chem. Mater. 13 (2001) 4618–4623, https://doi.org/10.1021/cm011105j.

[47] C. Yang, X. Peng, J. Yu, S. Li, H. Zhang, Engineering crystal-facet modulation to obtain stable Mn-based P2-layered oxide cathodes for sodium-ion batteries, J Colloid Interface Sci 629 (2023) 1061–1067, https://doi.org/10.1016/j.jcis.2022.09.065.

[48] T. Cui, X. Li, Y. Si, Y. Fu, Synergetic anion-cation co-doping in Na0.44MnO2 boosting a high-stability and improved-kinetics cathode for sodium ion battery, Energy Storage Mater 65 (2024), https://doi.org/10.1016/j.ensm.2023.103161.

[49] N. Yabuuchi, H. Yoshida, S. Komaba, Crystal structures and electrode performance of alpha-NaFeO2 for rechargeable sodium batteries, Electrochemistry 80 (2012) 716–719, https://doi.org/10.5796/electrochemistry.80.716.

[50] R.D. McAuliffe, G.E. Kamm, M.J. McDermott, R.P. Hermann, N. Vasquez-Garcia, R.L. Sacci, K.A. Persson, K.W. Chapman, G.M. Veith, Direct mechanochemical synthesis, phase stability, and electrochemical performance of α-NaFeO2, Inorg Chem 62 (2023) 3358–3367, https://doi.org/10.1021/acs.inorgchem.2c03286.

[51] J. Jayachitra, J. Richards Joshua, A. Balamurugan, N. Sivakumar, V. Sharmila, S. Shanavas, M. Abu Haija, M. Waqas Alam, A. BaQais, High electrode performance of hydrothermally developed activated C coated O3–NaFeO2 electrode for Na-ion batteries applications, Ceram Int 49 (2023) 48–56, https://doi.org/10.1016/j.ceramint.2022.07.110.

[52] Y. Zhuang, J. Zhao, Y. Zhao, X. Zhu, H. Xia, Carbon-coated single crystal O3-NaFeO2 nanoflakes prepared via topochemical reaction for sodium-ion batteries, Sustain. Mater. Technol. 28 (2021), https://doi.org/10.1016/j.susmat.2021.e00258.

[53] L. Wang, J. Wang, X. Zhang, Y. Ren, P. Zuo, G. Yin, J. Wang, Unravelling the origin of irreversible capacity loss in NaNiO2 for high voltage sodium ion batteries, Nano Energy 34 (2017) 215–223, https://doi.org/10.1016/j.nanoen.2017.02.046.

[54] M. Wable, B. Bal, Ö.Ö. Capraz, Probing electrochemical strain generation in sodium chromium oxide (NaCrO2) cathode in Na-ion batteries during charge/discharge, Energy Advances (2024), https://doi.org/10.1039/d3ya00563a.

[55] Z. Lu, J.R. Dahn, In Situ X-ray diffraction study of P2-Na[sub 2/3][Ni[sub 1/3]Mn[sub 2/3]]O[sub 2], J Electrochem Soc 148 (2001) A1225, https://doi.org/10.1149/1.1407247.

[56] S. Komaba, N. Yabuuchi, T. Nakayama, A. Ogata, T. Ishikawa, I. Nakai, Study on the reversible electrode reaction of Na 1-xNi 0.5Mn 0.5O 2 for a rechargeable sodium-ion battery, Inorg Chem 51 (2012) 6211–6220, https://doi.org/10.1021/ic300357d.

[57] Y. Chang, Y. Zhou, Z. Wang, X. Li, D. Wang, J. Duan, J. Wang, G. Yan, Synthesis of NaNi0.5Mn0.5O2 cathode materials for sodium-ion batteries via spray pyrolysis method, J Alloys Compd 922 (2022), https://doi.org/10.1016/j.jallcom.2022.166283.

[58] X. Peng, H. Zhang, C. Yang, Z. Lui, Z. Lin, Y. Lei, S. Zhang, S. Li, S. Zhang, Promoting threshold voltage of P2-Na0.67Ni0.33Mn0.67O2 with Cu2+ cation doping toward high-stability cathode for sodium-ion battery, J Colloid Interface Sci 659 (2024) 422–431, https://doi.org/10.1016/j.jcis.2023.12.170.

[59] M. Aranda, P. Lavela, J.L. Tirado, A novel potassium-containing layered oxide for the cathode of sodium-ion batteries, Battery Energy (2024), https://doi.org/10.1002/bte2.20230057.

[60] D. Carlier, J.H. Cheng, R. Berthelot, M. Guignard, M. Yoncheva, R. Stoyanova, B. J. Hwang, C. Delmas, The P2-Na2/3Co2/3Mn1/3O2 phase: Structure, physical properties and electrochemical behavior as positive electrode in sodium battery, Journal of the Chemical Society Dalton Trans. 40 (2011) 9306–9312, https://doi.org/10.1039/c1dt10798d.

[61] X. Wang, M. Tamaru, M. Okubo, A. Yamada, Electrode properties of P2-Na2/3MnyCo 1- yO2 as cathode materials for sodium-ion batteries, J. Phys. Chem. C 117 (2013) 15545–15551, https://doi.org/10.1021/jp406433z.

[62] N. Bucher, S. Hartung, J.B. Franklin, A.M. Wise, L.Y. Lim, H.Y. Chen, J.N. Weker, M.F. Toney, M. Srinivasan, P2-NaxCoyMn1-yO2 (y = 0, 0.1) as cathode materials in sodium-ion batteries - effects of doping and morphology to enhance cycling stability, Chem. Mater. 28 (2016) 2041–2051, https://doi.org/10.1021/acs.chemmater.5b04557.

[63] N. Yabuuchi, M. Kajiyama, J. Iwatate, H. Nishikawa, S. Hitomi, R. Okuyama, R. Usui, Y. Yamada, S. Komaba, P2-type Nax [Fe1/2 Mn1/2[O2 made from earth-abundant elements for rechargeable NaÂ batteries, Nat Mater 11 (2012) 512–517, https://doi.org/10.1038/nmat3309.

[64] B. Mortemard de Boisse, D. Carlier, M. Guignard, C. Delmas, Structural and electrochemical characterizations of P2 and New O3-Na x Mn 1-y Fe y O 2 phases prepared by auto-combustion synthesis for Na-ion batteries, J Electrochem Soc 160 (2013) A569–A574, https://doi.org/10.1149/2.032304jes.

[65] W.M. Dose, N. Sharma, J.C. Pramudita, J.A. Kimpton, E. Gonzalo, M.H. Han, T. Rojo, Cystallographic evolution of P2 Na2/3Fe0.4Mn0.6O2 electrodes during electrochemical cycling, Chem. Mater. 28 (2016) 6342–6354, https://doi.org/10.1021/acs.chemmater.6b02714.

[66] Y. Xi, Y. Lu, Mechanochemical synthesis of Fe/Mn-based binary hexacyanoferrate for sodium-ion battery, Powder Technol 423 (2023), https://doi.org/10.1016/j.powtec.2023.118500.

[67] J. Billaud, G. Singh, A.R. Armstrong, E. Gonzalo, V. Roddatis, M. Armand, T. Rojo, P.G. Bruce, Na0.67Mn1-xMgxO2 ($0 \leq x \leq 0.2$): A high capacity cathode for sodium-ion batteries, in: Energy Environ Sci, Royal Society of Chemistry, 2014: pp. 1387–1391. https://doi.org/10.1039/c4ee00465e.

[68] D. Buchholz, C. Vaalma, L.G. Chagas, S. Passerini, Mg-doping for improved long-term cyclability of layered Na-ion cathode materials - The example of P2-type NaxMg0.11Mn0.89O2, J Power Sources 282 (2015) 581–585, https://doi.org/10.1016/j.jpowsour.2015.02.069.

[69] H. Yu, S. Guo, Y. Zhu, M. Ishida, H. Zhou, Novel titanium-based O3-type NaTi0.5Ni0.5O2 as a cathode material for sodium ion batteries, Chem. Commun. 50 (2014) 457–459, https://doi.org/10.1039/c3cc47351a.

[70] S. Guo, H. Yu, P. Liu, Y. Ren, T. Zhang, M. Chen, M. Ishida, H. Zhou, High-performance symmetric sodium-ion batteries using a new, bipolar O3- type material, Na0.8Ni0.4Ti0.6O2, Energy Environ. Sci. 8 (2015) 1237–1244.

[71] G. Li, W. Zhu, W. Liu, First-principles calculations of the Ti-doping effects on layered NaNiO2 cathode materials for advanced Na-ion batteries, J. Indian Chem. Soc. 99 (2022), https://doi.org/10.1016/j.jics.2022.100424.

[72] W. Li, Y. Wang, G. Hu, Z. Peng, Y. Cao, Y. Zeng, K. Du, Ti-doped NaCrO2 as cathode materials for sodium-ion batteries with excellent long cycle life, J Alloys Compd 779 (2019) 147–155, https://doi.org/10.1016/j.jallcom.2018.11.257.

[73] N. Sabi, S. Doubaji, K. Hashimoto, S. Komaba, K. Amine, A. Solhy, B. Manoun, E. Bilal, I. Saadoune, Layered P2-Na2/3Co1/2Ti1/2O2 as a high-performance cathode material for sodium-ion batteries, J Power Sources 342 (2017) 998–1005, https://doi.org/10.1016/j.jpowsour.2017.01.025.

[74] H.Y.D.L.W.T.X.L.N.H.M.I. and H.Z. Shaohua Guo, A novel tunnel Na0.61Ti0.48Mn0.52O2 cathode material for sodium-ion batteries, ChemComm 50 (2014) 7998–8001.

[75] Y. Wang, J. Liu, B. Lee, R. Qiao, Z. Yang, S. Xu, X. Yu, L. Gu, Y.S. Hu, W. Yang, K. Kang, H. Li, X.Q. Yang, L. Chen, X. Huang, Ti-substituted tunnel-type Na0.44MnO2 oxide as a negative electrode for aqueous sodium-ion batteries, Nat Commun 6 (2015), https://doi.org/10.1038/ncomms7401.

[76] H. Yoshida, N. Yabuuchi, S. Komaba, NaFe0.5Co0.5O2 as high energy and power positive electrode for Na-ion batteries, Electrochem Commun 34 (2013) 60–63, https://doi.org/10.1016/j.elecom.2013.05.012.

[77] J.A.K. Satrughna, A. Kanwade, A. Srivastava, M.K. Tiwari, S.C. Yadav, S.T. Akula, P.M. Shirage, Experimental and ab initio based DFT calculation of NaFe0.5Co0.5O2 as an excellent cathode material for futuristic sodium ion batteries, J Energy Storage 65 (2023) 107371, https://doi.org/10.1016/j.est.2023.107371.

[78] X. Wang, G. Liu, T. Iwao, M. Okubo, A. Yamada, Role of ligand-to-metal charge transfer in O3-type NaFeO 2-NaNiO2 solid solution for enhanced electrochemical properties, J. Phys. Chem. C 118 (2014) 2970–2976, https://doi.org/10.1021/jp411382r.

[79] I. Moeez, D. Susanto, G. Ali, H.G. Jung, H.D. Lim, K.Y. Chung, Effect of the interfacial protective layer on the NaFe0.5Ni0.5O2cathode for rechargeable sodium-ion batteries, J Mater Chem A Mater 8 (2020) 13964–13970, https://doi.org/10.1039/d0ta02837a.

[80] Z.Y. Li, R. Gao, L. Sun, Z. Hu, X. Liu, Designing an advanced P2-Na0.67Mn0.65Ni0.2Co0.15O2 layered cathode material for Na-ion batteries, J Mater Chem A Mater 3 (2015) 16272–16278, https://doi.org/10.1039/c5ta02450a.

[81] C. Hakim, H.D. Asfaw, R. Younesi, D. Brandell, K. Edström, I. Saadoune, Development of P2 or P2/P3 cathode materials for sodium-ion batteries by controlling the Ni and Mn contents in Na0.7CoxMnyNizO2 layered oxide, Electrochim Acta 438 (2023), https://doi.org/10.1016/j.electacta.2022.141540.

[82] X. Li, D. Wu, Y.N. Zhou, L. Liu, X.Q. Yang, G. Ceder, O3-type Na(Mn0.25Fe0.25Co0.25Ni0.25)O2: A quaternary layered cathode compound for rechargeable Na ion batteries, Electrochem Commun 49 (2014) 51–54, https://doi.org/10.1016/j.elecom.2014.10.003.

[83] J.Y. Hwang, S.T. Myung, Y.K. Sun, Quaternary Transition Metal Oxide Layered Framework: O3-Type Na[Ni0.32Fe0.13Co0.15Mn0.40]O2 Cathode Material for High-Performance Sodium-Ion Batteries, J. Phys. Chem. C 122 (2018) 13500–13507, https://doi.org/10.1021/acs.jpcc.7b12140.

[84] L. Wang, Y.G. Sun, L.L. Hu, J.Y. Piao, J. Guo, A. Manthiram, J. Ma, A.M. Cao, Copper-substituted Na0.67Ni0.3-:XCuxMn0.7O2 cathode materials for sodium-ion batteries with suppressed P2–O2 phase transition, J Mater Chem A Mater 5 (2017) 8752–8761, https://doi.org/10.1039/c7ta00880e.

[85] M. Kouthaman, K. Kannan, R. Subadevi, M. Sivakumar, Study on the effect of co-substitution of transition metals on O3-type Na-Mn-Ni-O cathode materials for promising sodium-ion batteries, J Taiwan Inst Chem Eng 140 (2022), https://doi.org/10.1016/j.jtice.2022.104565.

[86] D. Zhou, W. Huang, X. Kang, F. Zhao, L. Zhao, Z. Deng, X. Yan, Y. Yu, M. Xiang, Titanium-doped P2-type Na0.67Co0.67Mn0.33-xTixO2 ($0 \leq x \leq 0.2$) as Novel Cathodes for sodium ion batteries with superior-rate, Int J Electrochem Sci 13 (2018) 2010–2021, https://doi.org/10.20964/2018.02.62.

[87] D. Pahari, S. Puravankara, On controlling the P2–O2 phase transition by optimal Ti-substitution on Ni- site in P2-type Na0.67Ni0.33Mn0.67O2 (NNMO) cathode for Na-ion batteries, J Power Sources 455 (2020), https://doi.org/10.1016/j.jpowsour.2020.227957.

[88] J. Deng, Y. Wang, Z. Wang, J. Li, Y. Luo, Ti and V co-doped P2-Na0.59Co0.10Mn0.90O2 cathode with excellent sodium storage performance, Chem Phys Lett 783 (2021), https://doi.org/10.1016/j.cplett.2021.139050.

[89] T. Li, M. Lu, Y. Zhang, X. Xiang, S. Liu, C. Chen, Structural evolution and redox chemistry of robust ternary layered oxide cathode for sodium-ion batteries, J Alloys Compd 978 (2024), https://doi.org/10.1016/j.jallcom.2024.173459.

[90] M. Leng, J. Bi, W. Wang, Z. Xing, W. Yan, X. Gao, J. Wang, R. Liu, Superior electrochemical performance of O3-type NaNi0.5-xMn0.3Ti0.2ZrxO2 cathode material for sodium-ion batteries from Ti and Zr substitution of the transition metals, J Alloys Compd 816 (2020), https://doi.org/10.1016/j.jallcom.2019.152581.

[91] Z. Wang, L. Fang, X. Fu, S. Zhang, H. Kong, H. Chen, F. Fu, A Ni/Co-free high-entropy layered cathode with suppressed phase transition and near-zero strain for high-voltage sodium-ion batteries, Chem. Eng. J. 480 (2024), https://doi.org/10.1016/j.cej.2023.148130.

[92] M. Nowak, K. Walczak, A. Milewska, J. Płotek, A. Budziak, J. Molenda, Electrochemical performance of different high-entropy cathode materials for Na-ion batteries, J Alloys Compd 968 (2023), https://doi.org/10.1016/j.jallcom.2023.172316.

[93] Y. Gupta, P. Siwatch, R. Karwasra, K. Sharma, S.K. Tripathi, Recent progress of layered structured P2- and O3- type transition metal oxides as cathode material for sodium-ion batteries, Renew. Sustain. Energy Rev. 192 (2024), https://doi.org/10.1016/j.rser.2023.114167.

[94] N.G. Garcia, J.M. Gonçalves, C. Real, B. Freitas, J.G. Ruiz-Montoya, H. Zanin, Medium- and high-entropy materials as positive electrodes for sodium-ion batteries: Quo Vadis? Energy Storage Mater 67 (2024) 103213 https://doi.org/10.1016/j.ensm.2024.103213.

[95] C.M. Rost, E. Sachet, T. Borman, A. Moballegh, E.C. Dickey, D. Hou, J.L. Jones, S. Curtarolo, J.P. Maria, Entropy-stabilized oxides, Nat Commun 6 (2015), https://doi.org/10.1038/ncomms9485.

[96] C. Zhao, F. Ding, Y. Lu, L. Chen, Y.S. Hu, High-Entropy Layered Oxide Cathodes for Sodium-Ion Batteries, Angewandte Chemie - International Edition 59 (2020) 264–269, https://doi.org/10.1002/anie.201912171.

[97] X.Y. Du, Y. Meng, H. Yuan, D. Xiao, High-entropy substitution: A strategy for advanced sodium-ion cathodes with high structural stability and superior mechanical properties, Energy Storage Mater 56 (2023) 132–140, https://doi.org/10.1016/j.ensm.2023.01.010.

[98] D. Chao, C. Zhu, X. Xia, J. Liu, X. Zhang, J. Wang, P. Liang, J. Lin, H. Zhang, Z. X. Shen, H.J. Fan, Graphene quantum dots coated VO2 arrays for highly durable electrodes for Li and Na ion batteries, Nano Lett 15 (2015) 565–573, https://doi.org/10.1021/nl504038s.

[99] F. Ding, C. Zhao, D. Zhou, Q. Meng, D. Xiao, Q. Zhang, Y. Niu, Y. Li, X. Rong, Y. Lu, L. Chen, Y.S. Hu, A novel Ni-rich O3-Na[Ni0.60Fe0.25Mn0.15]O2 cathode for Na-ion batteries, Energy Storage Mater 30 (2020) 420–430, https://doi.org/10.1016/j.ensm.2020.05.013.

[100] M.M. Rahman, J. Mao, W.H. Kan, C.J. Sun, L. Li, Y. Zhang, M. Avdeev, X.W. Du, F. Lin, An ordered P2/P3 composite layered oxide cathode with long cycle life in sodium-ion batteries, ACS Mater Lett 1 (2019) 573–581, https://doi.org/10.1021/acsmaterialslett.9b00347.

[101] B. Fu, X. Zhou, Y. Wang, High-rate performance electrospun Na0.44MnO2 nanofibers as cathode material for sodium-ion batteries, J Power Sources 310 (2016) 102–108, https://doi.org/10.1016/j.jpowsour.2016.01.101.

[102] L. Liu, X. Li, S.H. Bo, Y. Wang, H. Chen, N. Twu, D. Wu, G. Ceder, High-performance P2-type Na2/3(Mn1/2Fe1/4Co1/4)O2 cathode material with superior rate capability for Na-ion batteries, Adv Energy Mater 5 (2015), https://doi.org/10.1002/aenm.201500944.

[103] P. Barpanda, G. Liu, C.D. Ling, M. Tamaru, M. Avdeev, S.C. Chung, Y. Yamada, A. Yamada, Na2FeP2O7: A safe cathode for rechargeable sodium-ion batteries, Chem. Mater. 25 (2013) 3480–3487, https://doi.org/10.1021/cm401657c.

[104] R. Tripathi, S.M. Wood, M.S. Islam, L.F. Nazar, Na-ion mobility in layered Na2FePO4F and olivine Na[Fe, Mn]PO4, Energy Environ Sci 6 (2013) 2257–2264, https://doi.org/10.1039/c3ee40914g.

[105] H. Kim, I. Park, D.H. Seo, S. Lee, S.W. Kim, W.J. Kwon, Y.U. Park, C.S. Kim, S. Jeon, K. Kang, New iron-based mixed-polyanion cathodes for lithium and sodium rechargeable batteries: Combined first principles calculations and experimental study, J Am Chem Soc 134 (2012) 10369–10372, https://doi.org/10.1021/ja3038646.

[106] S.M. Oh, S.T. Myung, J. Hassoun, B. Scrosati, Y.K. Sun, Reversible NaFePO 4 electrode for sodium secondary batteries, Electrochem Commun 22 (2012) 149–152, https://doi.org/10.1016/j.elecom.2012.06.014.

[107] C. Tealdi, J. Heath, M.S. Islam, Feeling the strain: Enhancing ionic transport in olivine phosphate cathodes for Li- and Na-ion batteries through strain effects, J Mater Chem A Mater 4 (2016) 6998–7004, https://doi.org/10.1039/c5ta09418f.

[108] J. Kim, D.H. Seo, H. Kim, I. Park, J.K. Yoo, S.K. Jung, Y.U. Park, W.A. Goddard, K. Kang, Unexpected discovery of low-cost maricite NaFePO4 as a high-performance electrode for Na-ion batteries, Energy Environ Sci 8 (2015) 540–545, https://doi.org/10.1039/c4ee03215b.

[109] Y. Wang, M. Deng, X. Zhang, J. Zhang, Y. Sui, K. Sun, K. Rao, L. Wu, Sustainable synthesis of Ni, Mn co-doped FePO4@C cathode material for Na-ion batteries, J Colloid Interface Sci 661 (2024) 23–32, https://doi.org/10.1016/j.jcis.2024.01.198.

[110] FAST Na ION TRANSPORT IN SKELETON STRUCTURES, (n.d.).

[111] Z. Jian, L. Zhao, H. Pan, Y.S. Hu, H. Li, W. Chen, L. Chen, Carbon coated Na3V2(PO4)3 as novel electrode material for sodium ion batteries, Electrochem Commun 14 (2012) 86–89, https://doi.org/10.1016/j.elecom.2011.11.009.

[112] G. Li, D. Jiang, H. Wang, X. Lan, H. Zhong, Y. Jiang, Glucose-assisted synthesis of Na3V2(PO 4)3/C composite as an electrode material for high-performance sodium-ion batteries, J Power Sources 265 (2014) 325–334, https://doi.org/10.1016/j.jpowsour.2014.04.054.

[113] Y. Zhu, H. Xu, J. Ma, P. Chen, Y. Chen, The N-doped carbon coated Na3V2(PO4)3 with different N sources as cathode material for sodium-ion batteries: Experimental and theoretical study, Surf. Interfaces 45 (2024), https://doi.org/10.1016/j.surfin.2024.103888.

[114] A. Mukherjee, S. Mondal, D. Das, S. Banerjee, S.B. Majumder, Electrophoretically deposited Na3V2(PO4)3 and its carbonaceous composites as promising cathode for sodium-ion batteries, Mater Res Bull 170 (2024), https://doi.org/10.1016/j.materresbull.2023.112562.

[115] L. Li, Y. Jia, L. Song, J. Gao, Na2VSn(PO4)3: A novel NASICON-type electrode material for symmetric sodium-ion batteries, J Alloys Compd 942 (2023), https://doi.org/10.1016/j.jallcom.2023.169128.

[116] Y. Chen, X. Liao, P. Wang, J. Chen, X. Zhang, X. Wu, S.C. Smith, D. Lin, X. Tan, Q. Zheng, A high-energy-density NASICON-type Na3V1.25Ga0.75(PO4)3 cathode with reversible V4+/V5+ redox couple for sodium ion batteries, J Colloid Interface Sci 653 (2024) 1–10, https://doi.org/10.1016/j.jcis.2023.09.057.

[117] D. Wang, N. Su, Z.E. Yu, S. Lu, Y. Lyu, B. Guo, Reaction mechanisms of NASICON-type Na4MnV(PO4)3/C as a cathode for sodium-ion batteries, Electrochem Commun 159 (2024), https://doi.org/10.1016/j.elecom.2023.107651.

[118] Y. Wu, Q. Zou, C. Li, W. Wang, Structural reinforced NaTi2(PO4)3 composite by pillar effects for constructing a high-performance rocking-chair desalination battery, Chem. Eng. J. 480 (2024), https://doi.org/10.1016/j.cej.2023.147965.

[119] J. Wu, H. Liu, H. Bu, X. Zhang, H. Zhang, W. Wang, L. Yang, C. Zeng, S. Zhu, Manganese-based NASICON structured Na1+2xMnxTi2-x(PO4)3 as promising cathode in aqueous sodium ion battery, J Alloys Compd 934 (2023), https://doi.org/10.1016/j.jallcom.2022.167872.

[120] S.P. Guo, J.C. Li, Q.T. Xu, Z. Ma, H.G. Xue, Recent achievements on polyanion-type compounds for sodium-ion batteries: Syntheses, crystal chemistry and electrochemical performance, J Power Sources 361 (2017) 285–299, https://doi.org/10.1016/j.jpowsour.2017.07.002.

[121] H. Li, X. Chen, T. Jin, W. Bao, Z. Zhang, L. Jiao, Robust graphene layer modified Na2MnP2O7 as a durable high-rate and high energy cathode for Na-ion batteries, Energy Storage Mater 16 (2019) 383–390, https://doi.org/10.1016/j.ensm.2018.06.013.

[122] P. Barpanda, T. Ye, M. Avdeev, S.C. Chung, A. Yamada, A new polymorph of Na2MnP2O7 as a 3.6 v cathode material for sodium-ion batteries, J Mater Chem A Mater 1 (2013) 4194–4197, https://doi.org/10.1039/c3ta10210f.

[123] V.M. Kovrugin, J.N. Chotard, F. Fauth, C. Masquelier, Na7V3(P2O7)4as a high voltage electrode material for Na-ion batteries: Crystal structure and mechanism of Na+extraction/insertion by: Operando X-ray diffraction, J Mater Chem A Mater 8 (2020) 21110–21121, https://doi.org/10.1039/d0ta06230h.

[124] C. Deng, S. Zhang, 1D nanostructured Na7V4(P2O 7)4(PO4) as high-potential and superior-performance cathode material for sodium-ion batteries, ACS Appl Mater Interfaces 6 (2014) 9111–9117, https://doi.org/10.1021/am501072j.

[125] M. Nose, H. Nakayama, K. Nobuhara, H. Yamaguchi, S. Nakanishi, H. Iba, Na4Co3(PO4)2P2O 7: A novel storage material for sodium-ion batteries, J Power Sources 234 (2013) 175–179, https://doi.org/10.1016/j.jpowsour.2013.01.162.

[126] A. Gezović, M. Milović, D. Bajuk-Bogdanović, V. Grudić, R. Dominko, S. Mentus, M.J. Vujković, An effective approach to reaching the theoretical capacity of a low-cost and environmentally friendly Na4Fe3(PO4)2(P2O7) cathode for Na-ion batteries, Electrochim Acta 476 (2024), https://doi.org/10.1016/j.electacta.2023.143718.

[127] Y. Lu, S. Zhang, Y. Li, L. Xue, G. Xu, X. Zhang, Preparation and characterization of carbon-coated NaVPO4F as cathode material for rechargeable sodium-ion batteries, J Power Sources 247 (2014) 770–777, https://doi.org/10.1016/j.jpowsour.2013.09.018.
[128] N. Eshraghi, S. Caes, A. Mahmoud, R. Cloots, B. Vertruyen, F. Boschini, Sodium vanadium (III) fluorophosphate/carbon nanotubes composite (NVPF/CNT) prepared by spray-drying: good electrochemical performance thanks to well-dispersed CNT network within NVPF particles, Electrochim Acta 228 (2017) 319–324, https://doi.org/10.1016/j.electacta.2017.01.026.
[129] W.G. Morais, M.M. Leite, R.M. Torresi, Titanium- and niobium-doped fluorophosphates as positive electrodes for sodium-ion batteries, J. Electroanal. Chem. 897 (2021), https://doi.org/10.1016/j.jelechem.2021.115595.
[130] S. Mahato, S. Das, D. Gupta, K. Biswas, Vanadium substituted Fe, Cr co-doped high performance C/Na3V2(PO4)2F3 cathode for sodium-ion batteries, J. Electroanal. Chem. 955 (2024), https://doi.org/10.1016/j.jelechem.2024.118046.
[131] M. Ling, Q. Jiang, T. Li, C. Wang, Z. Lv, H. Zhang, Q. Zheng, X. Li, The mystery from tetragonal NaVPO4F to monoclinic NaVPO4F: crystal presentation, phase conversion, and Na-storage kinetics, Adv Energy Mater 11 (2021), https://doi.org/10.1002/aenm.202100627.
[132] W. Fu, B. Li, P. Wang, Z. Lin, K. Zhu, A high-entropy carbon-coated Na3V1.9(Mg, Cr, Al, Mo, Nb)0.1(PO4)2F3 cathode for superior performance sodium-ion batteries, Ceram Int (2024), https://doi.org/10.1016/j.ceramint.2024.02.096.
[133] W. Pan, W. Guan, S. Liu, B. Bin Xu, C. Liang, H. Pan, M. Yan, Y. Jiang, Na2Fe(SO4)2: An anhydrous 3.6 V, low-cost and good-safety cathode for a rechargeable sodium-ion battery, J Mater Chem A Mater 7 (2019) 13197–13204, https://doi.org/10.1039/c9ta02188d.
[134] T. Song, W. Yao, P. Kiadkhunthod, Y. Zheng, N. Wu, X. Zhou, S. Tunmee, S. Sattayaporn, Y. Tang, A low-cost and environmentally friendly mixed polyanionic cathode for sodium-ion storage, Angewandte Chemie - International Edition 59 (2020) 740–745, https://doi.org/10.1002/anie.201912272.
[135] R. Rajagopalan, Z. Wu, Y. Liu, S. Al-Rubaye, E. Wang, C. Wu, W. Xiang, B. Zhong, X. Guo, S.X. Dou, H.K. Liu, A novel high voltage battery cathodes of Fe2+/Fe3+ sodium fluoro sulfate lined with carbon nanotubes for stable sodium batteries, J Power Sources 398 (2018) 175–182, https://doi.org/10.1016/j.jpowsour.2018.07.066.
[136] D. Dwibedi, R.B. Araujo, S. Chakraborty, P.P. Shanbogh, N.G. Sundaram, R. Ahuja, P. Barpanda, Na2.44Mn1.79(SO4)3: a new member of the alluaudite family of insertion compounds for sodium ion batteries, J Mater Chem A Mater 3 (2015) 18564–18571, https://doi.org/10.1039/c5ta04527d.
[137] D. Dwibedi, R. Gond, A. Dayamani, R.B. Araujo, S. Chakraborty, R. Ahuja, P. Barpanda, Na2.32Co1.84(SO4)3 as a new member of the alluaudite family of high-voltage sodium battery cathodes, Dalton Trans. 46 (2017) 55–63, https://doi.org/10.1039/c6dt03767d.
[138] T. Jin, H. Li, K. Zhu, P.F. Wang, P. Liu, L. Jiao, Polyanion-type cathode materials for sodium-ion batteries, Chem Soc Rev 49 (2020) 2342–2377, https://doi.org/10.1039/c9cs00846b.
[139] C. Liu, K. Chen, H. Xiong, A. Zhao, H. Zhang, Q. Li, X. Ai, H. Yang, Y. Fang, Y. Cao, A novel Na8Fe5(SO4)9@rGO cathode material with high rate capability and ultra-long lifespan for low-cost sodium-ion batteries, Escience (2024), https://doi.org/10.1016/j.esci.2023.100186.
[140] Y. Li, W. Sun, J. Liang, H. Sun, I. Di Marco, L. Ni, S. Tang, J. Zhang, Understanding the electrochemical properties of A2MSiO4 (A = Li and Na; M = Fe, Mn, Co and Ni) and the Na doping effect on Li2MSiO4 from first-principles calculations, J Mater Chem A Mater 4 (2016) 17455–17463, https://doi.org/10.1039/c6ta05313k.
[141] Y. Kee, N. Dimov, A. Staykov, S. Okada, Investigation of metastable Na2FeSiO4 as a cathode material for Na-ion secondary battery, Mater Chem Phys 171 (2016) 45–49, https://doi.org/10.1016/j.matchemphys.2016.01.033.
[142] S. Li, J. Guo, Z. Ye, X. Zhao, S. Wu, J.X. Mi, C.Z. Wang, Z. Gong, M.J. McDonald, Z. Zhu, K.M. Ho, Y. Yang, Zero-strain Na2FeSiO4 as novel cathode material for sodium-ion batteries, ACS Appl Mater Interfaces 8 (2016) 17233–17238, https://doi.org/10.1021/acsami.6b03969.
[143] Y. Harishpal, Sharma, preparation, transport and Na-storage properties of monoclinic – Na2FeSiO4 for Na-ion batteries, Solid State Ion 388 (2022), https://doi.org/10.1016/j.ssi.2022.116084.
[144] C.Y. Chen, K. Matsumoto, T. Nohira, R. Hagiwara, Na2MnSiO4 as a positive electrode material for sodium secondary batteries using an ionic liquid electrolyte, Electrochem Commun 45 (2014) 63–66, https://doi.org/10.1016/j.elecom.2014.05.017.
[145] M. Law, V. Ramar, P. Balaya, Na2MnSiO4 as an attractive high capacity cathode material for sodium-ion battery, J Power Sources 359 (2017) 277–284, https://doi.org/10.1016/j.jpowsour.2017.05.069.
[146] J.C. Treacher, S.M. Wood, M.S. Islam, E. Kendrick, Na2CoSiO4 as a cathode material for sodium-ion batteries: Structure, electrochemistry and diffusion pathways, PCCP 18 (2016) 32744–32752, https://doi.org/10.1039/c6cp06777h.
[147] X. Rui, W. Sun, C. Wu, Y. Yu, Q. Yan, An advanced sodium-ion battery composed of carbon coated Na3V2(PO4)3 in a porous graphene network, Adv. Mater. 27 (2015) 6670–6676, https://doi.org/10.1002/adma.201502864.
[148] W. Zhou, L. Xue, X. Lü, H. Gao, Y. Li, S. Xin, G. Fu, Z. Cui, Y. Zhu, J. B. Goodenough, NaxMV(PO4)3 (M = Mn, Fe, Ni) structure and properties for sodium extraction, Nano Lett 16 (2016) 7836–7841, https://doi.org/10.1021/acs.nanolett.6b04044.
[149] H. Kim, C.S. Park, J.W. Choi, Y. Jung, Defect-controlled formation of triclinic Na 2 CoP 2 O 7 for 4 V sodium-ion batteries, Angew. Chem. 128 (2016) 6774–6778, https://doi.org/10.1002/ange.201601022.
[150] C.S. Park, H. Kim, R.A. Shakoor, E. Yang, S.Y. Lim, R. Kahraman, Y. Jung, J. W. Choi, Anomalous manganese activation of a pyrophosphate cathode in sodium ion batteries: A combined experimental and theoretical study, J Am Chem Soc 135 (2013) 2787–2792, https://doi.org/10.1021/ja312044k.
[151] J. Gao, Y. Tian, Y. Mei, L. Ni, H. Wang, H. Liu, W. Deng, G. Zou, H. Hou, X. Ji, Robust NASICON-type iron-based Na4Fe3(PO4)2(P2O7) cathode for high temperature sodium-ion batteries, Chem. Eng. J. 458 (2023), https://doi.org/10.1016/j.cej.2023.141385.
[152] Y. Qi, L. Mu, J. Zhao, Y. Hu, H. Liu, S. Dai, Superior Na-storage performance of low-temperature-synthesized Na 3 (VO 1–x PO 4) 2 F 1+2 x (0≤ x ≤1) nanoparticles for Na-ion batteries, Angew. Chem. 127 (2015) 10049–10054, https://doi.org/10.1002/ange.201503188.
[153] M. Peng, B. Li, H. Yan, D. Zhang, X. Wang, D. Xia, G. Guo, Ruthenium-oxide-coated sodium vanadium fluorophosphate nanowires as high-power cathode materials for sodium-ion batteries, Angew. Chem. 127 (2015) 6552–6556, https://doi.org/10.1002/ange.201411917.
[154] H. Chen, Q. Hao, O. Zivkovic, G. Hautier, L.S. Du, Y. Tang, Y.Y. Hu, X. Ma, C. P. Grey, G. Ceder, Sidorenkite (Na3MnPO4CO3): a new intercalation cathode material for Na-ion batteries, Chem. Mater. 25 (2013) 2777–2786, https://doi.org/10.1021/cm400805q.
[155] L. Tang, J. Zhang, Z. Li, X. Liu, Q. Xu, H. Liu, Y.G. Wang, Y. Xia, Z. Ma, Using Na7V4(P2O7)4(PO4) with superior Na storage performance as bipolar electrodes to build a novel high-energy-density symmetric sodium-ion full battery, J Power Sources 451 (2020), https://doi.org/10.1016/j.jpowsour.2020.227734.
[156] D. Wang, Y. Wu, J. Lv, R. Wang, S. Xu, Carbon encapsulated maricite NaFePO4 nanoparticles as cathode material for sodium-ion batteries, Colloids Surf A Physicochem Eng Asp 583 (2019), https://doi.org/10.1016/j.colsurfa.2019.123957.
[157] Q. Liu, D. Wang, X. Yang, N. Chen, C. Wang, X. Bie, Y. Wei, G. Chen, F. Du, Carbon-coated Na3V2(PO4)2F3 nanoparticles embedded in a mesoporous carbon matrix as a potential cathode material for sodium-ion batteries with superior rate capability and long-term cycle life, J Mater Chem A Mater 3 (2015) 21478–21485, https://doi.org/10.1039/c5ta05939a.
[158] S.J. Lim, D.W. Han, D.H. Nam, K.S. Hong, J.Y. Eom, W.H. Ryu, H.S. Kwon, Structural enhancement of Na3V2(PO4)3/C composite cathode materials by pillar ion doping for high power and long cycle life sodium-ion batteries, J Mater Chem A Mater 2 (2014) 19623–19632, https://doi.org/10.1039/c4ta03948c.
[159] Y. Qi, Z. Tong, J. Zhao, L. Ma, T. Wu, H. Liu, C. Yang, J. Lu, Y.S. Hu, Scalable Room-Temperature Synthesis of Multi-shelled Na3(VOPO4)2F Microsphere Cathodes, Joule 2 (2018) 2348–2363, https://doi.org/10.1016/j.joule.2018.07.027.
[160] X. Shen, Q. Zhou, M. Han, X. Qi, B. Li, Q. Zhang, J. Zhao, C. Yang, H. Liu, Y.S. Hu, Rapid mechanochemical synthesis of polyanionic cathode with improved electrochemical performance for Na-ion batteries, Nat Commun 12 (2021), https://doi.org/10.1038/s41467-021-23132-w.
[161] S. Qiao, S. Dong, L. Yuan, T. Li, M. Ma, Y. Wu, Y. Hu, T. Qu, S. Chong, Structure defects engineering in Prussian blue cathode materials for high-performance sodium-ion batteries, J Alloys Compd 950 (2023), https://doi.org/10.1016/j.jallcom.2023.169903.
[162] B. Xie, B. Sun, T. Gao, Y. Ma, G. Yin, P. Zuo, Recent progress of Prussian blue analogues as cathode materials for nonaqueous sodium-ion batteries, Coord Chem Rev 460 (2022), https://doi.org/10.1016/j.ccr.2022.214478.
[163] X. Wu, C. Wu, C. Wei, L. Hu, J. Qian, Y. Cao, X. Ai, J. Wang, H. Yang, Highly crystallized Na2CoFe(CN)6 with suppressed lattice defects as superior cathode material for sodium-ion batteries, ACS Appl Mater Interfaces 8 (2016) 5393–5399, https://doi.org/10.1021/acsami.5b12620.
[164] J. Qian, C. Wu, Y. Cao, Z. Ma, Y. Huang, X. Ai, H. Yang, Prussian blue cathode materials for sodium-ion batteries and other ion batteries, Adv Energy Mater 8 (2018), https://doi.org/10.1002/aenm.201702619.
[165] X. Bie, K. Kubota, T. Hosaka, K. Chihara, S. Komaba, Synthesis and electrochemical properties of Na-rich Prussian blue analogues containing Mn, Fe Co, and Fe for Na-Ion Batteries, J Power Sources 378 (2018) 322–330, https://doi.org/10.1016/j.jpowsour.2017.12.052.
[166] Z. Xu, Y. Sun, J. Xie, Y. Nie, X. Xu, J. Tu, C. Shen, Y. Jin, Y. Li, Y. Lu, A. Zhou, F. Chen, T. Zhu, X. Zhao, High-performance Ni/Fe-codoped manganese hexacyanoferrate by scale-up synthesis for practical Na-ion batteries, Materials Today Sustainability 18 (2022), https://doi.org/10.1016/j.mtsust.2022.100113.
[167] J. Chen, K. Huang, S. Liu, Insoluble metal hexacyanoferrates as supercapacitor electrodes, Electrochem Commun 10 (2008) 1851–1855, https://doi.org/10.1016/j.elecom.2008.07.046.
[168] C.D. Wessells, R.A. Huggins, Y. Cui, Copper hexacyanoferrate battery electrodes with long cycle life and high power, Nat Commun 2 (2011), https://doi.org/10.1038/ncomms1563.
[169] Y. Lu, L. Wang, J. Cheng, J.B. Goodenough, Prussian blue: A new framework of electrode materials for sodium batteries, Chem. Commun. 48 (2012) 6544–6546, https://doi.org/10.1039/c2cc31777j.
[170] D. Yang, J. Xu, X.Z. Liao, Y.S. He, H. Liu, Z.F. Ma, Structure optimization of Prussian blue analogue cathode materials for advanced sodium ion batteries, Chem. Commun. 50 (2014) 13377–13380, https://doi.org/10.1039/c4cc05830e.
[171] J. Song, L. Wang, Y. Lu, J. Liu, B. Guo, P. Xiao, J.J. Lee, X.Q. Yang, G. Henkelman, J.B. Goodenough, Removal of interstitial H2O in hexacyanometallates for a superior cathode of a sodium-ion battery, J Am Chem Soc 137 (2015) 2658–2664, https://doi.org/10.1021/ja512383b.
[172] K. Lu, B. Song, J. Zhang, H. Ma, A rechargeable Na-Zn hybrid aqueous battery fabricated with nickel hexacyanoferrate and nanostructured zinc, J Power Sources 321 (2016) 257–263, https://doi.org/10.1016/j.jpowsour.2016.05.003.

[173] W.J. Li, C. Han, G. Cheng, S.L. Chou, H.K. Liu, S.X. Dou, Chemical properties, structural properties, and energy storage applications of prussian blue analogues, Small 15 (2019), https://doi.org/10.1002/smll.201900470.
[174] S. Kang, S. Im, Y. Jeon, Acid-catalyzed synthesis and characterization of a nanocrystalline cobalt-based Prussian blue analogs (Co3[Co(CN)6]2·nH2O) by single-source method under hydrothermal conditions and its conversion to Co3O4, Bull Korean Chem Soc 36 (2015) 2387–2390, https://doi.org/10.1002/bkcs.10449.
[175] W. Li, C. Han, Q. Xia, K. Zhang, S. Chou, Y.M. Kang, J. Wang, H.K. Liu, S.X. Dou, Remarkable enhancement in sodium-ion kinetics of NaFe2(CN)6 by chemical bonding with graphene, Small Methods 2 (2018), https://doi.org/10.1002/SMTD.201700346.
[176] Y. You, H.R. Yao, S. Xin, Y.X. Yin, T.T. Zuo, C.P. Yang, Y.G. Guo, Y. Cui, L.J. Wan, J.B. Goodenough, Subzero-temperature cathode for a sodium-ion battery, Adv. Mater. 28 (2016) 7243–7248, https://doi.org/10.1002/adma.201600846.
[177] J. Luo, S. Sun, J. Peng, B. Liu, Y. Huang, K. Wang, Q. Zhang, Y. Li, Y. Jin, Y. Liu, Y. Qiu, Q. Li, J. Han, Y. Huang, Graphene-roll-wrapped prussian blue nanospheres as a high-performance binder-free cathode for sodium-ion batteries, ACS Appl Mater Interfaces 9 (2017) 25317–25322, https://doi.org/10.1021/acsami.7b06334.
[178] A. Johansson, E. Widenkvist, J. Lu, M. Boman, U. Jansson, Fabrication of high-aspect-ratio Prussian blue nanotubes using a porous alumina template, Nano Lett 5 (2005) 1603–1606, https://doi.org/10.1021/nl050964u.
[179] H. Zhang, Y. Gao, X.H. Liu, Z. Yang, X.X. He, L. Li, Y. Qiao, W.H. Chen, R.H. Zeng, Y. Wang, S.L. Chou, Organic cathode materials for sodium-ion batteries: from fundamental research to potential commercial application, Adv Funct Mater 32 (2022), https://doi.org/10.1002/adfm.202107718.
[180] W. Deng, X. Liang, X. Wu, J. Qian, Y. Cao, X. Ai, J. Feng, H. Yang, A low cost, all-organic Na-ion Battery Based on Polymeric Cathode and Anode, Sci Rep 3 (2013), https://doi.org/10.1038/srep02671.
[181] R. Thangavel, M. Moorthy, B.K. Ganesan, W. Lee, W.S. Yoon, Y.S. Lee, Nanoengineered organic electrodes for highly durable and ultrafast cycling of organic sodium-ion batteries, Small 16 (2020), https://doi.org/10.1002/smll.202003688.
[182] Y. Wu, W. Shuang, Y. Wang, F. Chen, S. Tang, X.L. Wu, Z. Bai, L. Yang, J. Zhang, Recent progress in sodium-ion batteries: advanced materials, reaction mechanisms and energy applications, Electrochemical Energy Reviews 7 (2024), https://doi.org/10.1007/s41918-024-00215-y.
[183] G. Zhou, Y.E. Miao, Z. Wei, L.L. Mo, F. Lai, Y. Wu, J. Ma, T. Liu, Bioinspired micro/nanofluidic ion transport channels for organic cathodes in high-rate and ultrastable lithium/sodium-ion batteries, Adv Funct Mater 28 (2018), https://doi.org/10.1002/adfm.201804629.
[184] Y. Fang, X. Yu, X.W. (David) Lou, A Practical High-Energy Cathode for Sodium-Ion Batteries Based on Uniform P2-Na 0.7 CoO 2 Microspheres, Angew. Chem. 129 (2017) 5895–5899, https://doi.org/10.1002/ange.201702024.
[185] D. Su, C. Wang, H.J. Ahn, G. Wang, Single crystalline Na0.7MnO2 nanoplates as cathode materials for sodium-ion batteries with enhanced performance, Chem. A Eur. J. 19 (2013) 10884–10889, https://doi.org/10.1002/chem.201301563.
[186] X. He, J. Wang, B. Qiu, E. Paillard, C. Ma, X. Cao, H. Liu, M.C. Stan, H. Liu, T. Gallash, Y.S. Meng, J. Li, Durable high-rate capability Na0.44MnO2 cathode material for sodium-ion batteries, Nano Energy 27 (2016) 602–610, https://doi.org/10.1016/j.nanoen.2016.07.021.
[187] P. Vassilaras, X. Ma, X. Li, G. Ceder, Electrochemical Properties of Monoclinic NaNiO 2, J Electrochem Soc 160 (2013) A207–A211, https://doi.org/10.1149/2.023302jes.
[188] Y. Yoda, K. Kubota, H. Isozumi, T. Horiba, S. Komaba, Poly-γ-glutamate binder to enhance electrode performances of P2-Na2/3Ni1/3Mn2/3O2 for Na-ion batteries, ACS Appl Mater Interfaces 10 (2018) 10986–10997, https://doi.org/10.1021/acsami.8b01362.
[189] W.M. Dose, N. Sharma, J.C. Pramudita, H.E.A. Brand, E. Gonzalo, T. Rojo, Structure-electrochemical evolution of a Mn-rich P2 Na2/3Fe0.2Mn0.8O2 Na-ion battery cathode, Chem. Mater. 29 (2017) 7416–7423, https://doi.org/10.1021/acs.chemmater.7b02397.
[190] J. Abou-Rjeily, I. Bezza, N.A. Laziz, D. Neacsa, C. Autret-Lambert, F. Ghamouss, P2-Na0.67Mn0.85Al0.15O2and NaMn2O4 blend as cathode materials for sodium-ion batteries using a natural β-MnO2 precursor, ACS Omega 6 (2021) 1064–1072, https://doi.org/10.1021/acsomega.0c01647.
[191] N. Yabuuchi, R. Hara, K. Kubota, J. Paulsen, S. Kumakura, S. Komaba, A new electrode material for rechargeable sodium batteries: P2-type Na2/3 [Mg0.28Mn0.72]O2 with anomalously high reversible capacity, J Mater Chem A Mater 2 (2014) 16851–16855, https://doi.org/10.1039/c4ta04351k.
[192] M. Kouthaman, K. Kannan, P. Arjunan, R. Subadevi, M. Sivakumar, Layered O3-type Na9/10Cr1/2Fe1/2O2 as new cathode for rechargeable sodium-ion battery, Colloids Surf A Physicochem Eng Asp 633 (2022), https://doi.org/10.1016/j.colsurfa.2021.127929.
[193] M. Sathiya, K. Hemalatha, K. Ramesha, J.M. Tarascon, A.S. Prakash, Synthesis, structure, and electrochemical properties of the layered sodium insertion cathode material: NaNi 1/3Mn 1/3Co 1/3O 2, Chem. Mater. 24 (2012) 1846–1853, https://doi.org/10.1021/cm300466b.
[194] H. Wang, J. Lin, X. Zhang, L. Wang, J. Yang, E. Fan, F. Wu, R. Chen, L. Li, Improved electrochemical performance of LiNi0.8Co0.1Mn0.1O2 cathode materials induced by a facile polymer coating for lithium-ion batteries, ACS Appl Energy Mater (2021), https://doi.org/10.1021/acsaem.1c00982.
[195] N.V. To, K.V. Nguyen, H.S. Nguyen, S.T. Luong, P.T. Doan, T.H.T. Nguyen, Q. Q. Ngo, N.V. Nguyen, P2-type layered structure Na1.0Li0.2Mn0.7Ti0.1O2 as a superb electrochemical performance cathode material for sodium-ion batteries, J. Electroanal. Chem. 880 (2021), https://doi.org/10.1016/j.jelechem.2020.114834.
[196] T.T. Wei, N. Zhang, Y.S. Zhao, Y.R. Zhu, T.F. Yi, Sodium-deficient O3–Na0.75Fe0.5-xCuxMn0.5O2 as high-performance cathode materials of sodium-ion batteries, Compos B Eng 238 (2022), https://doi.org/10.1016/j.compositesb.2022.109912.
[197] P. Zhou, Z. Che, F. Ma, J. Zhang, J. Weng, X. Wu, Z. Miao, H. Lin, J. Zhou, S. Zhuo, Designing water/air-stable P2-layered cathodes with delayed P2–O2 phase transition by composition and structure engineering for sodium-ion batteries at high voltage, Chem. Eng. J. 420 (2021), https://doi.org/10.1016/j.cej.2020.127667.
[198] M. Leng, J. Bi, Z. Xing, W. Wang, X. Gao, J. Wang, Z. Qian, A new perspective on the composition-structure-property relationships on Nb/Mo/Cr-doped O3-type layered oxide as cathode materials for sodium-ion batteries, Chem. Eng. J. 413 (2021), https://doi.org/10.1016/j.cej.2020.127824.
[199] J. Zhou Wang, Y. Xue Teng, G. Qiao Su, S. Bao, J. Lin Lu, A dual-modification strategy for P2-type layered oxide via bulk Mg/Ti co-substitution and MgO surface coating for sodium ion batteries, J Colloid Interface Sci 608 (2022) 3013–3021, https://doi.org/10.1016/j.jcis.2021.11.028.
[200] K. Walczak, A. Plewa, C. Ghica, W. Zając, A. Trenczek-Zając, M. Zając, J. Tobola, J. Molenda, NaMn0.2Fe0.2Co0.2Ni0.2Ti0.2O2 high-entropy layered oxide – experimental and theoretical evidence of high electrochemical performance in sodium batteries, Energy Storage Mater 47 (2022) 500–514, https://doi.org/10.1016/j.ensm.2022.02.038.
[201] H. Guo, M. Avdeev, K. Sun, X. Ma, H. Wang, Y. Hu, D. Chen, Pentanary transition-metals Na-ion layered oxide cathode with highly reversible O3–P3 phase transition, Chem. Eng. J. 412 (2021), https://doi.org/10.1016/j.cej.2021.128704.
[202] K. Kubota, K. Yokoh, N. Yabuuchi, S. Komaba, Na2CoPO4F as a high-voltage electrode material for na-ion batteries, Electrochemistry 82 (2014) 909–911, https://doi.org/10.5796/electrochemistry.82.909.
[203] P. Barpanda, J. Lu, T. Ye, M. Kajiyama, S.C. Chung, N. Yabuuchi, S. Komaba, A. Yamada, A layer-structured Na2CoP2O7 pyrophosphate cathode for sodium-ion batteries, RSC Adv 3 (2013) 3857–3860, https://doi.org/10.1039/c3ra23026k.
[204] W. Hong, J. Wang, E. Wang, Facile synthesis of highly active PdAu nanowire networks as self-supported electrocatalyst for ethanol electrooxidation, ACS Appl Mater Interfaces 6 (2014) 9481–9487.
[205] L. Wang, J. Song, R. Qiao, L. Andrew Wray, M.A. Hossain, Y.-D. Chuang, W. Yang, Y. Lu, D. Evans, J.-J. Lee, S. Vail, X. Zhao, M. Nishijima, S. Kakimoto, J.B. Goodenough, Rhombohedral Prussian White as Cathode for Rechargeable Sodium-Ion Batteries Rhombohedral Prussian White as Cathode for Rechargeable Sodi-um-Ion Batteries, 2015. http://pubs.acs.org.
[206] Y. Jiang, S. Yu, B. Wang, Y. Li, W. Sun, Y. Lu, M. Yan, B. Song, S. Dou, Prussian blue@C composite as an ultrahigh-rate and long-life sodium-ion battery cathode, Adv Funct Mater 26 (2016) 5315–5321, https://doi.org/10.1002/adfm.201600747.
[207] B. Wang, Y. Han, Y. Chen, Y. Xu, H. Pan, W. Sun, S. Liu, M. Yan, Y. Jiang, Gradient substitution: An intrinsic strategy towards high performance sodium storage in Prussian blue-based cathodes, J Mater Chem A Mater 6 (2018) 8947–8954, https://doi.org/10.1039/c8ta02291g.
[208] F. Peng, L. Yu, P. Gao, X.Z. Liao, J. Wen, Y.S. He, G. Tan, Y. Ren, Z.F. Ma, Highly crystalline sodium manganese ferrocyanide microcubes for advanced sodium ion battery cathodes, J Mater Chem A Mater 7 (2019) 22248–22256, https://doi.org/10.1039/c9ta08603j.
[209] W. Ren, M. Qin, Z. Zhu, M. Yan, Q. Li, L. Zhang, D. Liu, L. Mai, Activation of sodium storage sites in prussian blue analogues via surface etching, Nano Lett 17 (2017) 4713–4718, https://doi.org/10.1021/acs.nanolett.7b01366.
[210] K. Chihara, N. Chujo, A. Kitajou, S. Okada, Cathode properties of Na2C6O6 for sodium-ion batteries, Electrochim Acta 110 (2013) 240–246, https://doi.org/10.1016/j.electacta.2013.04.100.
[211] S. Wang, L. Wang, Z. Zhu, Z. Hu, Q. Zhao, J. Chen, All organic sodium-ion batteries with Na4C8H 2O6, Angewandte Chemie - International Edition 53 (2014) 5892–5896, https://doi.org/10.1002/anie.201400032.
[212] M. Zhou, L. Zhu, Y. Cao, R. Zhao, J. Qian, X. Ai, H. Yang, Fe(CN) 6–4-doped polypyrrole: A high-capacity and high-rate cathode material for sodium-ion batteries, RSC Adv 2 (2012) 5495–5498, https://doi.org/10.1039/c2ra20666h.
[213] R. Zhao, L. Zhu, Y. Cao, X. Ai, H.X. Yang, An aniline-nitroaniline copolymer as a high capacity cathode for Na-ion batteries, Electrochem Commun 21 (2012) 36–38, https://doi.org/10.1016/j.elecom.2012.05.015.
[214] Y. Huang, K. Li, J. Liu, X. Zhong, X. Duan, I. Shakir, Y. Xu, Three-dimensional graphene/polyimide composite-derived flexible high-performance organic cathode for rechargeable lithium and sodium batteries, J Mater Chem A Mater 5 (2017) 2710–2716, https://doi.org/10.1039/c6ta09754e.
[215] F. Yu, W. Tang, S. Wang, M. Guo, W. Deng, J. Hu, S. Jia, C. Fan, Organic-carbon core-shell structure promotes cathode performance for na-ion batteries, Adv Funct Mater 33 (2023), https://doi.org/10.1002/adfm.202300740.
[216] Y. Gambe, H. Kobayashi, I. Honma, A 3.5 V-class organic sodium-ion battery using a croconate cathode, Chem. Eng. J. 479 (2024), https://doi.org/10.1016/j.cej.2023.147760.
[217] Y. Yao, M. Pei, C. Su, X. Jin, Y. Qu, Z. Song, W. Jiang, X. Jian, F. Hu, A Small-molecule organic cathode with extended conjugation toward enhancing Na+ migration kinetics for advanced sodium-ion batteries, Small (2024), https://doi.org/10.1002/smll.202401481.
[218] K. Liu, S. Yang, L. Luo, Q. Pan, P. Zhang, Y. Huang, F. Zheng, H. Wang, Q. Li, From spent graphite to recycle graphite anode for high-performance lithium ion

batteries and sodium ion batteries, Electrochim Acta 356 (2020), https://doi.org/10.1016/j.electacta.2020.136856.
[219] Y. Yang Zhu, Y. Hua Wang, Y. Tong Wang, T. Jie Xu, P. Chang, Research progress on carbon materials as negative electrodes in sodium- and potassium-ion batteries, Carbon Energy 4 (2022) 1182–1213, https://doi.org/10.1002/cey2.221.
[220] D. Saritha, R. Sujithra, A concise review on cathode materials for Na-ion batteries, Mater Today Proc (2023), https://doi.org/10.1016/j.matpr.2023.03.401.
[221] F. Wei, Q. Zhang, P. Zhang, W. Tian, K. Dai, L. Zhang, J. Mao, G. Shao, Review—research progress on layered transition metal oxide cathode materials for sodium ion batteries, J Electrochem Soc 168 (2021) 050524, https://doi.org/10.1149/1945-7111/abf9bf.
[222] N. Ortiz-Vitoriano, N.E. Drewett, E. Gonzalo, T. Rojo, High performance manganese-based layered oxide cathodes: Overcoming the challenges of sodium ion batteries, Energy, Environ Sci 10 (2017) 1051–1074, https://doi.org/10.1039/c7ee00566k.
[223] C. Vaalma, D. Buchholz, M. Weil, S. Passerini, A cost and resource analysis of sodium-ion batteries, Nat Rev Mater 3 (2018).
[224] K.M. Abraham, How comparable are sodium-ion batteries to lithium-ion counterparts? ACS Energy Lett 5 (2020) 3544–3547, https://doi.org/10.1021/acsenergylett.0c02181.
[225] K. Du, C. Wang, L.U. Subasinghe, S.R. Gajella, M. Law, A. Rudola, P. Balaya, A comprehensive study on the electrolyte, anode and cathode for developing commercial type non-flammable sodium-ion battery, Energy Storage Mater 29 (2020) 287–299, https://doi.org/10.1016/j.ensm.2020.04.021.
[226] A. Rudola, C.J. Wright, J. Barker, Reviewing the Safe Shipping of Lithium-Ion and Sodium-Ion Cells: A Materials Chemistry Perspective, Energy Material Advances 2021 (2021), https://doi.org/10.34133/2021/9798460.
[227] J. Chen, G. Adit, L. Li, Y. Zhang, D.H.C. Chua, P.S. Lee, Optimization strategies toward functional sodium-ion batteries, Energy and Environmental Materials 6 (2023), https://doi.org/10.1002/eem2.12633.
[228] S. Nandy, E. Fortunato, R. Martins, Green economy and waste management: An inevitable plan for materials science, Prog. Nat. Sci.: Mater. Int. 32 (2022) 1–9, https://doi.org/10.1016/j.pnsc.2022.01.001.
[229] L. Zhao, T. Zhang, W. Li, T. Li, L. Zhang, X. Zhang, Z. Wang, Engineering of sodium-ion batteries: opportunities and challenges, Engineering 24 (2023) 172–183, https://doi.org/10.1016/j.eng.2021.08.032.
[230] C. Xu, B. Steubing, M. Hu, C. Harpprecht, M. van der Meide, A. Tukker, Future greenhouse gas emissions of automotive lithium-ion battery cell production, Resour Conserv Recycl 187 (2022), https://doi.org/10.1016/j.resconrec.2022.106606.
[231] S. Zhang, B. Steubing, H. Karlsson Potter, P.A. Hansson, Å. Nordberg, Future climate impacts of sodium-ion batteries, Resour Conserv Recycl 202 (2024), https://doi.org/10.1016/j.resconrec.2023.107362.
[232] F. Wu, Z. Zhou, A.L. Hicks, Life cycle impact of titanium dioxide nanoparticle synthesis through physical, chemical, and biological routes, 2019. http://www.lib.ed.ac.uk.
[233] J. Peters, D. Buchholz, S. Passerini, M. Weil, Life cycle assessment of sodium-ion batteries, Energy Environ Sci 9 (2016) 1744–1751, https://doi.org/10.1039/c6ee00640j.
[234] W. Guo, T. Feng, W. Li, L. Hua, Z. Meng, K. Li, Comparative life cycle assessment of sodium-ion and lithium iron phosphate batteries in the context of carbon neutrality, J Energy Storage 72 (2023), https://doi.org/10.1016/j.est.2023.108589.
[235] S. Wickerts, R. Arvidsson, A. Nordelöf, M. Svanström, P. Johansson, Prospective life cycle assessment of sodium-ion batteries made from abundant elements, J Ind Ecol 28 (2024) 116–129, https://doi.org/10.1111/jiec.13452.
[236] S. Tian, H. He, A. Kendall, S.J. Davis, O.A. Ogunseitan, J.M. Schoenung, S. Samuelsen, B. Tarroja, Environmental benefit-detriment thresholds for flow battery energy storage systems: A case study in California, Appl Energy 300 (2021), https://doi.org/10.1016/j.apenergy.2021.117354.
[237] Y. Yang, E.G. Okonkwo, G. Huang, S. Xu, W. Sun, Y. He, On the sustainability of lithium ion battery industry – A review and perspective, Energy Storage Mater 36 (2021) 186–212, https://doi.org/10.1016/j.ensm.2020.12.019.
[238] C.M. Costa, J.C. Barbosa, R. Gonçalves, H. Castro, F.J.D. Campo, S. Lanceros-Méndez, Recycling and environmental issues of lithium-ion batteries: Advances, challenges and opportunities, Energy Storage Mater 37 (2021) 433–465, https://doi.org/10.1016/j.ensm.2021.02.032.
[239] J.F. Peters, M. Baumann, J.R. Binder, M. Weil, On the environmental competitiveness of sodium-ion batteries under a full life cycle perspective-a cell-chemistry specific modelling approach, (2021). https://doi.org/10.5281/zenodo.4742246.
[240] L.A. Ma, A.J. Naylor, L. Nyholm, R. Younesi, Strategies for mitigating dissolution of solid electrolyte interphases in sodium-ion batteries, Angewandte Chemie - International Edition 60 (2021) 4855–4863, https://doi.org/10.1002/anie.202013803.
[241] Y. Zhao, Y. Kang, J. Wozny, J. Lu, H. Du, C. Li, T. Li, F. Kang, N. Tavajohi, B. Li, Recycling of sodium-ion batteries, Nat Rev Mater 8 (2023) 623–634, https://doi.org/10.1038/s41578-023-00574-w.
[242] Y. Wang, N. An, L. Wen, L. Wang, X. Jiang, F. Hou, Y. Yin, J. Liang, Recent progress on the recycling technology of Li-ion batteries, Journal of Energy Chemistry 55 (2020) 391–419, https://doi.org/10.1016/j.jechem.2020.05.008.
[243] S. Sloop, L. Crandon, M. Allen, K. Koetje, L. Reed, L. Gaines, W. Sirisaksoontorn, M. Lerner, A direct recycling case study from a lithium-ion battery recall, Sustain. Mater. Technol. 25 (2020), https://doi.org/10.1016/j.susmat.2020.e00152.
[244] R. Zhang, X. Shi, O.C. Esan, L. An, Organic electrolytes recycling from spent lithium-ion batteries, Global Chall. 6 (2022), https://doi.org/10.1002/gch2.202200050.
[245] T. Liu, Y. Zhang, C. Chen, Z. Lin, S. Zhang, J. Lu, Sustainability-inspired cell design for a fully recyclable sodium ion battery, Nat Commun 10 (2019), https://doi.org/10.1038/s41467-019-09933-0.
[246] P. Meshram, B.D. Pandey, Abhilash, Perspective of availability and sustainable recycling prospects of metals in rechargeable batteries – A resource overview, Resour. Policy 60 (2019) 9–22, https://doi.org/10.1016/j.resourpol.2018.11.015.
[247] IRON AND STEEL SCRAP, n.d.
[248] S. Jiang, L. Zhang, H. Hua, X. Liu, H. Wu, Z. Yuan, Assessment of end-of-life electric vehicle batteries in China: Future scenarios and economic benefits, Waste Manag. 135 (2021) 70–78, https://doi.org/10.1016/j.wasman.2021.08.031.
[249] H. Zhang, G. Liu, J. Li, D. Qiao, S. Zhang, T. Li, X. Guo, M. Liu, Modeling the impact of nickel recycling from batteries on nickel demand during vehicle electrification in China from 2010 to 2050, Sci. Total Environ. 859 (2023), https://doi.org/10.1016/j.scitotenv.2022.159964.
[250] D. Brough, H. Jouhara, The aluminium industry: A review on state-of-the-art technologies, environmental impacts and possibilities for waste heat recovery, International Journal of Thermofluids 1–2 (2020), https://doi.org/10.1016/j.ijft.2019.100007.
[251] F. Gómez, J.I. Guzmán, J.E. Tilton, Copper recycling and scrap availability, Resour. Policy 32 (2007) 183–190, https://doi.org/10.1016/j.resourpol.2007.08.002.
[252] C. Samuelsson, B. Björkman, Copper Recycling, in: Handbook of Recycling: State-of-the-Art for Practitioners, Analysts, and Scientists, Elsevier Inc., 2014: pp. 85–94. https://doi.org/10.1016/B978-0-12-396459-5.00007-6.
[253] X. Pu, H. Wang, D. Zhao, H. Yang, X. Ai, S. Cao, Z. Chen, Y. Cao, Recent progress in rechargeable sodium-ion batteries: toward high-power applications, Small 15 (2019), https://doi.org/10.1002/smll.201805427.
[254] https://straitsresearch.com/report/sodium-ion-battery-market/request-sample, Sodium-Ion Battery Market Size, (2023).
[255] https://www.alliedmarketresearch.com/sodium-ion-battery-market-A10597, Sodium Ion Battery Market Size, Share, Competitive Landscape and Trend Analysis Report by Application, by End Use: Global Opportunity Analysis and Industry Forecast, 2022-2031, (2022).
[256] L. Rakhymbay, B. Shugay, M. Karlykan, A. Namazbay, A. Konarov, Z. Bakenov, Recent Advances in Layered Na2Mn3O7 Cathode Materials for Sodium-Ion Batteries, Eurasian, J. Chem. 109 (2023) 59–67, https://doi.org/10.31489/2959-0663/1-23-5.
[257] P. Yadav, V. Shelke, A. Patrike, M. Shelke, Sodium-based batteries: development, commercialization journey and new emerging chemistries, Oxford Open Materials Science 3 (2023), https://doi.org/10.1093/oxfmat/itac019.
[258] T. Duan, L. Gan, Y. Chen, Analysis on sustainable development capacity of new energy enterprises: A case study of CATL, Frontiers in Business Econ. Manag. 8 (2023) 35–40.